Fall November 22, 2017

McTips 20171227 George McNamara, Ross Fluorescence Imaging Center - light microscopy, sample preparation, image analysis.pdf

George McNamara

McTips 20171227 George McNamara, PhD
Senior Laboratory Manager ('image core manager')
Ross Fluorescence Imaging Center
Johns Hopkins University School of Medicine
Ross S913A, 720 Rutland Ave, Baltimore, MD 21205-2195
305-764-2081 (cell)
gmcnama2@jhmi.edu
http://confocal.jhu.edu

geomcnamara@earthlink.net
http://home.earthlink.net/~tiki_goddess/TikiGoddess.jpg
(image core mascot) →
http://www.geomcnamara.com/data
http://www.geomcnamara.com/**fluorescent-proteins**-photophysics-data
http://www.geomcnamara.com/fluorescent-**biosensors**
https://works.bepress.com/gmcnamara
McNamara 2017 CPHG (open access):
http://onlinelibrary.wiley.com/doi/10.1002/cphg.42/abstract

Local users: I suggest copy to your computer, and check back for updates, in:
S:\Image Core Manuals
(JHU SOM users: please contact GM for name and access to our "S: drive" local server).

Notes:

- newest tips at top.
- I sometimes add information to older sections, with 'heading 3' appearing indented in the table of contents, and dated (ex. 20170731).
- JHU I.T. may block some web sites, such as
- http://home.earthlink.net/~tiki_goddess
- Some web browsers (Google Chrome!) may not display some web sites (and/or JHU I.T. block).

Image Core guidelines:

- Take great care of our microscopes and computers, so we can all get excellent data.
- I do not want you infecting out computers with viruses, so:
  - Use (a) server to transfer your files, not USB sticks.

If you want to surf the web during a session, bring your own laptop and use that.

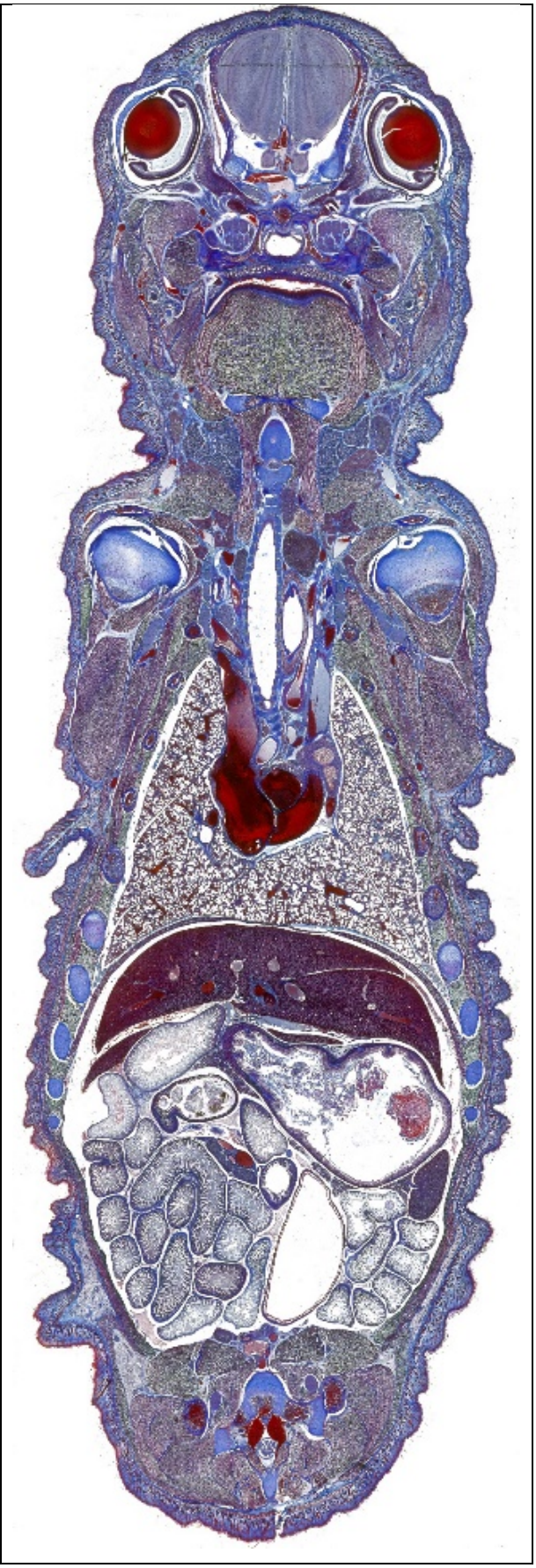

Do you prefer raw (left) or deconvolved (right)? (more on this in **Deconvolution**; tyramide signal amplification "TSA" of mitochondrial protein, ~100x brighter than direct or indirect fluorescent antibody).

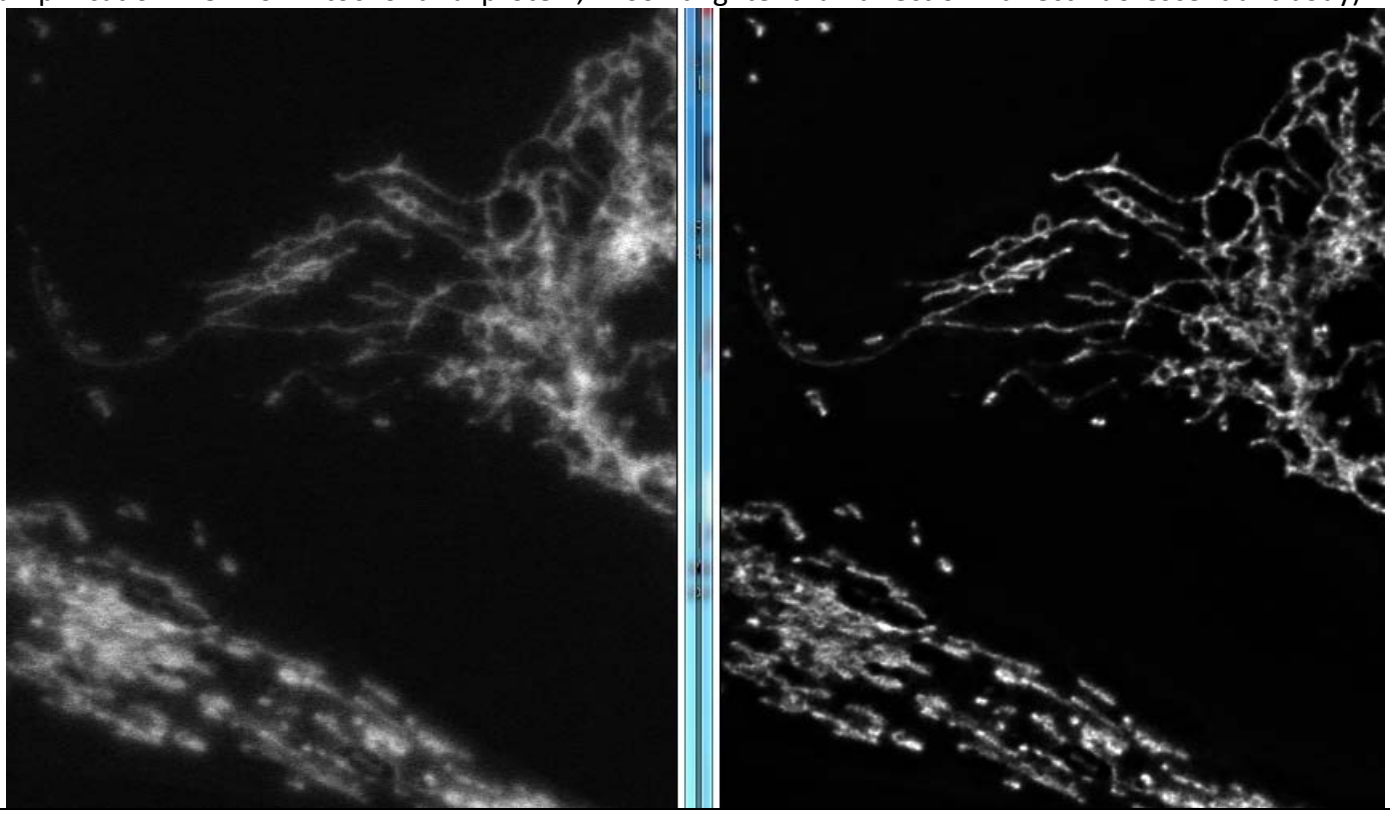

Ross Fluorescence Imaging Center current line up http://confocal.jhu.edu/calendar 1. Andor Spinning Disk 2. Computer Workstation #1 3. Keyence BZ-X700 4. MetaMorph Key 1 (#34135) 5. Metamorph Key 2 (#4646) 6. Olympus FV1000 MP 7. Perkin-Elmer EnVision Plate Reader 8. Perkin-Elmer Volocity Imaging Software 9. PTI-QuantMaster 1 10. PTI-QuantMaster 2 11. Zeiss Axio Imager Upright Microscope/PTI-RatioMaster 12. Zeiss Axio Observer Inverted Microscope 13. Zeiss LSM 510 Meta	Instruments are available 24/7 for fully trained users. 1. Confocal, 2 EMCCDs 2. PC for MetaMorph 3. Automated microscope 4. MetaMorph imaging system license 5. MetaMorph imaging system license 6. Multiphoton microscope, Mai Tai DeepSee 7. Plate reader (multi mode) 8. Volocity imaging software: quantitation, visualization, restoration [CPU deconvolution]. 9. Monochromator based physiology 10. Monochromator based physiology 11. Upright microscope, conventional fluorescence lamp and monochromator 12. Inverted microscope, Olympus DP72 camera 13. Confocal microscope (ten years old, no more service contract)
Olympus Imaging Center – demo equipment Ask John Gibas.	The Olympus instruments are demo equipment that visit for ~1-2 month periods (and not just these). Contact John Gibas, john.gibas@olympus-ossa.com

Contents

Garry Nolan's CODEX (CO-Detection by indEXing) 30plex (or more) immunofluorescence preprint and Akoya Biosciences (products)

20171227W: GM notes:

- "n * 30plex" cycles of cycles would be possible by stripping the set of ~30 primary antibodies (that are conjugated to the DNA tags), and repeating with another set.
- Instead of DNA tagging (barcoding) the primary antibodies, I suggest instead barcoding secondary nanobodies, i.e. nanobobdy anti-mouse IgG (anti-Kappa/Lambda and anti-Heavy chain) as is Pleiner 2017 JCB and www.nano-tag.com (see section below; 2ndary nanobodies to rabit, ginea pig, chicken, etc also doable). This would enable having one "universal' set of tagged nanobodies, usable in any order, instead of having to prepare individual primary antibodies.

https://www.biorxiv.org/content/early/2017/10/20/203166

Deep profiling of mouse splenic architecture with CODEX multiplexed imaging.

Yury Goltsev, Nikolay Samusik, Julia Kennedy-Darling, Salil Bhate, Matthew Hale, Gustavo Vasquez, Garry Nolan

doi: https://doi.org/10.1101/203166
This article is a preprint and has not been peer-reviewed [what does this mean?].
Posted October 20, 2017.

Abstract

A cytometric imaging approach, called CO-Detection by indEXing (CODEX), that enables high parameter multiplexing of antibody-tagged target epitopes is used here to create high parameter imaging datasets of normal mouse and lupus (MRL/lpr) spleens. In this procedure, antibody binding events are rendered iteratively using DNA barcodes, fluorescent dNTP analogs, and an in-situ polymerization-based indexing procedure. Fluorescent signals from multiple rounds of indexing are computationally combined into a multi-channel image stack and subjected to image segmentation and quantification. A segmentation and linear model algorithm was developed to accurately quantify membrane antigen levels on dissociated cells as well as tissue sections. Leveraging the spatially resolved nature of CODEX multiplexed single-cell imaging data, quantitative de novo characterization of lymphoid tissue architecture

was enabled and overlaid onto previously described morphological features. We observed an unexpected, profound impact of the cellular neighborhood on the expression of protein receptors on immune cells. By comparing normal murine spleen to spleens from animals with systemic autoimmune disease (MRL/lpr), extensive and previously uncharacterized splenic cell interaction dynamics in the healthy versus diseased state was observed. The fidelity of multiplexed imaging data analysis demonstrated here will allow deep proteomic analysis and systematic characterization of complex tissue architecture in normal and clinically aberrant samples.

https://www.akoyabio.com/technology/

Rapid Multi-Parameter Tissue Imaging

While tissue imaging studies to date have been highly illuminating, the low number of simultaneous measurements has limited their power. Current systems measure up to five parameters using typical microscopes, and up to twelve using specialty instruments. This limitation is largely based on the number of fluorophores which can be simultaneously imaged. Approaches have been developed to overcome such limitations, but to date they are primarily brute force methods which require multiple time consuming stain/strip/wash cycles and can degrade the sample over time.

As such, deep proteomic profiling that capitalizes on knowledge of tissue organization in situ remains a critical unmet need. High parameter imaging is essential in deciphering the complexity of cellular populations with dynamically changing composition such as a bone marrow or tumor microenvironments.

Our CODEX™ (CO-Detection by indEXing) technology enables this high parameter deep proteomic profiling, initially measuring 30-50 parameters in less than a day. The technology utilizes a “single stain, multiple images” approach. The tissue is first labeled with the entire antibody panel in one step (~50 markers). Antibody binding events are then revealed and imaged in cycles by adding and removing cognate CODEX-tagged dyes.

This process is iterated such that the binding of 30-50 antibodies has been analyzed for all cells in the tissue section. Fluorescent signals from each round are computationally combined into a multi-channel image stack and can be subjected to image segmentation, quantification and analysis.

This multidimensional data enables the user to identify novel cellular neighborhoods and delineate profoundly different tissue micro-architectures, providing a basis for a wide range of novel applications, particularly within immunology and oncology.

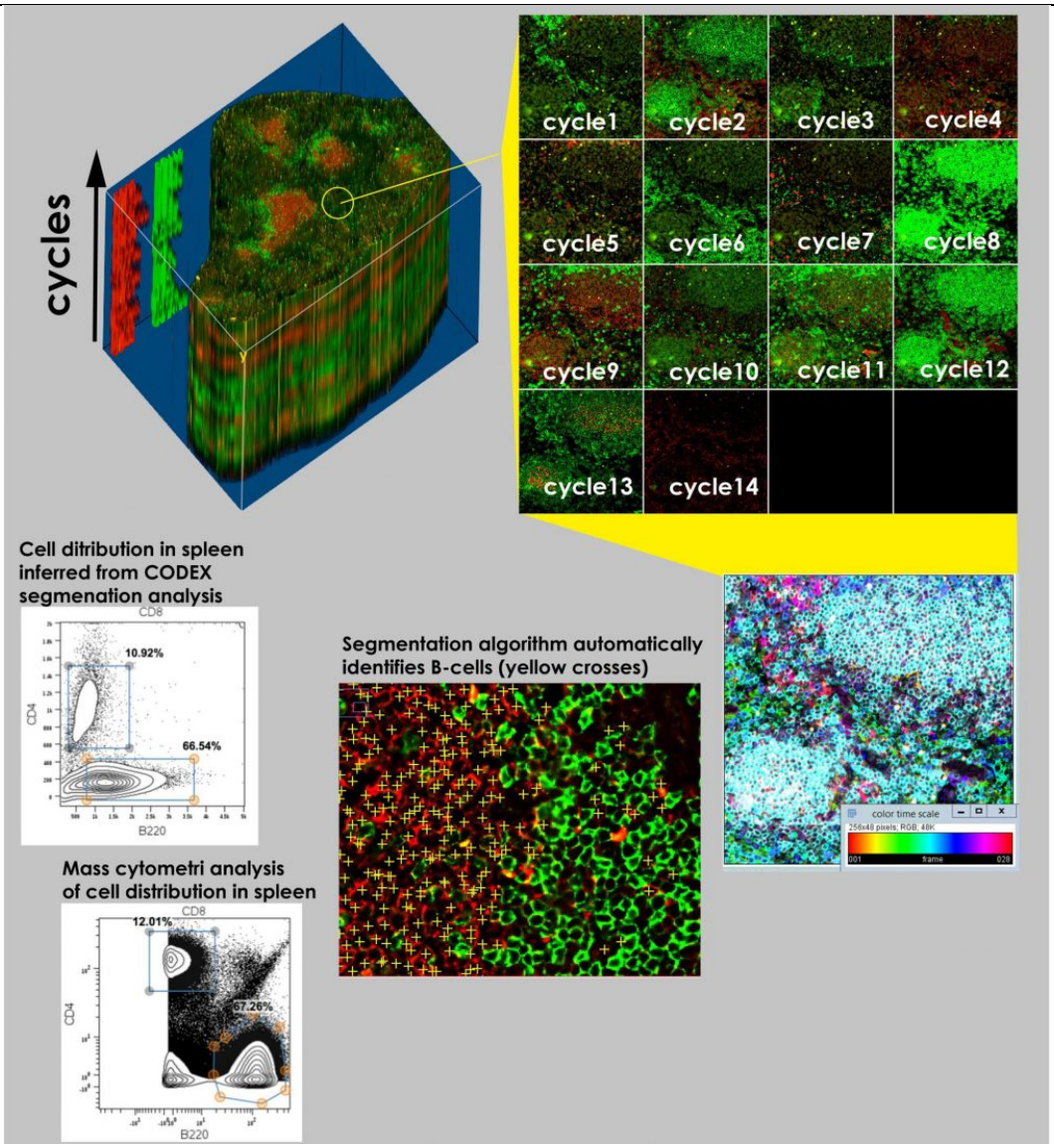

Eosin (tetrabromofluorescein) was named for …

20171227W: the December 2017 issue of RMS InFocus cited the web article below for how Eosin received its name – which is a lot cooler than tetrabromofluorescein(s).

http://www.agarscientific.net/h-and-e-part-one-history-background-and-solutions/

H and E Part One: History, Background and Solutions

October 30, 2014 by PB

In the previous articles we looked at tissue preparation, sectioning and making slides. Now that you have slides ready for use, the next stage is immunohistochemistry or staining.

One of the most commonly used stains for examining tissue is haematoxylin and eosin (or H&E). This is another of those lab techniques which can easily be taken for granted, however, if you understand the science, the materials and the method, this should help you achieve optimal results every time you stain. In this article we'll

take a brief look at the history of the technique followed by the solutions used (and the materials needed for each one to help you set up your own H&E station) and finally, the method itself.

A tree and a girl: a bit of history

The origins of haematoxylin date back to the 17th Century. This dye is actually named after the tree from which it is extracted: *Haematoxylum campechianum*. A native tree of Mexico and Central America, this logwood was exported to Europe for use in fabric dyeing. In 1863, a German anatomist called Heinrich Wilhelm Gottfried von Waldeyer-Hartz (or 'Waldeyer' for short) published the first article in which he had been experimenting in the use of haematoxylin as a histochemical dye (he was also credited as naming the 'chromosome'). However, these initial results were poor and it wasn't until 1865 when Böhmer realised that the extracted dye needed to be combined with a 'mordant' to facilitate the staining of tissue. A 'mordant' is simply a metallic salt which helps the dye bind to tissue, the most commonly used are aluminium and iron. Independently of Böhmer, Heinrich Caro was a Polish chemist working for the chemical company which later became BASF. Working with a sample of fluorescein, Caro synthesised a yellow-red dye which he named 'Eosin' (after the nickname of a girl he admired!). Emil Fischer was another German chemist working in the field and in 1875 he published a paper on Eosin Y which is the commonly used eosin dye in histology. The 'Y' stands for 'yellowish'! Skip forward a year and Wissowzky published his work on a combined staining using both haematoxylin and eosin.

Haematoxylin

The haematoxylin which is extracted from the wood is not actually a very good histological dye in itself. It needs to be oxidised to 'haematein'. Even then, this dye is not directly used in histology. This is where the mordant comes in. This metal cation enables the haematoxylin to bind to the nuclear proteins (specifically the histones). You may come across the term 'haematoxylin lake', but this doesn't refer to some vast expanse of liquid! This term just means a solution of haematoxylin and metal salt with some additional chemicals.

Eosin Y

Eosin Y is an anionic acidic dye which binds to positively charged components of the cytoplasm such as amino groups. This counterstain helps to differentiate between the nucleus and non-nuclear components in cells. Even though the 'Y' stands for 'yellowish', the stain is actually pink. Another type of eosin is 'eosin B'. The 'B' stands for 'blueish'!

***

See also:

http://stainsfile.info/StainsFile/dyes/dyes.htm

http://stainsfile.info/StainsFile/dyes/45380.htm

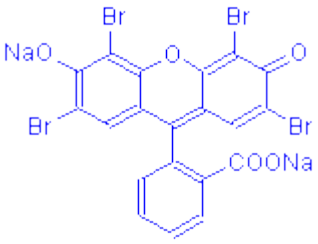

Property	Data

Eosin Y is the most common counterstain to alum hematoxylin in the Hematoxylin and Eosin

Common name	Eosin Y
Suggested name	Eosin Y ws
Other names	Eosine Yellowish Bromoeosine Tetrabromofluorescein
C.I. number	45380
C.I. name	Acid red 87
Class	Fluorone
Ionisation	Acid
Solubility aqueous	40%
Solubility ethanol	2%
Absorption maximum	515-518 (Conn) 517 (Gurr) 514 (Aldrich)
Colour	Red
Empirical formula	$C_{20}H_6O_5Br_4Na_2$
Formula weight	691.9

method (H&E). It stains satisfactorily from both aqueous and ethanolic solution. It is one of the dyes in Papanicolaou's EA solutions for staining exfoliative cytology for cervical cancer screening. It can be used to make Romanowsky stains. It is widely used in numerous procedures. It is strongly fluorescent, but this property is hardly ever used.
The free radical, eosinol Y is made by treating the dye with hydrochloric acid. It is sometimes called ***eosin Y, spirit soluble***. Eosinol Y is soluble in ethanol and slightly soluble in xylene, but not in water, and is useful for staining difficult tissues.

FSD and Flamma Fluorophores from BioActs

20171227W: info on two more families of fluorophores.

http://www.bioacts.com/eng/sub10.php?cate1=5M10UXU0FA&cate2=RGGHEO4656

FSD™ Fluorophore

FSD Fluor™	λ_{Ex} (nm)	λ_{Em} (nm)	Excitation Laser Line	Replacement for
FSD 488	495	519	488 nm Laser	Alexa® 488, Cy® 2, Dylight® 488
FSD 555	552	565	488, 532 nm Laser	Alexa® 555, Cy® 3, Dylight® 549
FSD 594	593	617	561, 594 nm Laser	Alexa® 594
FSD 647	650	667	594, 663 nm Laser	Alexa® 647, Cy® 5, Dylight® 649
FSD 750	749	774	680 nm Laser	Alexa® 750, Cy® 7, Dylight® 750
FSD 800	774	790	785 nm Laser	Alexa® 790, Dylight® 800, IRDye® 800

The FSD™ series is a new fluorescent dye with excellent fluorescence intensity and high quantum yield compared to conventional fluorescent dyes.

Available with reactive groups for conjugation:

Reactive FSD Fluor™	Reactive target group
NHS ester	Amine (-NH_2)
Sulfo-NHS ester	
Vinylsulfone	
Isothiocyanate	
Maleimide	Thiol (-SH)
Hydrazide	Aldehyde (-CHO) Ketone (>C=O) Hydroxyl group (-OH)
Dichlorotriazine	

Functionalized FSD Fluor™
Carboxylic acid
Amine
Thiol
Click-chemistry FSD Fluor™
Alkyne
PEG4-Alkyne
ADIBO

Flamma® Fluorophore

Flamma® Fluor	λ_{Ex} (nm)	λ_{Em} (nm)	Excitation Laser Line	Replacement for
Flamma® 406	401	434	UV	Alexa Fluor® 405, Cascade Blue®, DyLight® 405, CF™ 405, Pacific Blue®
Flamma® 496	496	516	488 nm Laser	FAM, FITC, Fluorescein
Flamma® 488	495	519	488 nm Laser	Alexa Fluor® 488, Cy® 2, DyLight® 488, CF™ 488, ATTO 488
Flamma® 552	550	565	532, 543, 546, 555 or 568 nm Laser	Alexa Fluor® 555, Cy® 3, DyLight® 549, CF™ 488, ATTO 488
Flamma® 553	554	584	532, 543, 546, 555 or 568 nm Laser	Alexa Fluor® 546, TRITC
Flamma® 560	560	589	532, 543, 546, 555 or 568 nm Laser	Alexa Fluor® 568, CF™ 568, ATTO 565, RITC
Flamma® 648	648	663	663, 635, or 640 nm Laser	Alexa Fluor® 647, Cy® 5, DyLight® 649, CF™ 647, ATTO 647N
Flamma® 675	675	691	680 or 685 nm Laser	Alexa Fluor® 680, Cy® 5.5, DyLight® 680, CF™ 680, IRDye® 680LT
Flamma® 749	749	774	680 or 685 nm Laser	Alexa Fluor® 750, Cy® 7, DyLight® 750, CF™ 750, IRDye® 750
Flamma® 774	774	800	785 nm Laser	Cy® 7.5, CF™ 770
Flamma® 800	775	795	785 nm Laser	Alexa Fluor® 790, DyLight® 800, CF™ 790, IRDye® 800CW

Adobe Photoshop Tip: Scientific Imaging With Photoshop book – Gerry Sedgewick

20171222F.

Available in paperback or amazon kindle edition:

https://www.amazon.com/Scientific-Imaging-Photoshop-Methods-Measurement/dp/0321514335

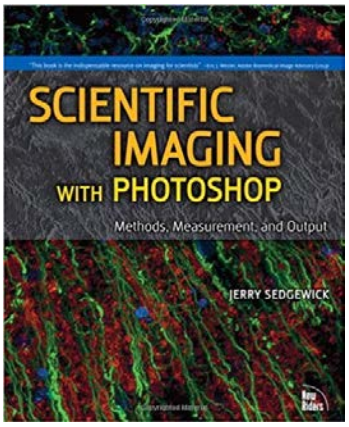

Scientific Imaging with Photoshop: Methods, Measurement, and Output 1st Edition

by Jerry Sedgewick (Author)

Paperback: 312 pages
Publisher: New Riders; 1 edition (June 2, 2008)
Language: English
ISBN-10: 0321514335
ISBN-13: 978-0321514332

https://www.researchgate.net/publication/259687962_Scientific_Imaging_with_Photoshop_Methods_Measurement_and_Output

Abstract

Adobe Photoshop is one of the more powerful tools available to scientists today. It is indispensable in the preparation of digital images of specimens for measurement, especially for separating relevant features from background detail. Scientific Imaging with Photoshop is the authoritative guide to the use of Photoshop in scientific research, with a special emphasis on the ethical ramifications of the use of image-enhancement software to extract data from digital images. Beginning Photoshop users will benefit from its tutorials in the basics of image processing, and more sophisticated users will appreciate the sections on automating Photoshop operations with actions. In addition, the book lays out procedures in straightforward language for acquiring digital images as well as outputting processed images in digital and hard-copy formats. Scientific Imaging with Photoshop provides all this and more: • Little-known methods separating features of interest from the background for subsequent quantification • How to make dense colors and subtle visual detail reproduce properly in publication • Correct Photoshop methods and techniques for all user levels • Procedures that are usable in legacy versions of Photoshop as well as Photoshop Elements and Photoshop Extended

Scientific Imaging with Photoshop: Methods, Measurement and Output. Available from: https://www.researchgate.net/publication/259687962_Scientific_Imaging_with_Photoshop_Methods_Measurement_and_Output [accessed Dec 22 2017].

My “Color Balancing Histology Images” article is available online (open access, with permission from editor) home.earthlink.net/~geomcnamara/McNamara2005JoH28n2pp81-88.pdf

Adobe Photoshop Tip: dealing with Leica SP8 confocal data, especially with the HyD detectors

20171222F (see also ‘Scientific Imaging With Photoshop’ above, and ‘Color Balancing Histology Images’ below).

1. if you like the color scheme you see in the Leica LAS X software, File --> Export --> JPEG, will result in "what you see is what you get" image file.
2. Plan "PS" for Photoshop: LAS File --> Export --> TIF --> Raw (no overlay), and then open the images in Photoshop (convert to 8-bit if 16-bit: Image menu --> Mode --> check "8bit/channel" if currently "16bit/channel), copy & paste into appropriate CHANNELS, contrast adjust each channel.

Note: the raw data images when using HyD photon counting mode (as I recommend) may be only in the 10's out of 255 (8-bit) or 65535 (16-bit). These will look dark in Photoshop!!! Use Image --> Adjust --> Levels

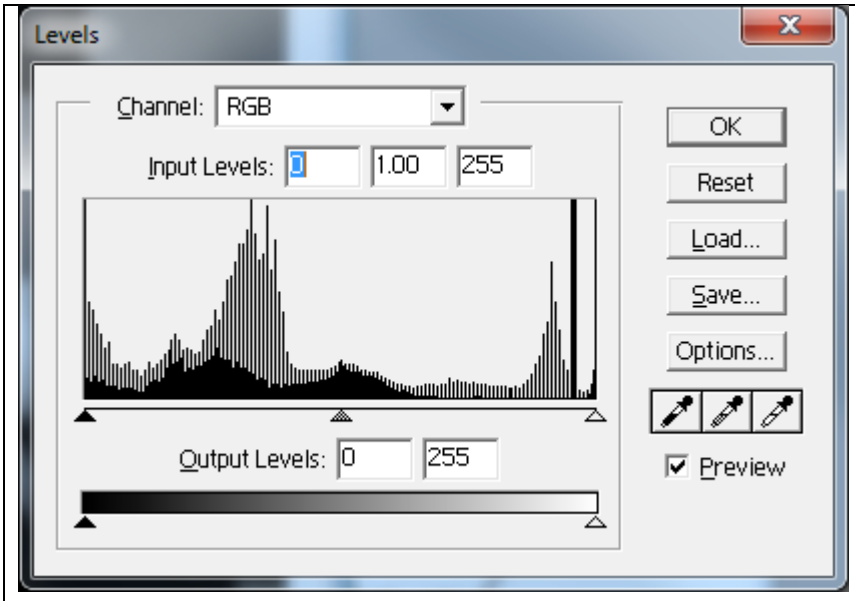

(typically change Output level 'high' = right hand, value ... easiest to do on the single channel images.
➔HyD photon counting mode might output values in the range of zero to ten counts (photons detected!) per pixel. This differs from "the usual PMT" output of zero to 255 (or when I am training users or operating a PMT based confocal, ~10 to ~200 intensity, making sure detector offset is above zero and maximum is not close to saturating), but in fact PMT is simply "photomultiplying, then digitizing" a few photons (photoelectrons) to integer numbers. The HyD's are more sensitive than standard PMTs, and the HyD photon count numeric output is more likely to be "usefully linear" with respect to both laser power and number of fluorophores in the acquisition volume, than standard PMT behavior. A simple test any user can perform is to change laser power while imaging a very thin, sparse, specimen (ex. Alexa Fluor 647-phalloidin labeling of F-actin in the periphery of a very thin cell).

Fit it: Glyoxol or PFA+GA as possibly superior fixatives for immunofluorescence and/or smFISH

20171220W: recent abstracts on potentially better fixatives. PFA (paraformaldehyde, "formalin") has a long history, so will be hard to displace from "standard of care". On the other hand, horses have a long history as "transporters": imagine if every automobile and truck in Baltimore was replaced with horse(s) [hint: one tank of gasoline = a whole lot of food and poop].

Glyoxal (pH 4 or 5, optional Ethanol permeabilization agent)

EMBO J. 2017 Nov 16. pii: e201695709. doi: 10.15252/embj.201695709. [Epub ahead of print]
Glyoxal as an alternative fixative to formaldehyde in immunostaining and super-resolution microscopy.
Richter KN[1,2], Revelo NH[1], Seitz KJ[1,3], Helm MS[1,3], Sarkar D[4], Saleeb RS[5], D'Este E[6], Eberle J[7], Wagner E[8,9], Vogl C[10,11], Lazaro DF[12,13], Richter F[3,14], Coy-Vergara J[15], Coceano G[16], Boyden ES[17], Duncan RR[5], Hell SW[6], Lauterbach MA[7], Lehnart SE[8,9], Moser T[10,11], Outeiro T[12,13], Rehling P[14,18], Schwappach B[15], Testa I[16], Zapiec B[19], Rizzoli SO[20,2].
Author information
Paraformaldehyde (PFA) is the most commonly used fixative for immunostaining of cells, but has been associated with various problems, ranging from loss of antigenicity to changes in morphology during fixation. We show here that the small dialdehyde glyoxal can successfully replace PFA Despite being less toxic than PFA, and, as most aldehydes, likely usable as a fixative, glyoxal has not yet been systematically tried in modern fluorescence microscopy. Here, we tested and optimized glyoxal fixation and surprisingly found it to be more efficient than PFA-based protocols. Glyoxal acted faster than PFA, cross-linked proteins more effectively, and improved the preservation of cellular morphology. We validated glyoxal fixation in multiple laboratories against

different PFA-based protocols and confirmed that it enabled better immunostainings for a majority of the targets. Our data therefore support that glyoxal can be a valuable alternative to PFA for immunostaining.

KEYWORDS: PFA ; fixation; glyoxal; immunocytochemistry; super-resolution Microscopy
PMID: 29146773 DOI: 10.15252/embj.201695709

GAF = glyoxal acid-free fixative
GM: contradicting the richter 2017 (above) approach of pH 4 or 5.

PLoS One. 2017 Aug 10;12(8):e0182965. doi: 10.1371/journal.pone.0182965. eCollection 2017.
Acid-free glyoxal as a substitute of formalin for structural and molecular preservation in tissue samples.
Bussolati G[1], Annaratone L[1], Berrino E[2], Miglio U[2], Panero M[2], Cupo M[1], Gugliotta P[1], Venesio T[2], Sapino A[1,2], Marchiò C[1,3].
Author information
Tissue fixation in phosphate buffered formalin (PBF) remains the standard procedure in histopathology, since it results in an optimal structural, antigenic and molecular preservation that justifies the pivotal role presently played by diagnoses on PBF-fixed tissues in precision medicine. However, toxicity of formaldehyde causes an environmental concern and may demand substitution of this reagent. Having observed that the reported drawbacks of commercially available glyoxal substitutes of PBF (Prefer, Glyo-fix, Histo-Fix, Histo-CHOICE, and Safe-Fix II) are likely related to their acidity, we have devised a neutral fixative, obtained by removing acids from the dialdehyde glyoxal with an ion-exchange resin. The resulting glyoxal acid-free (GAF) fixative has been tested in a cohort of 30 specimens including colon (N = 25) and stomach (N = 5) cancers. Our results show that GAF fixation produces a tissue and cellular preservation similar to that produced by PBF. Comparable immuno-histochemical and molecular (DNA and RNA) analytical data were obtained. We observed a significant enrichment of longer DNA fragment size in GAF-fixed compared to PBF-fixed samples. Adoption of GAF as a non-toxic histological fixative of choice would require a process of validation, but the present data suggest that it represents a reliable candidate.
PMID: 28796828 PMCID: PMC5552132 DOI: 10.1371/journal.pone.0182965

PFA/GA

Biol Open. 2016 Sep 15;5(9):1343-50. doi: 10.1242/bio.019943.
Critical importance of appropriate fixation conditions for faithful imaging of receptor microclusters.
Stanly TA[1], Fritzsche M[1], Banerji S[1], García E[2], Bernardino de la Serna J[3], Jackson DG[4], Eggeling C[5].
Author information
Receptor clustering is known to trigger signalling events that contribute to critical changes in cellular functions. Faithful imaging of such clusters by means of fluorescence microscopy relies on the application of adequate cell fixation methods prior to immunolabelling in order to avoid artefactual redistribution by the antibodies themselves. Previous work has highlighted the inadequacy of fixation with paraformaldehyde (PFA) alone for efficient immobilisation of membrane-associated molecules, and the advantages of fixation with PFA in combination with glutaraldehyde (GA). Using fluorescence microscopy, we here highlight how inadequate fixation can lead to the formation of artefactual clustering of receptors in lymphatic endothelial cells, focussing on the transmembrane hyaluronan receptors LYVE-1 and CD44, and the homotypic adhesion molecule CD31, each of which displays their native diffuse surface distribution pattern only when visualised with the right fixation techniques, i.e. PFA/GA in combination. Fluorescence recovery after photobleaching (FRAP) confirms that the artefactual receptor clusters are indeed introduced by residual mobility. In contrast, we observed full immobilisation of membrane proteins in cells that were fixed and then subsequently permeabilised, irrespective of whether the fixative was PFA or PFA/GA in combination. Our study underlines the importance of choosing appropriate sample preparation protocols for preserving authentic receptor organisation in advanced fluorescence microscopy.
KEYWORDS: FRAP; Fixation; Immunolabelling; LYVE-1; Membrane receptors; Receptor clustering; Super-resolution
PMID: 27464671 PMCID: PMC5051640 DOI: 10.1242/bio.019943

Nanobodies for efficient multiplex immunofluorescence with many mouse mAbs and/or rabbit, guinea pig, chicken IgGs … that is, all primaries can be same species.

- www.nano-tag.com … X4 products (4 dyes per target) and/or "service" http://nano-tag.com/services
- www.chromotek.com
- Rockland Immunochemicals … development https://rockland-inc.com/Product.aspx?id=49989 …

➔ Key feature of any company that offers nanobody (or phage display library) development is you own the nanobodies protein AND the VHH single domain antibody (sdAb) DNA sequence.

http://nano-tag.com/products/product-features/
Our current product lines are based on recombinant single-domain antibodies (sdAbs) derived from llamas or alpacas. This type of affinity Tags (also known as "Nanobodies"; trademark owned by Ablynx) provides significant advantages over conventional IgG molecules. All our Tags have been developed in-house. They are highly specific with affinities tailored for a wide range of applications.

http://nano-tag.com/products now (12/2017 ASCB-EMBO exhibit) has nanobodies for each of:
* rabbit IgG
* mouse IgG
These are not yet on their web site (they already had anti-guinea pig and anti-chicken) -- I spoke with them at the ASCB-EMBO meeting exhibition Sunday (Dec 3, 2017). Currently have four colors (equivalent to Alexa Fluor's 488, 546, 594, 647), hopefully will have more "soon".
the key feature is the workflow could be:
1. combine mouse monoclonal antibody #1 + nanobody #1 (with latter in excess).
2. incubate for (say) 30 minutes.
3. add modest amount of unlabeled nanobody (to bind all remaining sites on the mAb).
1', 2',3'. Repeat for antibody#2+nanobody#2, and other pairs.
4. Combine all "pairs" (#1mAb+#1nano, #2mAb+#2nano, etc) in one tube. Optional: DAPI or other counterstain(s).
5. Aliquot onto slides or imaging dishes.
6. incubate (60 minutes?).
7. Wash.
8. mounting medium (i.e. Prolong Diamond).
9. image.

➔20171214 update: we are expecting some Nanotag X4 samples in early January 2018.

Nano-Tag fluorophore dyes (20171207 info):

Atto488
Atto542
Atto565

Atto647N
Abberior Star 580
Abberior Star 635P
Sulfo-Cyanin 3
Sulfo-Cyanin 5

Spectra of ATTO-TEC dyes available on Nano-Tag nanobodies:

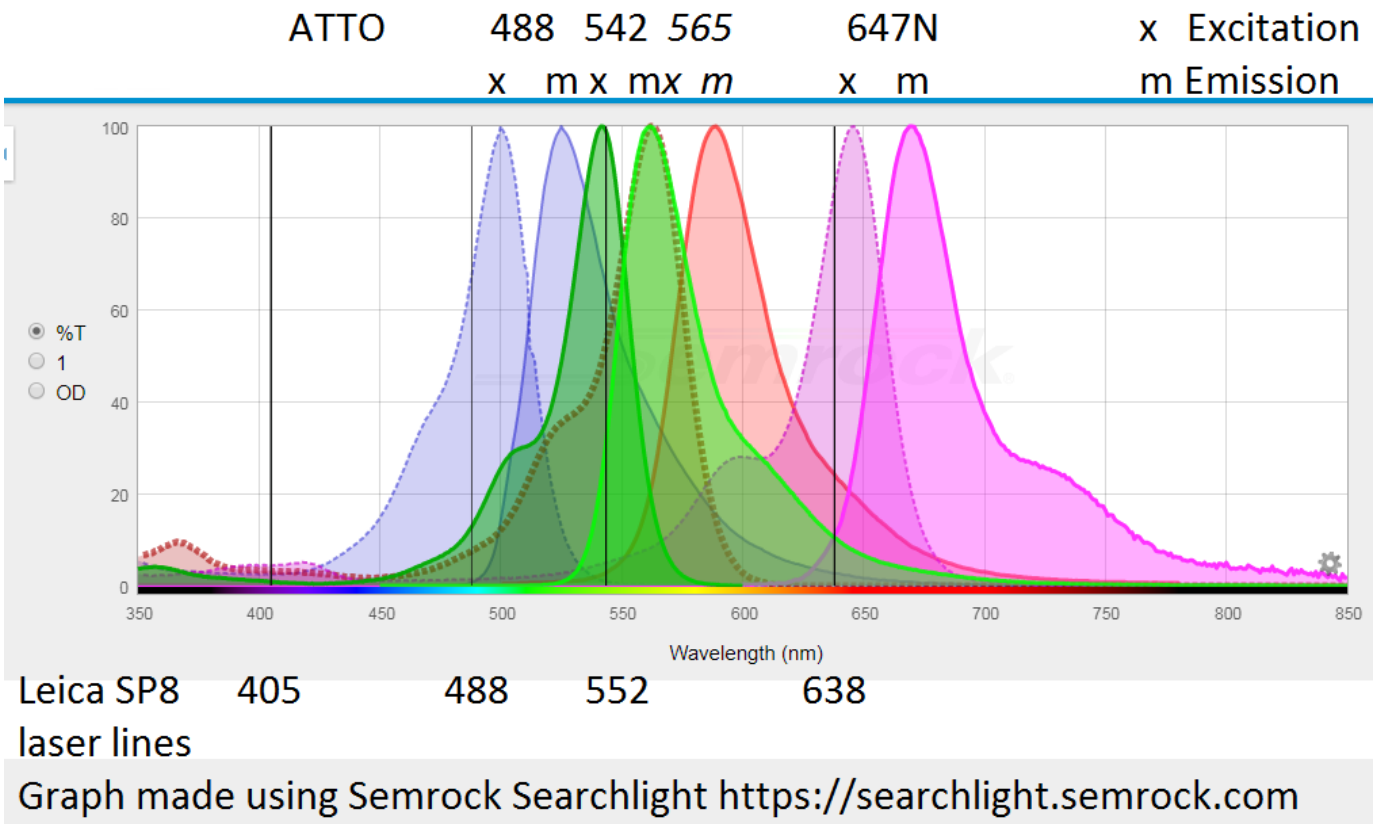

20171221H: part of a press release (Pleiner et al 2017 JCB journal article reference below):

https://www.eurekalert.org/pub_releases/2017-12/m-fla122117.php
PUBLIC RELEASE: 21-DEC-2017

Fewer laboratory animals thanks to secondary nanobodies

MAX-PLANCK-GESELLSCHAFT
Antibodies are indispensable in biological research and medical diagnostics. However, their production is time-consuming, expensive, and requires the use of many animals. Scientists at the Max Planck Institute for Biophysical Chemistry in Göttingen, Germany, have now developed so-called secondary nanobodies that can replace the most-used antibodies and may drastically reduce the number of animals in antibody production. This is possible because the secondary nanobodies can be produced in large scale by bacteria. Moreover, the secondary nanobodies outperform their traditional antibody counterparts in key cell-biological applications.

As a central part of our immune system, antibodies protect us humans and other vertebrates against pathogens. They are, however, also essential tools in medical diagnostics, therapy, and basic research - for example in

fluorescence microscopy. When researchers want to study a certain protein within a cell, they can mark it selectively with antibodies directed against this protein. Once these so-called primary antibodies have bound their target, secondary antibodies are applied. These bind the primary antibodies, carry fluorescent dyes that light up under the microscope, and thus make the protein of interest visible.

The great variety of primary antibodies is traditionally produced in small mammals such as rabbits and mice: First, the animals are immunized with the purified protein - this is comparable to vaccinating humans. As a result, the animals' immune system forms antibodies against the protein. The antibodies are finally collected from the blood of the animals, and processed. As antibodies are used by thousands of labs worldwide and because most of their applications rely on secondary antibodies, the latter are in enormous demand. Therefore, the production of secondary antibodies necessitates not only many, but also large animals such as donkeys, goats, or sheep. This poses an ethical problem.

Secondary nanobodies can be produced in bacteria

Researchers at the Max Planck Institute for Biophysical Chemistry now present a sustainable alternative that can replace secondary antibodies directed against primary ones from mice or rabbits. It relies on so-called nanobodies and may drastically reduce the number of animals used for antibody production. Nanobodies are fragments of special antibodies from camels and related species such as alpacas. "We have developed secondary nanobodies that not only perform very well, but also, they can be produced microbiologically at any scale - just like beer in a fermenter," explains Dirk Görlich, Director at the Max Planck Institute in Göttingen and head of the project.

"Secondary antibodies have to meet extremely stringent quality requirements and must detect only primary antibodies of a single species and no structures in the analyzed cells or medical samples. Thus, the problem was to obtain construction plans for truly perfect secondary nanobodies. We started with a vast number of variants that we extracted from a small amount of blood from two immunized alpacas. By so-called phage display, we then fished out the best variants and eventually used them to program bacteria for nanobody production," elucidates Tino Pleiner, first author of the work.

Nanobodies were first described in 1993 by a Belgian pioneering group of scientists. Since then, researchers try to take advantage of them for their work in the lab. However, replacing secondary antibodies with nanobodies turned out to be not trivial at all. One reason is the nanobodies' size: They are ten times smaller than normal antibodies. Therefore, they offer much less space for coupling fluorescent molecules and thus appear far dimmer in the microscope than conventional antibodies.

"Indeed, our first experiments with secondary nanobodies were rather disappointing and produced only dark and noisy images. However, we did not give up, and immunized the two alpacas again to stimulate their immune system to improve the initial nanobodies. Further evolution in the test tube, a special coupling strategy for the fluorescent dyes, and combining two or more compatible nanobodies did the rest," Görlich tells about initial difficulties. By now, the nanobodies at least match conventional antibodies in terms of signal strength.

Improved resolution in light microscopy

Nanobodies have clear advantages over secondary antibodies. "Super-resolution fluorescence microscopy, for example, can optically resolve cellular structures in the range of a few nanometers. However, such images get blurred when primary and secondary antibodies are used that each measure 15 nanometers already. Using nanobodies with a size of just three nanometers indeed improves resolution," Pleiner says.

"We have tested the secondary nanobodies in other applications besides microscopy, and the results are very promising," Görlich emphasizes. Especially the new route of production in bacteria facilitates their modification and

fusion to other reporter proteins, for instance enzymes. "We expect that in many applications our nanobodies will replace conventional secondary antibodies from donkeys, goats, or sheep."

Pleiner 2017 JCB - a toolbox of anti-mouse and anti-rabbit IgG secondary nanobodies Gorlich see www.nano-tag.com

doi: 10.1083/jcb.201709115
Pleiner T, Bates M, Görlich D. A toolbox of anti-mouse and anti-rabbit IgG secondary nanobodies. J Cell Biol. 2017 Dec 20. pii: jcb.201709115. doi: 10.1083/jcb.201709115. [Epub ahead of print]

1. Department of Cellular Logistics, Max Planck Institute for Biophysical Chemistry, Göttingen, Germany tino.pleiner@mpibpc.mpg.de.
2. Department of NanoBiophotonics, Max Planck Institute for Biophysical Chemistry, Göttingen, Germany mark.bates@mpibpc.mpg.de.
3. Department of Cellular Logistics, Max Planck Institute for Biophysical Chemistry, Göttingen, Germany goerlich@mpibpc.mpg.de.

Abstract
Polyclonal anti-immunoglobulin G (anti-IgG) secondary antibodies are essential tools for many molecular biology techniques and diagnostic tests. Their animal-based production is, however, a major ethical problem. Here, we introduce a sustainable alternative, namely nanobodies against all mouse IgG subclasses and rabbit IgG. They can be produced at large scale in *Escherichia coli* and could thus make secondary antibody production in animals obsolete. Their recombinant nature allows fusion with affinity tags or reporter enzymes as well as efficient maleimide chemistry for fluorophore coupling. We demonstrate their superior performance in Western blotting, in both peroxidase- and fluorophore-linked form. Their site-specific labeling with multiple fluorophores creates bright imaging reagents for confocal and superresolution microscopy with much smaller label displacement than traditional secondary antibodies. They also enable simpler and faster immunostaining protocols, and allow multitarget localization with primary IgGs from the same species and of the same class.
PMID: 29263082 DOI: 10.1083/jcb.201709115

→ T. Pleiner and D. Görlich are inventors on a European patent application encompassing the nanobodies described in this article.

http://jcb.rupress.org/content/early/2017/12/19/jcb.201709115/tab-pdf (this "early' URL may become non-functional when the final volume:page version is published – you can use the DOI to access).

Gorris 2017 JI & Parra 2017 Sci Rep – 7plex Tyramide signal amplification + DAPI counterstain

20171122W update (today is my 6 month work anniversary here at JHU G.I. Ross F.I.C.).

I note that in 1999 Brian Van Tine did 6plex TSA on human white blood cells with CD markers (i.e. CD3, CD4, CD20, CD68, more) – Brian was a student at the Cold Spring Harbor Labs (CSHL) In Situ Hybridization course run by David Speector. I was there as a commercial faculty member, as part of Applied Spectral Imaging's contingent.

Gorris et al 2017 J. Immunology - new example of multicolor fluorescent tyramide signal amplification ... will probably be simpler to use Biocare's PeroxAbolish than "MWT" (microwave treatment) to kill HRP ... no need to go 7plex initially!

Parra 2017 – more of the same.

Both PerkinElmer (Opal TSA kits) and ThermoFisher/Molecular Probes (Alexa Fluor tyramides) have lots of colors (the Opal fluorophores may even be Alexa's). these are discussed in tyramide section(s) here in McTips (near the bottom = beginning).

The Sato 2017 "click tyrosine" (bookmark) discussed previously may enable an additional 10x improvement in sensitivity compared to Tyramide.

Gorris reference and abstract:

Eight-Color **Multiplex** Immunohistochemistry for Simultaneous Detection of Multiple Immune Checkpoint Molecules within the Tumor Microenvironment.
Gorris MAJ, Halilovic A, Rabold K, van Duffelen A, Wickramasinghe IN, Verweij D, Wortel IMN, Textor JC, de Vries IJM, Figdor CG.
J Immunol. 2017 Nov 15. pii: ji1701262. doi: 10.4049/jimmunol.1701262. [Epub ahead of print]
PMID: 29141863

Therapies targeting immune checkpoint molecules CTLA-4 and PD-1/PD-L1 have advanced the field of cancer immunotherapy. New mAbs targeting different immune checkpoint molecules, such as TIM3, CD27, and OX40, are being developed and tested in clinical trials. To make educated decisions and design new combination treatment strategies, it is vital to learn more about coexpression of both inhibitory and stimulatory immune checkpoints on individual cells within the tumor microenvironment. Recent advances in multiple immunolabeling and multispectral imaging have enabled simultaneous analysis of more than three markers within a single formalin-fixed paraffin-embedded tissue section, with accurate cell discrimination and spatial information. However, multiplex immunohistochemistry with a maximized number of markers presents multiple difficulties. These include the primary Ab concentrations and order within the multiplex panel, which are of major importance for the staining result. In this article, we report on the development, optimization, and application of an eight-color multiplex immunohistochemistry panel, consisting of PD-1, PD-L1, OX40, CD27, TIM3, CD3, a tumor marker, and DAPI. This multiplex panel allows for simultaneous quantification of five different immune checkpoint molecules on individual cells within different tumor types. This analysis revealed major differences in the immune checkpoint expression patterns across tumor types and individual tumor samples. This method could ultimately, by characterizing the tumor microenvironment of patients who have been treated with different immune checkpoint modulators, form the rationale for the design of immune checkpoint-based immunotherapy in the future.
PMID: 29141863 DOI: 10.4049/jimmunol.1701262

Parra 2017
Validation of **multiplex** immunofluorescence panels using multispectral microscopy for immune-profiling of formalin-fixed and paraffin-embedded human tumor tissues.
Parra ER, Uraoka N, Jiang M, Cook P, Gibbons D, Forget MA, Bernatchez C, Haymaker C, Wistuba II, Rodriguez-Canales J.
Sci Rep. 2017 Oct 17;7(1):13380. doi: 10.1038/s41598-017-13942-8.
PMID: 29042640
Immune-profiling is becoming an important tool to identify predictive markers for the response to immunotherapy. Our goal was to validate multiplex immunofluorescence (mIF) panels to apply to formalin-fixed and paraffin-embedded tissues using a set of immune marker antibodies, with the Opal™ 7 color Kit (PerkinElmer) in the same tissue section. We validated and we described two panels aiming to characterize the expression of PD-L1, PD-1, and subsets of tumor associated immune cells. Panel 1 included pancytokeratin (AE1/AE3), PD-L1, CD4, CD8, CD3, CD68, and DAPI, and Panel 2 included pancytokeratin, PD-1, CD45RO, granzyme B, CD57, FOXP3, and DAPI. After all primary antibodies were tested in positive and negative controls by immunohistochemistry and uniplex IF, panels were developed and simultaneous marker expressions were quantified using the Vectra 3.0™ multispectral microscopy and image analysis InForm™ 2.2.1 software (PerkinElmer).These two mIF panels demonstrated specific co-localization in different cells that can identify the expression of PD-L1 in malignant cells and macrophages, and different T-cell subpopulations. This mIF methodology can be an invaluable tool for tumor tissue immune-profiling to allow multiple targets in the same tissue section and we provide that is accurate and reproducible method when is performed carefully under pathologist supervision.
PMID: 29042640 PMCID: PMC5645415 DOI: 10.1038/s41598-017-13942-8

See also the Carstens "8plex" paper discussed previously.

Spatial computation of intratumoral T cells correlates with survival of patients with pancreatic cancer.
Carstens JL, Correa de Sampaio P, Yang D, Barua S, Wang H, Rao A, Allison JP, LeBleu VS, **Kalluri** R.
Nat Commun. 2017 Apr 27;8:15095. doi: 10.1038/ncomms15095.
PMID: 28447602

"Block all FcR's" ➔"Light Me Up" … CD16, CD32, CD64 and especially FcRn

Many immunostaining protocols include one or more "blocking reagents", such as "Normal Goat Serum" ("NGS") to block 'non-specific' binding of primary and/or secondary antibodies.

Enterocytes express FcRn (Fc Receptor Neonatal) and monocytes/macrophages and other cell types express FcRgamma's CD16, CD32, CD64 and other FcReceptors (there are a lot of Fc Receptors). FcRn is special in that it binds with high affinity at pH 6 to rescue IgG's and albumin (possibly different binding site) from endosomes/lysosomes and release at cell surface at pH 7.2 (and above).

Wikipedia entry: " Therefore, FcRn can bind IgG from the slightly acidic intestinal lumen and ensure efficient, unidirectional transport to the basolateral side where the pH is neutral to slightly basic.[5]"

Rather than merely "block" these FcR's I propose to "light them up".

For example, instead of just using 638 nm laser → Alexa Fluor 647 (or ATTO 647N etc), I propose adding an additional fluorophore-antibody (or antibodies) to "light up" these molecules. For example, an anti-FcRn might light up the entire recycling pathway of human enterocytes (and maybe Microfold M-cells?).

Purified Rat Anti-Mouse CD16/CD32 (Mouse BD Fc Block™) Clone 2.4G2 (RUO)
http://www.bdbiosciences.com/us/applications/research/b-cell-research/surface-markers/mouse/purified-rat-anti-mouse-cd16cd32-mouse-bd-fc-block-24g2/p/553142

Alternative Name: FcγRIII/FcγRII; Fcgr3/Fcgr2
The 2.4G2 antibody reacts specifically with a common nonpolymorphic epitope on the extracellular domains of the mouse Fc γ III and Fc γ II receptors. It has also been reported to bind the Fc γ I receptor (CD64) via its Fc domain. 2.4G2 mAb blocks non-antigen-specific binding of immunoglobulins to the Fc γ III and Fc γ II, and possibly Fc γ I, receptors *in vitro* and *in vivo* . CD16 and/or CD32 are expressed on natural killer cells, monocytes, macrophages, dendritic cells (at low levels), Kupffer cells, granulocytes, mast cells, B lymphocytes, immature thymocytes, and some activated mature T lymphocytes.
This antibody is routinely tested by flow cytometric analysis. Other applications were tested at BD Biosciences Pharmingen during antibody development only or reported in the literature.

Human BD Fc Block™

http://www.bdbiosciences.com/us/reagents/research/antibodies-buffers/immunology-reagents/anti-mouse-antibodies/cell-surface-antigens/human-bd-fc-block/p/564220
Brand BD Pharmingen™
Concentration 0.5 mg/ml

Fcγ Receptors belong to the immunoglobulin superfamily and are expressed at varying levels in multiple cell lineages including high expression in myeloid and B cells. The major functions of Fc receptors are protective functions of the immune system. There are multiple different types of Fc receptors reflecting a variety of different biological activities, which are modulated when they are aggregated by multivalent antigen-antibody complexes.

While normally serving important physiological roles in the immune system, Fc Receptors can also be the cause of nonspecific, false-positive antibody staining of cells. Human BD Fc Block™ is designed and formulated to block or significantly reduce potential non-specific antibody staining caused by receptors for IgG that may be encountered in various applications including the flow cytometric analysis of human cells. Moreover, it can increase the specificity of antibody labeling of extremely rare target cells such as antigen-specific B cells, fetal cells in maternal blood, hematopoietic progenitor cells, or disseminated epithelial tumor cells.

2012 review on FcRn

Monoclonal antibodies directed against human FcRn and their applications

Gregory J. Christianson,Victor Z. Sun,Shreeram Akilesh,Emanuele Pesavento,Gabriele Proetzel &**Derry C. Roopenian**

MAbs. 2012 Mar-Apr; 4(2): 208–216.
http://dx.doi.org/10.4161/mabs.4.2.19397

The MHC class I-like Fc receptor (FcRn) is an intracellular trafficking Fc receptor that is uniquely responsible for the extended serum half-life of antibodies of the IgG subclass and their ability to transport across cellular barriers. By performing these functions, FcRn affects numerous facets of antibody biology and pathobiology. Its critical role in controlling IgG pharmacokinetics has been leveraged for the design of therapeutic antibodies and related biologics. FcRn also traffics serum albumin and is responsible for the enhanced pharmacokinetic properties of albumin-conjugated therapeutics. The understanding of FcRn and its therapeutic applications has been limited by a paucity of reliable serological reagents against human FcRn. Here, we describe the properties of a new panel of highly specific monoclonal antibodies (mAbs) directed against human FcRn with diverse epitope specificities. We show that this antibody panel can be used to study the tissue expression pattern of human FcRn, to selectively block IgG and serum albumin binding to human FcRn in vitro and to inhibit FcRn function in vivo. This mAb panel provides a powerful resource for probing the biology of human FcRn and for the evaluation of therapeutic FcRn blockade strategies.

Key words: FcRn, IgG, monoclonal antibody, albumin, therapy

Introduction

Although originally referred to as the neonatal Fc receptor, FcRn influences IgG serum levels and tissue distribution at all stages of life.[1–5] This divergent member of the MHC class I family molecule is a heterodimer composed of an evolutionally distinct α-chain in complex with the β_2-microglobulin (β_2M) light chain that is common to most other class I molecules. FcRn is an intracellular trafficking, integral membrane Fc receptor for IgG. It resides primarily in the early acidic endosomes where it captures endocytosed IgG by binding to the Fc region only at a low pH.[6–8] FcRn rescues bound IgG from degradation in the lysosomal compartment and transports its ligand to the cell surface for release at neutral extracellular pH. Through this mechanism, FcRn is responsible for the long serum half-life of IgG.[9] FcRn transports IgG across the tight epithelial barriers of the endothelium and mucosa, thus influencing its bioavailability.[7,10] In antigen presenting cells, FcRn controls the presentation of antigens in IgG immune complexes to T cells[11,12] and IgG-Fc fusion protein vaccines.[13,14] FcRn also controls serum albumin homeostasis by an analogous trafficking mechanism as for IgG.[5,15,16] These properties have proven to be critical for maximizing the pharmacokinetics immunofluorescence and bioavailability of IgG monoclonal antibodies (mAbs) and IgG-Fc fusion proteins and albumin conjugated protein therapeutics.[5,17,18] While the biological and therapeutic importance of FcRn's varied and expanding functional attributes are increasingly documented, major gaps remain in the

understanding of the cell biology of FcRn, its tissue sites of action, and methods to exploit this biology for therapeutic purposes.

Of particular relevance is the need for reliable serological reagents for detection of human FcRn (hFcRn) and for probing its biology in normal and pathological states. This report describes the generation, characterization and applications of a part of mAbs with varied epitope specificities directed against human (h)FcRn. Our data demonstrate that the mAbs can readily detect hFcRn by flow cytometry and on tissue sections, which makes them valuable tools for defining the sites of hFcRn expression. Furthermore, the ability of certain mAbs to differentially block hIgG or human serum albumin binding supports a model of distinct binding sites for these ligands to hFcRn.[5,16] Finally, treatment of hFcRn transgenic mice with a hIgG blocking mAb provides a proof-of-principle that anti-hFcRn mAbs can be applied therapeutically to specifically control the serum persistence of human IgG in vivo.

https://en.wikipedia.org/wiki/Neonatal_Fc_receptor

Fc fragment of IgG, receptor, transporter, alpha

The neonatal Fc receptor (FcRn), also known as the Brambell receptor, is a protein that in humans is encoded by the FCGRT gene.[1][2]

The neonatal Fc receptor is an Fc receptor which is similar in structure to the MHC class I molecule and also associates with beta-2-microglobulin.[3] It was first discovered in rodents as a unique receptor capable of transporting IgG from mother's milk across the epithelium of newborn rodent's gut into the newborn's bloodstream.[4] Further studies revealed a similar receptor in humans, leading to the naming as a neonatal Fc receptor. In humans, however, it is found in the placenta to help facilitate transport of mother's IgG to the growing fetus and it has also been shown to play a role in monitoring IgG turnover.[3] Neonatal Fc receptor expression is up-regulated by the proinflammatory cytokine, TNF-α, and down-regulated by IFN-γ.[5]

Transcytosis and recycling of IgG[edit]

FcRn helps transport IgG from the gut to the bloodstream. FcRn-mediated transcytosis of IgG across epithelial cells is possible because FcRn binds IgG at acidic pH (<6.5) but not at neutral or higher pH. Therefore, FcRn can bind IgG from the slightly acidic intestinal lumen and ensure efficient, unidirectional transport to the basolateral side where the pH is neutral to slightly basic.[5]

This receptor also helps with the recovery of IgG in adults through the process of endocytosis in endothelial cells. FcRn in acidic endosomes bind to IgG internalized through pinocytosis, recycling it to the cell surface and releasing it at the basic pH of blood, and thereby preventing IgG from undergoing lysosomal degradation. This mechanism may provide an explanation for the greater half-life of IgG in the blood compared to that of other antibody isotypes (3 weeks).[6] It has been shown that conjugation of some drugs to the Fc domain of IgG significantly increases their half-life.[7]

5. *Kuo, Timothy T.; Baker, Kristi; Yoshida, Masaru; Qiao, Shuo-Wang; Aveson, Victoria G.; Lencer, Wayne I.; Blumberg, Richard S. (2010). "Neonatal Fc receptor: from immunity to therapeutics". Journal of Clinical Immunology.* ***30*** *(6): 777–789. doi:10.1007/s10875-010-9468-4.*

Kuo 2010:

In humans, FcRn is detected in both fetal and adult intestines and can mediate bidirectional transcytosis across the intestinal epithelium both in vitro and in vivo [28, 49–51]. FcRn in the intestine and other mucosal tissues therefore continues to play a significant role beyond the neonatal period, especially in immune surveillance and adaptive immunity. Using mice that were humanized to express human FcRn under the control of its endogenous promoter and β2m as transgenes within intestinal epithelial cells, FcRn at the intestinal epithelium was found to deliver IgG to

the luminal surface where it bound to a cognate antigen before returning the complex back to the lamina propria for processing and presentation by dendritic cells to CD4+ T cells [51].
In a murine model of intestinal infection using Citrobacter rodentium, which only infects intestinal epithelial cells and is dependent upon IgG for eradication, FcRn within the intestinal epithelium was shown to be essential in directing C. rodentium-associated antigens within the epithelium to regional lymph nodes for initiation of an adaptive immune response [52, 53]. In the absence of FcRn, C. rodentium elimination was slowed. These observations also help to explain the role of the high levels of antibacterial IgG that are observed within intestinal tissues and the lumen in inflammatory bowel disease (IBD). Using a murine model of colitis, antibacterial IgG was shown to drive colitis and was dependent upon FcRn expression in antigen presenting cells [54]. These studies thus show an important role for FcRn in mediating IgG-dependent anti-infective immunity and potentially autoimmunity in immune-mediated disorders such as IBD. Such observations have important implications for adaptive immunity in general.

"Light me up":
Rolling Stones Start Me Up https://www.youtube.com/watch?v=ZzlgJ-SfKYE
The Doors (1967) Light My Fire https://www.youtube.com/watch?v=deB_u-to-IE
Ingrid Michaelson (2016) Light Me Up https://www.youtube.com/watch?v=KsF86vz-xD4

Leica recommendations for coverglasses and mounting media

GM notes:

- See this doc (many sections) for more recommendations wrt optical clearing and mounting media.
- d = 0.61 * lambda / (*n sin alpha*) = d = 0.61 * lambda / NA … is for XY resolution. In practice equation can be simplified to d_{george} = 0.6 * 500 nm / NA = 300 nm / NA. For NA=1.4 this is $d_{george(NA\ 1.4)}$ = 214 nm. For XY pixel size, I recommend XYPixelSize = d / 3 so $XYPixelSize_{george(NA\ 1.4)}$ = 60 nm. For Z-step size, I recommend 3x XYPixelSize, which happens do by "d" (it's a small, small world). For 0.7NA, simply double these numbers.
- Leica mentions "Prolong/Prolong Gold" … current "state of the art" of this series for R.I. 1.515 immersion oil lens imaging (i.e. new Leica SP8 confocal) is **Prolong Diamond without DAPI**. Specifically, I now recommend adding the DAPI (or Hoechst or other DNA counterstain) to the Primary antibody (if 'direct labels') or secondary antibody (if 'indirect' label), then brief wash, then mount. I do note that the Prolong media series may shrink as it hardens AND needs 'to breathe' to allow a solvent to vaporize. *My thanks to Kelli Johnson (JHU G.I.) and Dr. Sarah Crowe (Leica) for discussions.*

Useful Equations and Numbers

Rayleigh Criterion

$$d = \frac{0.61\lambda}{n \sin \alpha}$$

Distance of two point sources at which the maximum of the second PSF overlaps with the first minimum of the first PSF. Details see page 7.

Full Width Half Maximum

$$\mathrm{FWHM}_{\mathrm{lateral}} = \frac{0.51\lambda}{n \sin \alpha}$$

Lateral FWHM of PSF for a fluorescent point object, with PH ≥ 1 AU.

STED Resolution

$$\Delta x \sim \frac{\lambda}{n \sin \alpha \sqrt{1 + \frac{I}{I_s}}}$$

Mountant	Manufacturer	RI
Fluoromount-G™	Southern Biotech Assoc. Inc.	1.40
ProLong®/ProLong® Gold	Molecular Probes	1.46 after curing
VECTASHIELD®	Vector Laboratories	1.44
VECTASHIELD® Hard+Set™	Vector Laboratories	1.46 after hardening
Mowiol®	Kuraray Europe GmbH	1.41–1.49
TDE/Water	–	1.33–1.52

Immersion Medium	RI
Air	1.000
Water	1.333
Immersion Type G at 23°C (Glycerol/Water)	1.450
Glycerol 100%	1.474
Immersion Type F (Oil)	1.518

How sensitive an objective is to varying coverglass thickness depends on the immersion medium and the numerical aperture (NA). For objectives designed for use with coverglass (0.17 mm), the following table can be referenced as a general rule.

Immersion Medium	With or Without Coverglass	Coverglass No 1.5 (0.16 – 0.19 mm)	Coverglass No 1.5H (0.17 mm ± 0.005 mm)
Air	NA <0.30	NA <0.70	NA >0.70
Water	NA <0.60	NA <0.90	NA >0.90
Immersion Type G	NA <0.80	NA <1.10	NA >1.10
Immersion Type F	NA <0.90	NA <1.30	NA >1.30

ThermoFisher AlexaFluorPlus … improved conjugation technology

- Real or marketing hype?
- Main new feature is improved conjugation … my guess is they have (i) a longer spacer between the antibody and the fluorophore, (ii) less fluorophore-fluorophore quenching (maybe better spatial separation for a given D.o.L. Degree of Labeling).
- "Highly cross adsorbed secondary antibodies" … I suggest thinking about "going direct", a'la most flow cytometry antibodies (and see "Resolution Blues" section).

GM note: if you want to really amplify your signal, optimize Tyramide signal amplification (TSA) (ThermoFisher offers TSA with entire Alexa Fluor product line). … see also "Click tyrosine".

www.thermofisher.com/AlexaFluorPlus
link goes to

https://www.thermofisher.com/us/en/home/life-science/antibodies/secondary-antibodies/fluorescent-secondary-antibodies/alexa-fluor-plus-secondary-antibodies.html

A new conjugate technology that provides higher signal to noise ratios for fluorescent imaging and western blotting
Invitrogen Alexa Fluor Plus secondary antibodies represent an advancement in fluorescent conjugate technology, designed to provide brighter signal, enhanced sensitivity, and minimal cross-reactivity in a variety of applications. Obtain superior images with Alexa Fluor Plus secondary antibodies. Make your low-abundance targets visible, spend less time optimizing, and make every one of your precious samples count. Alexa Fluor Plus secondary antibodies have up to 4.2 times higher signal to noise in IF/ICC imaging and up to 5.8 times higher signal to noise ratio in western fluorescent blotting while having lower cross-reactivity compared to leading Alexa Fluor secondary antibodies, providing you with higher sensitivity and better signal-to-noise ratios for your critical experiments.
The development of Alexa Fluor Plus secondary antibodies is supported by two decades of our industry-leading research and experience with fluorescent probe technologies. With over 30,000 publications citing their use in research, Alexa Fluor secondary antibodies are the trusted name in fluorescent applications.
Features of Alexa Fluor Plus secondary antibodies

- Higher signal-to-noise ratio, enabling detection of low-abundance targets

Alexa Fluor Plus: Up to 4.2 times higher to signal noise in IF/ICC imaging (AF488, 555, 647, 680, 800)

  - Up to 5.8 times higher signal to noise in western fluorescent blotting
- Enhanced sensitivity and greater range of linear detection

Compare the technology
See how Alexa Fluor Plus secondary antibody conjugates compare to original Alexa Fluor and classical dye secondary antibody conjugates.

	Classical fluorophore conjugates	**Alexa Fluor conjugates**	**Alexa Fluor Plus conjugates**
What are they?	Affordable, traditional dyes conjugated to secondary antibodies	Bright and stable industry-leading dyes conjugated to secondary antibodies	Innovative, proprietary dyes conjugated to highly cross-adsorbed secondary antibodies
Signal-to-noise ratio	Low	Medium	High
Photostability	Varying levels of photostability, depending on dye	Photostable	Photostable
Specificity	Various options available	Various options available	Highly specific, low cross-reactivity (highly cross-adsorbed)
Sensitivity and brightness	Lower sensitivity and brightness compared to leading Alexa Fluor conjugates	Widely recognized standard for brightness and sensitivity	Improved sensitivity and brightness over leading Alexa Fluor conjugates in IF/ICC imaging and fluorescent western blotting
Research areas	Designed for detection of high-abundance targets in	Designed for detection of medium- to high-	Designed for detection of low-abundance targets in research

	research areas with easy-to-obtain samples	abundance targets in most research areas	areas with hard-to-obtain samples, e.g., neuroscience
Range of linear detection	Low	Medium	High

New packaging helps save time and space

- **Storage made easier**—the new vials have flagless labels. No more struggling to wrap the flag around the vial to fit it into racks or centrifuges.
- **Identifying made easier**—vials have colored caps corresponding to the Alexa Fluor Plus dye of the secondary antibody conjugate. If you are looking for an Alexa Fluor Plus 488 antibody, just look for the green cap.
- **Easier to see how much antibody you have left**—vials are clear so you can easily see the volume remaining. No need to pipette from an opaque or solid-colored vial just to estimate how much antibody remains.

https://www.thermofisher.com/us/en/home/life-science/antibodies/secondary-antibodies/fluorescent-secondary-antibodies/alexa-fluor-plus-secondary-antibodies.html

All 10 initial Alexa Fluor Plus products are 1 mg for $269.

Catalog #	Name
A32723	Goat anti-Mouse IgG (H+L) Highly Cross-Adsorbed Secondary Antibody, Alexa Fluor Plus 488
A32727	Goat anti-Mouse IgG (H+L) Highly Cross-Adsorbed Secondary Antibody, Alexa Fluor Plus 555
A32728	Goat anti-Mouse IgG (H+L) Highly Cross-Adsorbed Secondary Antibody, Alexa Fluor Plus 647
A32729	Goat anti-Mouse IgG (H+L) Highly Cross-Adsorbed Secondary Antibody, Alexa Fluor Plus 680
A32730	Goat anti-Mouse IgG (H+L) Highly Cross-Adsorbed Secondary Antibody, Alexa Fluor Plus 800
A32731	Goat anti-Rabbit IgG (H+L) Highly Cross-Adsorbed Secondary Antibody, Alexa Fluor Plus 488
A32732	Goat anti-Rabbit IgG (H+L) Highly Cross-Adsorbed Secondary Antibody, Alexa Fluor Plus 555
A32733	Goat anti-Rabbit IgG (H+L) Highly Cross-Adsorbed Secondary Antibody, Alexa Fluor Plus 647
A32734	Goat anti-Rabbit IgG (H+L) Highly Cross-Adsorbed Secondary Antibody, Alexa Fluor Plus 680
A32735	Goat anti-Rabbit IgG (H+L) Highly Cross-Adsorbed Secondary Antibody, Alexa Fluor Plus 800

GM note:

- I expect the AF+ 488, 555, 647, 680 to be usable together on the new Leica SP8 confocal microscope (the emission spectral range is 380-800 nm, since the AF800 and AF+800 emission spectra >800nm, too long for our SP8).
- First graph: the four (probably) usable together AF+'s.
- Second graph: a potentially more useful set, replacing AF+680 with conventional AF700, and adding more AF's and other ThermoFisher fluorophores compatible with our SP8's four laser lines (405, 488, 552, 638

nm). Note that I do not bother with a DNA counterstain. Note in graph: BD's Brilliant Violet's, Brilliant Blues or NIRvana Sciences narrow emission spectra fluorophores.

Graph 1: 4plex from 3 (preferably sequential) laser lines:

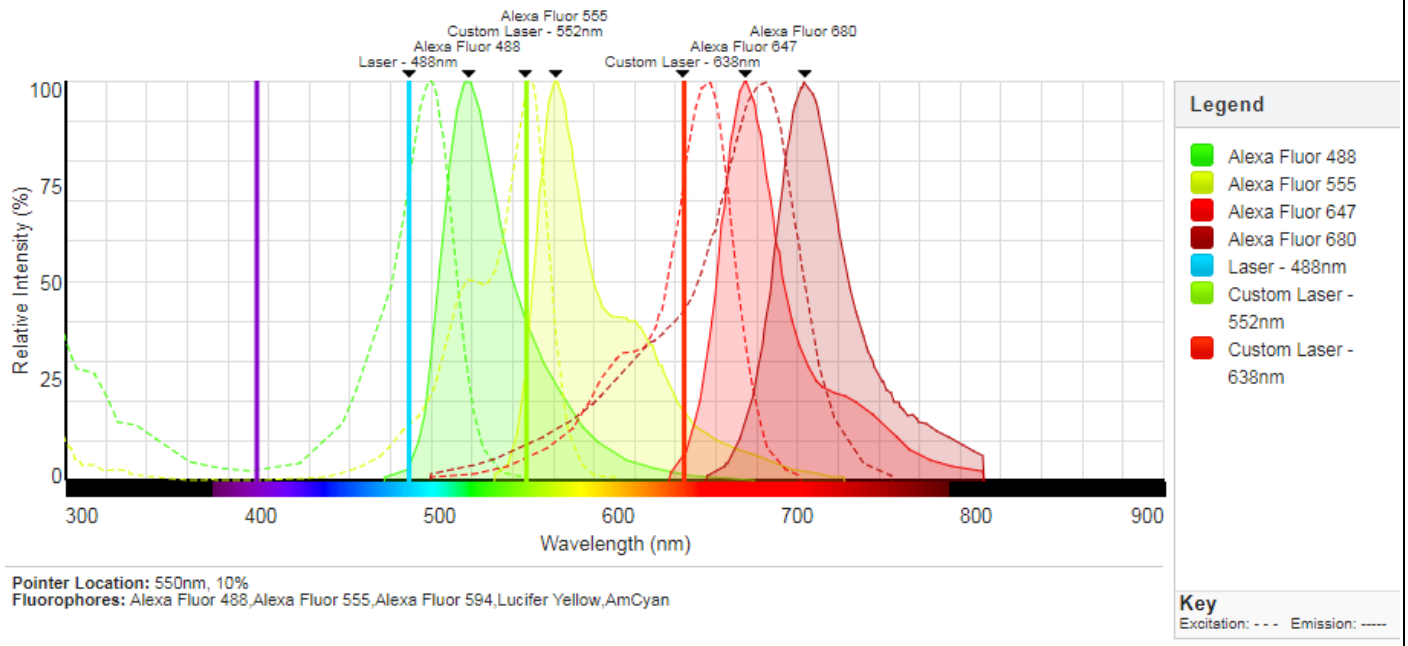

Graph 2: GM 11plex from four sequential laser lines (I am not claiming this is the perfect 11plex, these only include ThermoFisher fluorophores whereas BD Biosciences Brilliant Violet's and Brilliant Blues would enable higher plex):

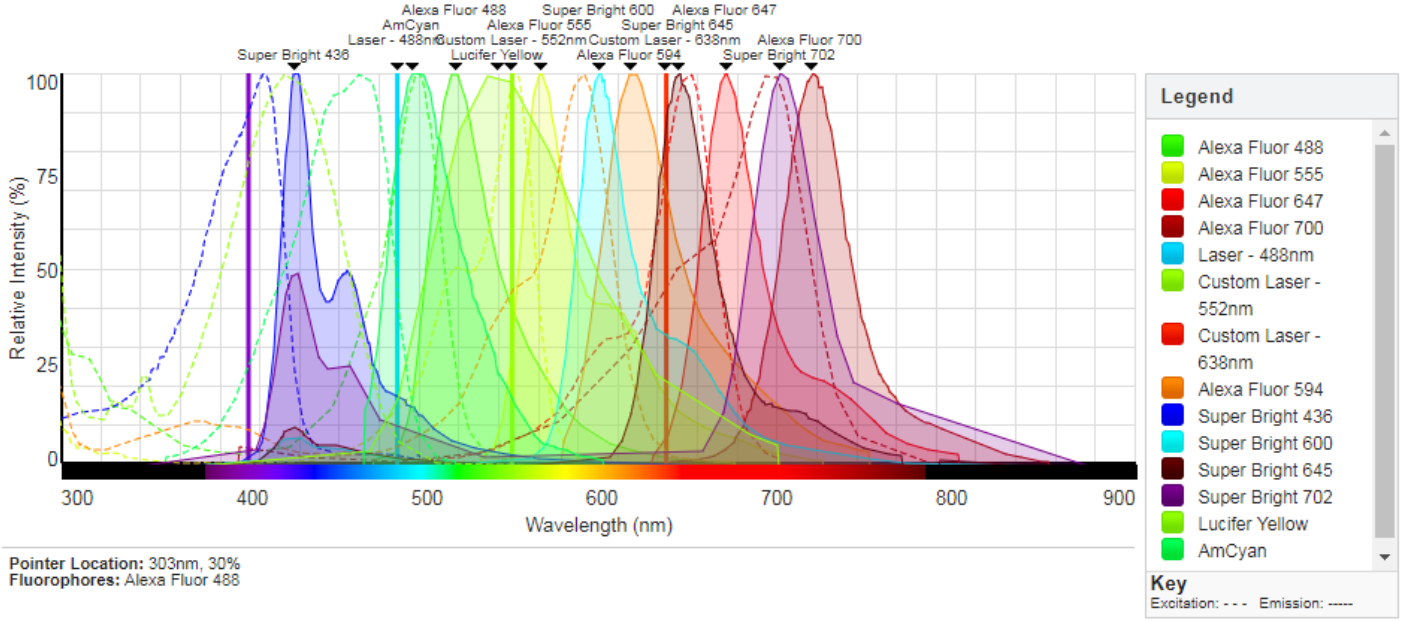

Addgene guest blog by Doug Richardson: which fluorescence microscope technique is best?

20171010

http://blog.addgene.org/fluorescence-microscopy-techniques-which-is-best-for-me

First paragraphs:

post was contributed by Doug Richardson, Director of the Harvard Center for Biological Imaging and a Lecturer on Molecular and Cellular Biology at Harvard University.

No matter whether you are a sports photographer at the Super Bowl, a medical technologist taking an x-ray, or a biologist imaging the smallest structures of life; the key to a great image is contrast. The human visual system relies primarily on contrast to identify individual objects and perceive the world around us. Without contrast, objects simply vanish into noise.

Due to its unrivaled contrast, fluorescence imaging has emerged as the dominant light microscopy contrast technique in modern biology (1). When performed correctly, fluorescence microscopy provides a high contrast image in which a bright signal overlays a perfectly black background. In addition to this, the use of multiple fluorophores can add a second layer of contrast, color contrast, to an image and thereby provide molecular or structural specificity to the viewer. Finally, modern microscope designs may further exploit the unique characteristics of fluorophores to block out of focus fluorescence from reaching a detector or restricting fluorescence to specific excitation volumes to enhance spatial contrast (i.e. optical sectioning (2) or super-resolution (3).

GM Idea: optimal high resolution fluorescence microscopy with R.I. matched specimen, thin coverglass, immersion oil – all R.I. 1.525 – then quantitative deconvolution

Why R.I. 1.525? The Zeiss 170 um coverglasses made by Marienfeld are 1.525 versus standard glass is assumed to be 1.515. Hopefully these are also (or will be) available in high precision 120 um (+/- 5 um) thickness *since this would enable 50 um deeper specimen imaging*.

The coverglass is normally a "two plane" perpendicular to the optical axis" pair of surfaces, and light rays are expected to enter and exit at symmetric angles, if R.I. matched on both sides. In reality, coverglasses are not necessarily either:

- Flat (zero terrain)
- Perpendicular to the optical axis (that is, can be tilted … especially by user error but sometimes bad design of specimen or microscope holder).

➔ You can examine and quantify both flatness and perpendiularity by "reflection contrast microscopy" (reviewed by Ploem & Prins 2017 RMS InFocus 47: 38-56, please see GM for PDF) – see my section(s) on Interference Reflection Contrast Microscopy (IRM, RICM). Perfect R.I. matching would (in theory) cause the interface to disappear (no reflection!). In reality, the dynamic range of research microscopes would still see stuff. Might be useful to put a very sparse distribution of scattering or fluorescence objects (ex. 10 nm colloidal gold or 20 nm Fluospheres) on each surface to facilitate finding the coverglass surfaces).

Note: Perfect R.I. matching is most critical for high N.A. objective lenses (usually considered 1.2 – 1.49 NA), but would likely benefit "moderate" NA (i.e. 0.7 – 1.15 N.A.) and may even benefit lower N.A.

The ultimate "clear sandwich" would be ALL R.I. 1.525:

- Cleared specimen in mounting medium
- Thin coverglass (that is, 120 +/- 5 um would be even better than 170 +/- 5 um)
- Immersion oil

Imaging would also benefit from R.I. matching live specimens with LOW R.I. coverglass, such as R.I. 1.405:

- Iodixanol in live cell culture media – see Boothe 2017 eLIFE, section below.
- R.I. 1.405 coverglass
- Olympus silicone oil and Silicone Oil objective lens (several available).

More optical clearing: Chan, Kaufman, Tanaka (Deisseroth, Uhlen), Yu, Orlich 2017 papers

Note: Sarah Crowe, Leica, suggests for stabilizing specimen:

- 80% glycerol
- 1 or 2% low melting point temperature agarose (102% by weight)
- PBS or other buffer

And then to solidify faster, put in refrigerator.

See also other optical clearing sections (Ce3D and more).

Both GM and Sarah Crowe recommend "DAPI first", then wash, then "DAPI Free" mounting medium. See also GM's section below, "Resolution Blues" for ditching DAPI in favor of BUV's, BV's, SB's (can use a NIR DNA counterstain if you need nucleus, but how about immunofluorescence of nuclear pore complex, nuclear lamins, telomere repeats, histones, nucleoli, smFISH … I suggest NIRvana Sciences narrow emission spectra fluorophores with antibodies and/or FISH probe sets).

Chen L, Li G, Li Y, Li Y, Zhu H, Tang L, French P, McGinty J, Ruan S 2017 UbasM: An effective balanced optical clearing method for intact biomedical imaging. Sci Rep 7: 12218. doi: 10.1038/s41598-017-12484-3. PMID: 28939860 UbasM = Urea-Based Amino-Sugar Mixture.

Garvalov BK, Erturk A 2017 Seeing whole-tumour heterogeneity. Nat Biomed Eng 1: 772-774. https://www.nature.com/articles/s41551-017-0150-5 News&views for Tanaka et al 2017 "DIPCO".

Kaufman JA, Castro MJ, Sandoval-Skeet N, Al-Nakkash L 2017 Optical clearing of small intestine for three-dimensional visualization of cellular proliferation within crypts. J Anat. 2017 Oct 1. doi: 10.1111/joa.12711. [Epub ahead of print] PMID: 28967147 Triton X-100 (low concentration), DMSO, Delipidization.

Tanaka N ... Deisseroth K, Uhlen P 2017 Whole-tissue biopsy phenotyping of three-dimensional tumours reveals patterns of cancer heterogeneity. Nat Biomed Eng 1: 796–806. https://www.nature.com/articles/s41551-017-0139-0 FFPE tissue blocks -> optical clearing (~14 days) -> diagnosis in 3D. DIPCO = diagnosing immunolabelled paraffin-embedded cleared organs) pipeline.

Orlich M, Kiefer F 2017 A qualitative comparison of ten tissue clearing techniques. Histol Histopathol. 2017 May 12:11903. doi: 10.14670/HH-11-903. [Epub ahead of print] PMID: 28497438

Yu T, Qi Y, Gong H, Luo Q, Zhu D 2017 Optical clearing for multi-scale biological tissues. J Biophotonics. 2017 Oct 12. doi: 10.1002/jbio.201700187. [Epub ahead of print] **Review**. PMID: 29024450

Notes:

- see also Li, Gerner, Germain 2017 "Ce3D" and other optical clearing and refractive index matching sections herein.

- The pasted tables (Chan 2017; Yu 2017) are to draw your attention to the information available. Best to read the journal articles, not the tiny text below.

Table: Chan et al 2017 Sci Rep.

Method (Ref)	Agents		Clearing Performance						
	Main (Detergent)	Clearing Mode (steps)	Capability	Efficiency		FP preservation	DiI compatibility	Handling	Incubation Temp.
				Slice (~mm)	Hemisphere (~cm)				
Organic solvent-based methods									
BABB (ref.[24])	Benzyl alcohol Benzyl Benzoate	Replacing water with organic solvents (5–6 steps)	**Very Strong**	**Slow > 4.5 hr**	**Very Fast 3–7 d**	**Very poor**	**Poor**	**Needs Care**	**RT**
3DISCO (ref.[25])	Benzyl Ether	Replacing water with organic solvents (6 steps)	**Very Strong**	**Slow > 3.5 hr**	**Very Fast 3–7 d**	**Poor**	**Poor**	**Needs Care**	**RT**
iDISCO (ref.[40])	Benzyl Ether	Replacing water with organic solvents (6 steps)	Very Strong	Slow >3.5 hrr	Very Fast 3–7 d	Poor	Poor	Needs Care	RT
uDISCO (ref.[30])	BABB(4): DBE(1)	Replacing water with organic solvents (8–9 steps)	**Very Strong**	**Very Slow > 15 hr**	**Very Fast 3–7 d**	**Medium**	**Poor**	**Needs Care**	**> 26 °C**
Aqueous solution-based methods									
Scale (ref.[31])	Urea Glycerol (0.1%Triton X-100)	Water-based chemical agents (1–2 steps)	**Medium**	**Very Slow > 15 hr**	**Very Slow months**	**Excellent**	**N.T.**	**Very Easy**	**RT**
SeeDB (ref.[34])	Fructose	Sugar solutions (6 steps)	**Weak**	**Slow > 2 hr**	—	**Excellent**	**Good**	**Easy (viscous)**	**37 °C**
CUBIC (ref.[32])	Urea Amino-alcohol (Triton X-100 15%, Reagent-1 0.1%, Reagent-2)	Detergent-based chemical agents (3 steps)	**Strong**	**Fast 1–2 hr**	**Fast 7–12 d**	**Excellent**	**Poor**	**Very Easy**	**RT (or 37 °C)**
ScaleS (ref.[33])	Urea Sorbitol (0.2% Triton X-100)	Water-based chemical agents (5 steps)	**Strong**	**Medium > 2 hr**	**Medium 2–4 weeks**	**Excellent**	**Good (Poor for SQ(5))**	**Very Easy**	**37 °C**
UbasM	Urea Amino-sugar (0.2% Triton X-100)	Water-based chemical agents (3 steps)	**Strong**	**Fast 1–2 hr**	**Fast 7–12 d**	**Excellent**	**Good**	**Very Easy**	**RT (or 30 °C)**
Hydrogel embedding methods									
CLARITY (ref.[37])	SDS Boric acid (SDS 4%)	Hydrogel embedding + removal of lipids with electrophoresis	Very Strong	- N.T.	Medium 2–4 weeks	N.T.	N.T.	Complicated Needs device Careful	37 °C
PACT (ref.[38])	SDS Histodenz (SDS 8%)	Hydrogel embedding + removal of lipids with 8% SDS	Very Strong	- N.T.	Medium 2–4 weeks	Medium	Poor	Careful	37 °C

see also:
* Li, Germain, Gerner 2017 PNAS "Ce3D"
* Kaufman 2017 J Anat, doi: 10.1111/joa.12711
* FocusClear

Table 1. Comparison of UbasM properties with other optical clearing methods. The table summarizes general properties and performance indicators for UbasM and other major published clearing methods. These methods are categorized mainly into aqueous solution-/organic solvent-based and hydrogel embedding methods. To evaluate clearing efficiency, mm-thick adult mouse brain slice and 4-week old mouse hemisphere were used as small (~mm) and large samples (~cm). SeeDB was only demonstrated to embryos and young mice and the resulting sample transparency is insufficient for one-photon imaging of the adult organ. The complex uDISCO processing (i.e. 8–9 steps) required at least 15 hours[30]. Conclusions were evaluated from experiments performed in this paper (indicated by bold text) and also based on published information. (RT – room temperature; N.T. – not tested)

Table: Yu 2017 J Biophotonics

Table 1. Comparison of *in vitro* tissue optical clearing methods.

Method	Time to clear	Species(age)	Fluorescent labels		Molecular phenotyping		Final RI	Morphology alternation	Complexity
			FPs	Lipophilic dyes	Immunostaining	FISH			
Small samples/ neonatal samples/embryos									
FocusClear	hours-days	Insect	yes	yes	yes	N.T.	1.45	Shrinkage	Incubation
Sucrose	1 day	Rat(A), Mouse	yes	no	yes	N.T.	1.44	Shrinkage	Incubation
SeeDB	days	Mouse(E,A)	yes	yes	yes	N.T.	1.50	no	Incubation
SeeDB2	days	Insect, Mouse(E,N,A)	yes	yes	yes	N.T.	1.52	no	Incubation
FRUIT	days	Rabbit(A), Mouse(A)	yes	yes	N.T.	N.T.	1.48	Slight expansion	Incubation
ScaleS	days	Human(O), Mouse(A,O)	yes	yes	yes	N.T.	1.44	Transient shrinkage /expansion	Incubation
Clear$^{T/T2}$	hours-days	Mouse(E,A)	yes	yes	yes	N.T.	1.44	no	Incubation
TDE	days-weeks	Human(C), Mouse(A)	yes	no	yes	N.T.	1.42	no	Incubation
DMSO/D-sorbitol	days	Mouse	yes	no	N.T.	N.T.	1.47	no	Incubation
RapiClear	days-weeks	Mouse, Rat, Insect, Zebrafish Biomaterial, Plant	yes	N.T.	N.T.	N.T.	1.47-1.55	no	Incubation
Intact & adult samples									
BABB	days	Insect, Mouse(E,A)	yes	no	yes	N.T.	1.55	Shrinkage	Incubation
3DISCO	hours-days	Mouse(E,A), Human(E)	yes	no	yes	N.T.	1.56	Shrinkage	Incubation
iDISCO	hours-days	Mouse(E,A)	yes	no	yes	N.T.	1.56	Shrinkage	Incubation
iDISCO+	hours-days	Mouse(A)	yes	no	yes	N.T.	1.56	Shrinkage	Incubation
FluoClearBABB	hours-days	Mouse(A)	yes	no	N.T.	N.T.	1.56	Shrinkage	Incubation
Ethanol-ECi	Hours-days	Mouse(A)	yes	no	yes	N.T.	1.56	Shrinkage	Incubation
CLARITY	days	Human(C) Mouse(A), Zebrafish(A)	yes	no	yes	yes	1.45	Transient expansion	Embedding, customed set-up
PACT	days-weeks	Human Rat(A), Mouse(A)	yes	no	yes	yes	1.42-1.48	Slight expansion	Embedding, Incubation
SCM	days-weeks	Mouse(A), Human	yes	no	yes	N.T.	1.46	expansion	Embedding, Incubation
FASTClear	weeks	Human	no	no	yes	N.T.	1.42/1.56	no or shrinkage	Incubation
Stochastic electrotransport	days	Mouse(A)	yes	no	yes	N.T.	1.46	Transient expansion	Embedding, customed set-up

SWITCH	days	Human, Marmoset Rat(A), Mouse(A)	no	yes	yes	yes	1.47	Slight expansion	Embedding
EDC-CLARITY	days	Human(A) Mouse(A)	yes	no	yes	yes	1.45	Transient expansion	Embedding, customed set-up
Bone CLARITY	weeks	Mouse(A)	yes	no	yes	N.T.	1.47	no	Embedding, Incubation
PEA-CLARITY	weeks	Plant	yes	no	yes	N.T.	1.33/1.45/1.46	no	Embedding, Incubation
Scale	weeks-months	Mouse(E,A)	yes	N.T.	yes	N.T.	1.38	Expansion	Incubation
CUBIC	days	Marmoset(N) Mouse(N,Y,A)	yes	no	yes	N.T.	1.45	Transient expansion	Incubation
ClearSee	days-weeks	Plant	yes	yes	N.T.	N.T.	1.41	no	Incubation
Whole-body									
PARS	days-weeks	Rat# (A), Mouse# (A)	yes	no	yes	yes	1.42-1.48	no	Perfusion, embedding, customed set-up
CB-Perfusion	days-weeks	Mouse# (N,A)	yes	no	yes	N.T.	1.45	Transient expansion	Perfusion, Incubation
CUBIC-cancer	days-weeks	Mouse#(A)	yes	no	yes	N.T.	1.44-1.52	Transient expansion	Perfusion, Incubation
ACT-PRESTO	hours-days	Human, Rabbit(A) Rat(E,A), Mouse#(N,A)+	yes	no	yes	yes	1.43-1.48	Expansion	Embedding, customed set-up
uDISCO	hours-days	Rat#(A), Mouse#(A,O), Human (O)	yes	no	yes	N.T.	1.56	Shrinkage	Incubation

***Abbreviations: E, embryo; N, neonatal; A, adult; O, old; C, child. FPs, fluorescent proteins; RI, refractive index; FISH, fluorescent in-situ hybridization; +zebrafish, xenopus,chicken, octopus; Embedding, hydrogel embedding; #Applicable for whole-body clearing.**

***Glossary of some tissue clearing agent acronyms:**

BABB: Benzyl alcohol and benzyl-benzoate

3DISCO: Three-dimensional imaging of solvent-cleared organs

iDISCO: Immunolabeling-enabled 3D imaging of solvent-cleared organs

uDISCO: Ultimate three-dimensional imaging of solvent-cleared organs

Ethanol-ECi: Ethanol-ethyl cinnamate

SeeDB: See Deep Brain

TDE: 2,2′-thiodiethanol

FRUIT: A method based on fructose and urea

CLARITY: Clear Lipid-exchanged Acrylamide-hybridized Rigid Imaging/ Immunostaining/ In situ hybridization-compatible Tissue-hYdrogel

PACT: PAssive CLARITY Technique

PARS: Perfusion-assisted Agent Release in Situ

EDC-CLARITY: 1-Ethyl-3-3-dimethyl-aminopropyl carbodiimide-CLARITY

PEA-CLARITY: Plant Enzyme Assisted (PEA)-CLARITY

Bone CLARITY: A bone tissue clearing method based on CLARITY

SCM: Simplified CLARITY method

ACT-PRESTO: Active Clarity Technique-Pressure Related Efficient and Stable Transfer of macromolecules into Organs

SWITCH: System-Wide control of Interaction Time and kinetics of CHemicals

FASTClear: Free of Acrylamide SDS-based Tissue Clearing

Scale: an aqueous reagent that renders biological samples transparent

ScaleS: a sorbitol-based Scale

CUBIC: Clear Unobstructed Brain Imaging Cocktails & computational analysis

CB-Perfusion: CUBIC based on transcardial perfusion

Table: Orlich 2017 (see article for additional table on volume changes per method and organ)

	Murray's clear	3DISCO	Sca*l*e	SeeDB	FRUIT	CUBIC	CB-Perfusion	Clear^{T2}	CLARITY	PACT
E10.5	++++	+++	++	-	++	+++	/	+	/	+++
E12.5	++++	+++	++	-	++	+++	/	+	++	+++
E15.5	++++	++	-	-	+	++	/	-	+	+++
Brain	++	++++	-	-	+	++	+++	-	+++	+++
Lung	++++	++++	-	-	+	++	+++	-	++	+++
Heart	++++	++++	-	-	+	++	+++	-	++	++
Kidney	++++	++++	-	-	+	++	+++	-	++	+++
Muscle(thigh)	++++	++++	-	+	+	++	+++	-	++	+++
Fluorescence preservation	-	-	+	/	/	++	++	/	/	+
Size change	-1	-3	+2	-1	+1	-1/+1	-1/+1	+1	+2	+1
Sample characteristic	stiff	stiff	fragile	stiff	stiff	spongy	spongy	stiff	spongy	spongy
Viscosity of fluids	+	+	+	++++	+++	++	++	+	++	++
Duration	1 d	1d	7 d	3d	3d	14d	10d	1d	10d	14d
Handling	++^{T}	++^{T}	+	+	+	+	++^{PTG}	+	+++^{PTG}	++^{TG}

Refractive Index Matching Media for R.I. 1.518 Oil Immersion Objective Lenses and Fixed Specimens (including optical clearing)

Notes:

- Sarah Crowe, Leica, now (2017) prefers Prolong Diamond over Prolong Gold … partly because P.D. reaches R.I. ~1.47 (but still not close to 1.518). Please note that both Prolong's may shrink the specimen during solidification. GM recommends "DAPI free" Prolong, that is, do the DAPI as a step after the final antibody wash.
- Key is – for any high resolution objective lens that you need best image quality – is to match the refractive index of the immersion medium (ex. immersion oil) and the mounting medium (ex. CFM-3 or Prolong Gold or Prolong Diamond).
- **pH 6.5 is not optimal for many fluorophores or fluorescent proteins.** For example, fluorescein is dim at 6.5 (you should not be using fluorescein in 2017+ anyway). The Fouquet table below claims TDE is pH 6.5 … I suggest TDE could be diluted (from 100% to ~97%) with borate buffer pH 8.0 (or higher) or whatever is most appropriate.
- Live specimens: see also Iodixanol (R.I. tunable to 1.4 addition to aqueous media) for live specimens (Boothe 2017, Fadero & Maddox 2017) with Olympus R.I. 1.4 Silicone Oil objective lenses (we host an Olympus Imaging Center – John Gibas can arrange for an Silicone Oil immersion lens for evaluation … budgeting to

purchase one for the image core may be challenging). Our Olympus FV1000MP multiphoton excitation fluorescence microscope has a 25x/1.05NA water (saline dipping) immersion lens, designed for R.I. 1.33 (saline). My guess is Iodixanol could be added to your "saline" media, and be compatible with both tissues and live mouse body parts – your time and money to evaluate performance (I am happy to help).

Fouquet C, Gilles JF, Heck N, Dos Santos M, Schwartzmann R, Cannaya V, Morel MP, Davidson RS, Trembleau A, Bolte S. Improving axial resolution in confocal microscopy with new high refractive index mounting media. PLoS One. 2015 Mar 30;10(3):e0121096. doi: 10.1371/journal.pone.0121096. PMID: 2582278

Resolution, high signal intensity and elevated signal to noise ratio (SNR) are key issues for biologists who aim at studying the localisation of biological structures at the cellular and subcellular levels using confocal microscopy. The resolution required to separate sub-cellular biological structures is often near to the resolving power of the microscope. When optimally used, confocal microscopes may reach resolutions of 180 nm laterally and 500 nm axially, however, axial resolution in depth is often impaired by spherical aberration that may occur due to **refractive** index mismatches. Spherical aberration results in broadening of the point-spread function (PSF), a decrease in peak signal intensity when imaging in depth and a focal shift that leads to the distortion of the image along the z-axis and thus in a scaling error. In this study, we use the novel mounting medium CFM3 (Citifluor Ltd., UK) with a **refractive** index of 1.518 to minimize the effects of spherical aberration. This mounting medium is compatible with most common fluorochromes and fluorescent proteins. We compare its performance with established mounting media, harbouring **refractive** indices below 1.500, by estimating lateral and axial resolution with sub-resolution fluorescent beads. We show furthermore that the use of the high **refractive** index media renders the tissue transparent and improves considerably the axial resolution and imaging depth in immuno-labelled or fluorescent protein labelled fixed mouse brain tissue. We thus propose to use those novel high **refractive** index mounting media, whenever optimal axial resolution is required.

Table 1. Comparison of mounting media.

Mounting medium	Manufacturer	Refractive index	pH	Base compound	Fluorophore compatibility*
2,2'-Thiodiethanol	Sigma-Aldrich, France	1.518	6.5	2,2'-Thiodiethanol	most organic dyes and fluorochromes, RFP, however causes strong GFP quenching (8)
CFM-1	Citifluor Ltd., UK	1.515	7.5	glycerol-PBS-based	nd
CFM-3	Citifluor Ltd., UK	1.518	6.5	glycerol-based	DAPI, Hoechst, Alexa and Cyanine dyes, Venus, GFP#, Tomato, mCherry
Vectashield H-1000	Vector Laboratories Ltd., UK	1.454	nd	glycerol-based	fluorescein, rhodamine, Texas Red, AMCA, DyLight fluorescent dyes and other fluorescent reagents such as Cy3, Cy5, Alexa Fluor 488, and Alexa Fluor 594. GFP, RFP, YFP
Prolong Gold	ProLong Gold	1.390–1.460 depending on curing time	nd	glycerol-based	most organic dyes, however, fluorescent proteins less well preserved
Fluoromount-G	Southern Biotechnology	1.400	7.4	acrylate-PBS	most organic dyes
Mowiol Tris MWL 4–88	Citifluor Ltd., UK	1.410–1.490	9.5	polyvinyl alcohol	most organic dyes

*fluorochrome compatibility was experimentally evaluated only for CFM3, data for other mounting media were taken out of the manufacturers datasheets.
GFP shows enhanced photobleaching in CFM3

Below R.I.
Mowiol ~1.41
VectaShield ~1.45
CFM-3 1.518

Z-series 100 um, oil immersion objective lens. R.I. matching of oil immersion medium and mounting medium for best results

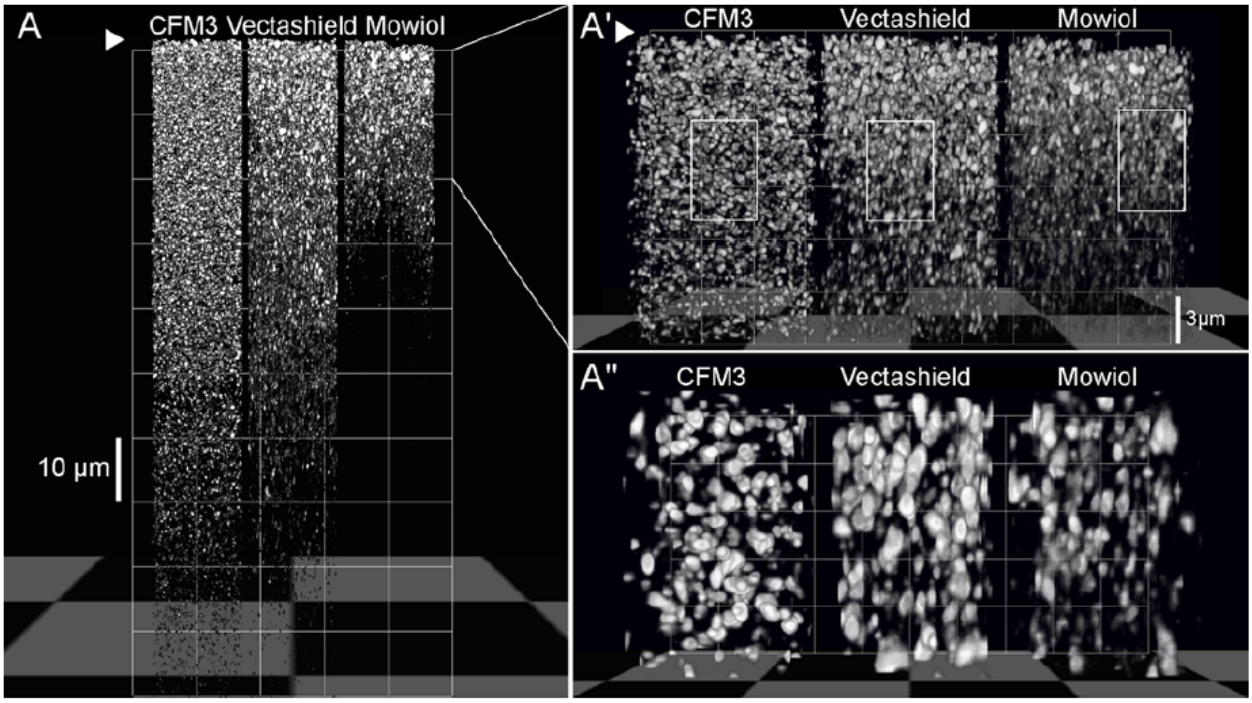

Fig 5. Depth penetration and resolution improvement in VGLUT1-Venus mouse brain slices. 100 µm vibratome sections of brain of adult transgenic mice (VGLUT1^{Venus}) were mounted in CFM3, Vectashield or Mowiol and imaged using the 514 nm laser line. Imaging was carried out using an optimal z-section. 3D-reconstructions of the entire z-stack (A) with the coverslip position at the top (arrowhead) and the first 20 µm (A') of VGLUT1^{Venus}-labelled synaptic boutons were carried out to demonstrate depth penetration in the different media. (A") is a magnified view of the insert in (B) showing synaptic boutons in a depth of 5–15 µm. Note that the boutons mounted in Vectashield appear elongated in comparison to CFM3 mounted sections. Scalebars are 10 and 3 µm.

PAINT Molecules: 5plex sequential immunofluorescence single molecules RTK oncosurfaceome (can go >>5 plex)

Please note that the scale bar in the Werbin et al Fig 3e below is 500 nm (*nano*meters!) – with colored dots representing *single* molecules (color legend at top, red = EGFR) and 'painted polygons' representing clusters of various molecules *on the plasma membrane of part of one cell*.

Werbin JL, Avendaño MS, Becker V, Jungmann R, Yin P, Danuser G, Sorger PK. Multiplexed Exchange-PAINT imaging reveals ligand-dependent EGFR and Met interactions in the plasma membrane. Sci Rep. 2017 Sep 22;7(1):12150. doi: 10.1038/s41598-017-12257-y. PMID: 28939861

Signal transduction by receptor tyrosine kinases (RTKs) involves complex ligand- and time-dependent changes in conformation and modification state. High resolution structures are available for individual receptors dimers, but less is known about receptor clusters that form in plasma membranes composed of many different RTKs with the potential to interact. We report the use of multiplexed super-resolution imaging (Exchange-PAINT) followed by mean-shift clustering and random forest analysis to measure the precise distributions of five receptor tyrosine kinases (RTKs) from the ErbB, IGF-1R and Met families in breast cancer cells. We find that these receptors are intermixed nonhomogenously on the plasma membrane. Stimulation by EGF does not appear to induce a change in the density of EGFR in local clusters but instead results in formation of EGFR-Met and EGFR-ErbB3 associations; non-canonical EGFR-Met interactions are implicated in resistance to anti-cancer drugs but have not been previously detected in drug-naïve cells.

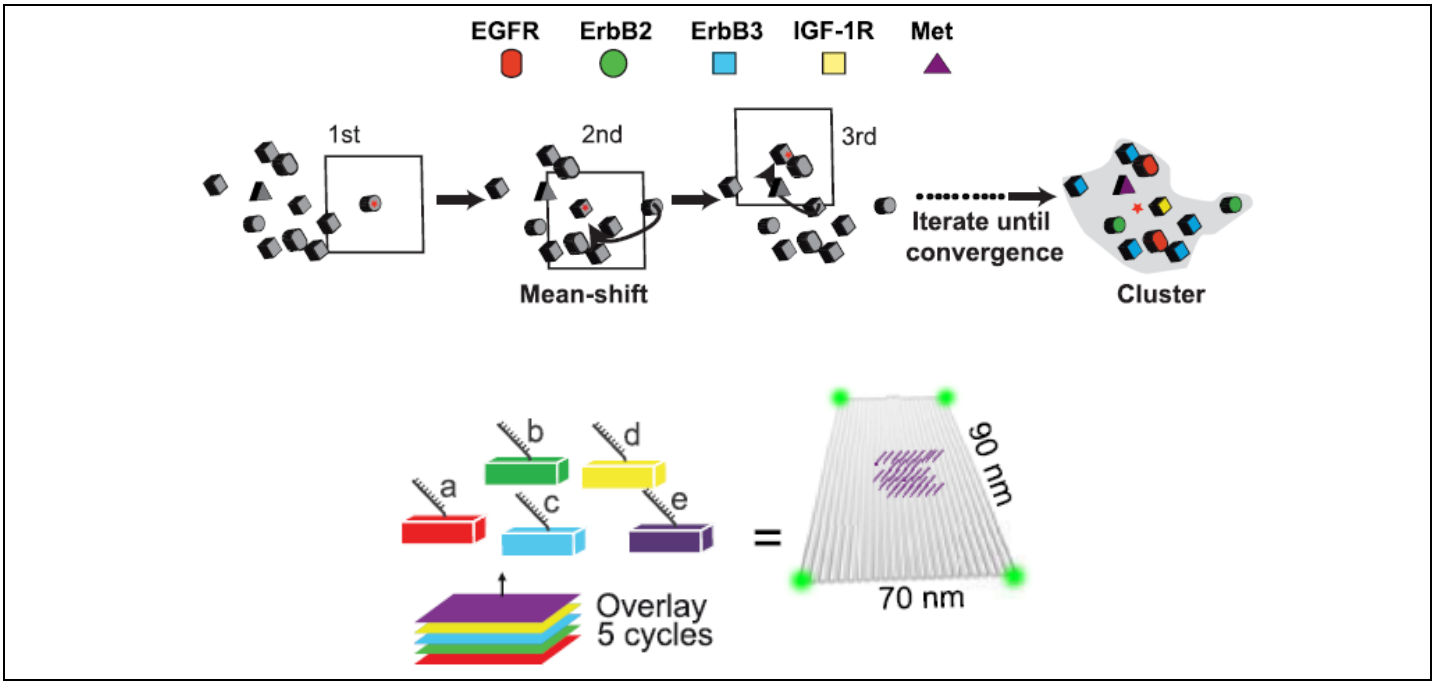
EGFR
ErbB2
ErbB3
IGF-1R
Met
1st
2nd
3rd
Iterate until convergence
Mean-shift
Cluster
a
b
c
d
e
Overlay 5 cycles
=
90 nm
70 nm

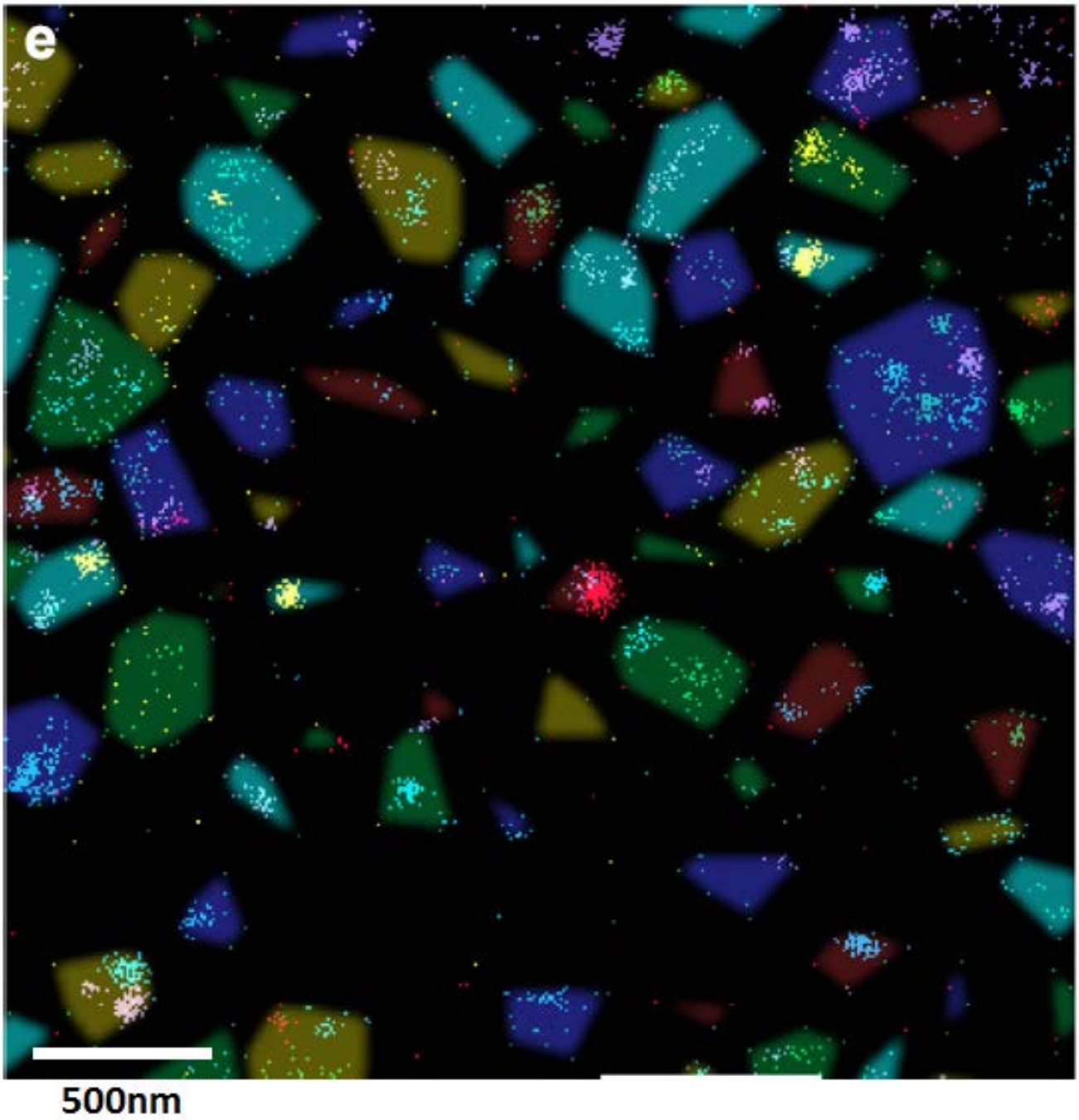

Figure 3. Computational clustering of receptors.
(**a**) A schematic of the mean-shift clustering algorithm used to group localizations detected by Exchange-PAINT into clusters based on local density.
(**b**) *In vitro* clustering validation. Five types of DNA origami structures (**a** to **e**), each displaying 48 DNA-PAINT docking strands, were mixed and then imaged sequentially as previously described.
(**e**) Clusters and their outlines in BT20 cells as detected by mean-shift clustering in the image shown in Fig. 2f. Scale bar: 500 nm.

Valm, Betzig, Lippincott-Schwartz: 6plex FP organelle painting in live cells

GM note: see also “Colorful Cell” for 6plex FP (Sladitschek HL, Neveu PA 2015 - MXS-Chaining Kit paper, has been available in addgene.org).

Valm AM, Cohen S, Legant WR, Melunis J, Hershberg U, Wait E, Cohen AR, Davidson MW, Betzig E, Lippincott-Schwartz J 2017 Applying systems-level spectral imaging and analysis to reveal the organelle interactome. Nature. 546 (7656): 162-167. doi: 10.1038/nature22369. PMID: 28538724

The organization of the eukaryotic cell into discrete membrane-bound organelles allows for the separation of incompatible biochemical processes, but the activities of these organelles must be coordinated. For example, lipid metabolism is distributed between the endoplasmic reticulum for lipid synthesis, lipid droplets for storage and transport, mitochondria and peroxisomes for β-oxidation, and lysosomes for lipid hydrolysis and recycling. It is increasingly recognized that organelle contacts have a vital role in diverse cellular functions. However, the spatial and temporal organization of organelles within the cell remains poorly characterized, as fluorescence imaging approaches are limited in the number of different labels that can be distinguished in a single image. Here we present a systems-level analysis of the organelle interactome using a multispectral image acquisition method that overcomes the challenge of spectral overlap in the fluorescent protein palette. We used confocal and lattice light sheet instrumentation and an imaging informatics pipeline of five steps to achieve mapping of organelle numbers, volumes, speeds, positions and dynamic inter-organelle contacts in live cells from a monkey fibroblast cell line. We describe the frequency and locality of two-, three-, four- and five-way interactions among six different membrane-bound organelles (endoplasmic reticulum, Golgi, lysosome, peroxisome, mitochondria and lipid droplet) and show how these relationships change over time. We demonstrate that each organelle has a characteristic distribution and dispersion pattern in three-dimensional space and that there is a reproducible pattern of contacts among the six organelles, that is affected by microtubule and cell nutrient status. These live-cell confocal and lattice light sheet spectral imaging approaches are applicable to any cell system expressing multiple fluorescent probes, whether in normal conditions or when cells are exposed to disturbances such as drugs, pathogens or stress. This methodology thus offers a powerful descriptive tool and can be used to develop hypotheses about cellular organization and dynamics.

News&Views:

Shim SH 2017 Cell imaging: An intracellular dance visualized. Nature 546 (7656): 39-40. doi: 10.1038/nature22500. PMID: 28538721

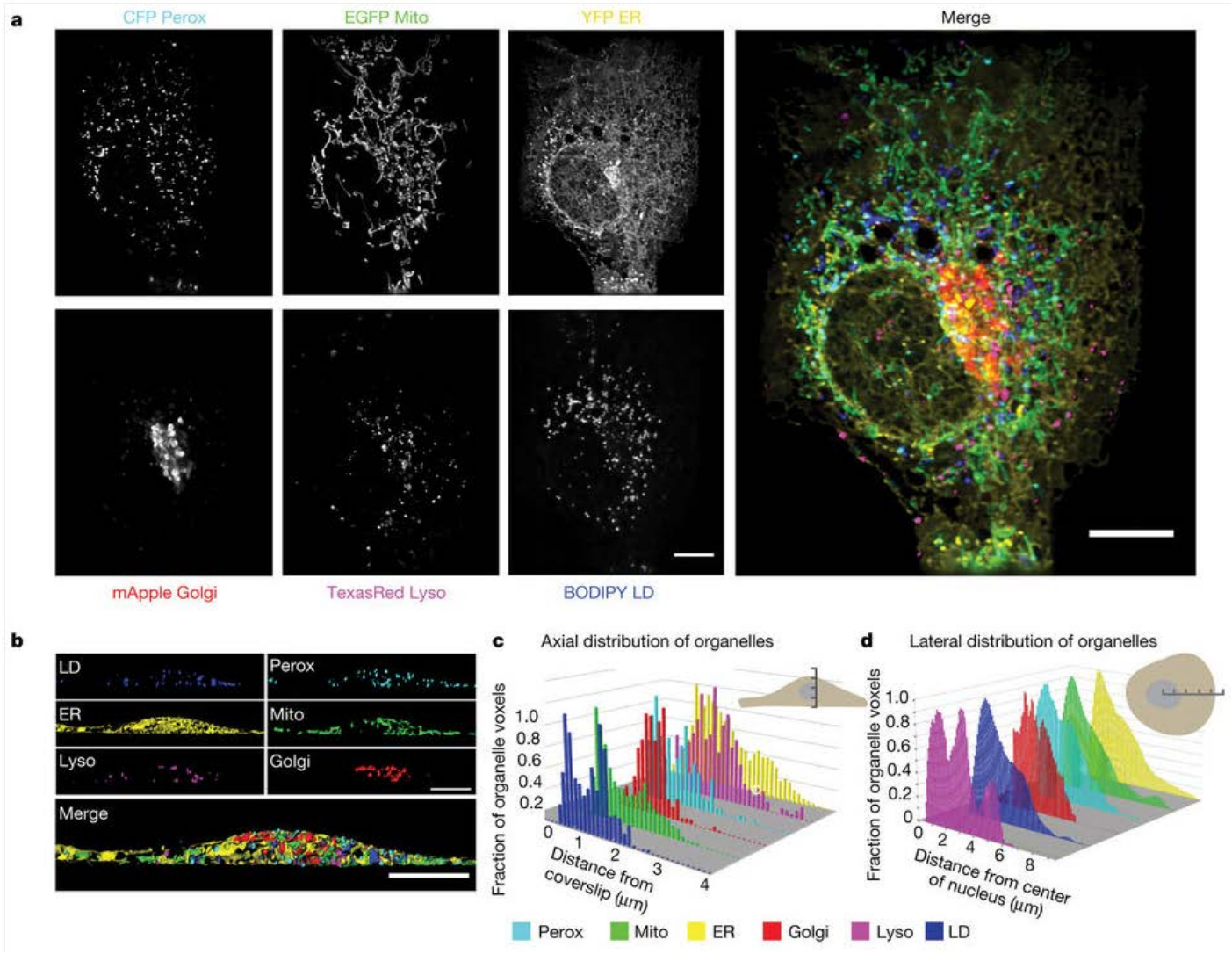

Fig 3a, Maximum intensity projections of a COS-7 cell expressing CFP–SKL, Mito–EGFP, ss-YFP–KDEL, and mApple–SiT, and labelled with Texas Red dextran and BODIPY 665/676.

Note: Sladitschek 2015 MXS-Chaining Kit colorful cell was already at 6plex.

Sladitschek HL, Neveu PA 2015 MXS-Chaining: A Highly Efficient Cloning Platform for Imaging and Flow Cytometry Approaches in Mammalian Systems. PLoS One 10: e0124958. doi: 10.1371/journal.pone.0124958. PMID: 25909630

Valm imaged a few cells – probably not enough (but were able to publish in Nature anyway). See **Schauer et al 2010** for a nice approach of using micropattern(s) to constrain cell shape (they suggest their favorite (-- micropattern and extracellular matrix induces apical-basolateral polarity in single cells):

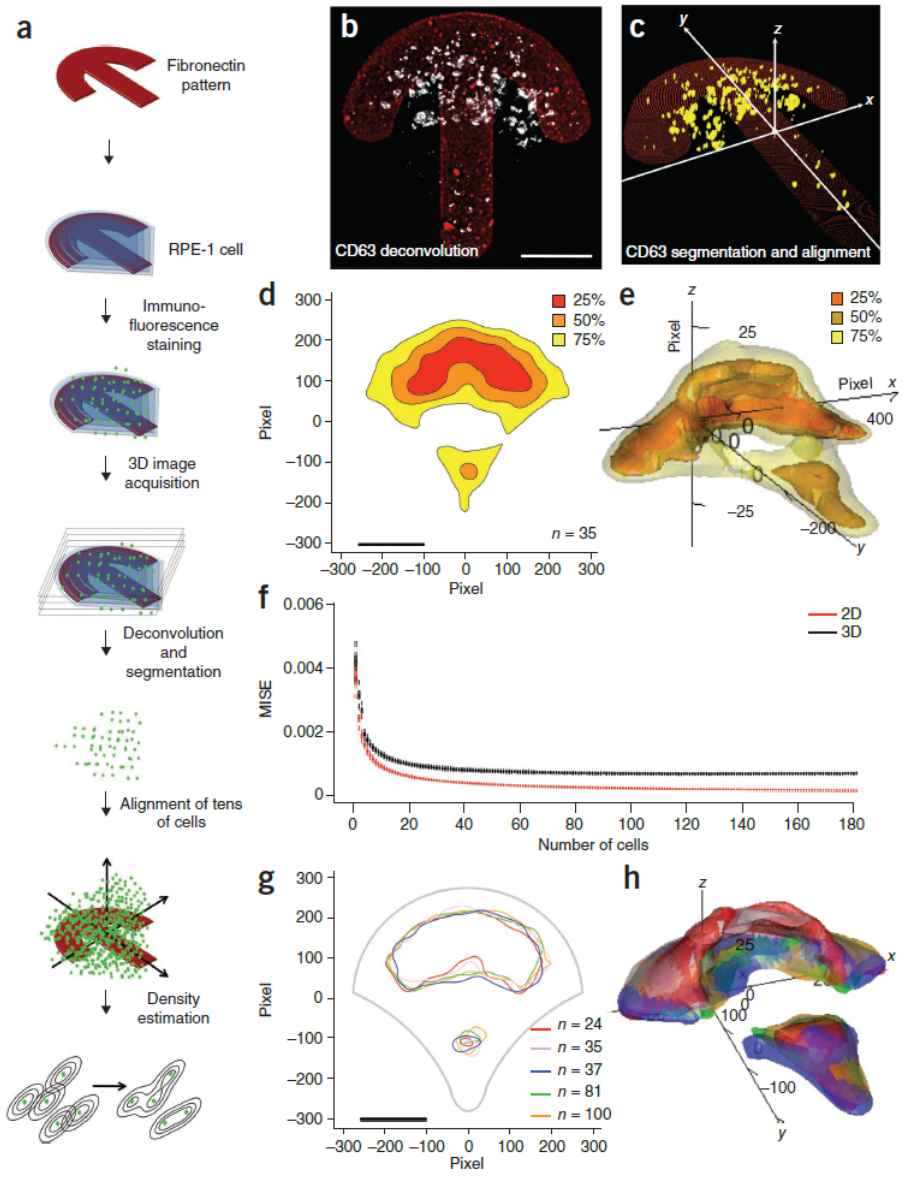

Figure 1 | Analysis of CD63-positive endomembranes from 35 cells on crossbow-shaped patterns. (**a**) Outline of experimental procedure. (**b**) Maximum intensity projection of the deconvolved fluorescence of CD63-positive endomembranes (white) and the fluorescently marked crossbow pattern (red). (**c**) Schematic representation of the segmentation and alignment procedure using the fluorescently marked crossbow pattern. (**d**) The 2D density estimation map with the indicated percentile probability contours representing the smallest regions in which the corresponding percentage of CD63-positive endomembranes were found. (**e**) The 3D density estimation map. For ease of visualization, the height (*z* axis) has been stretched fivefold. (**f**) Estimated MISE for 2D and 3D density estimation as a function of the number of CD63-positive cells analyzed. (**g**) Overlap of the 50% contour of the 2D estimation for five independent experiments. Each color represents an independent experiment using *n* cells. The outer gray outline represents spread of crossbow-shaped cells. (**h**) Overlap of the 50% contour of the 3D estimation for five independent experiments; color-code for independent experiments as in **g**. Scale bars, 10 μm.

marker proteins and fluorophore-coupled antibodies; alternatively, we constructed stable cell lines expressing EGFP-tagged marker proteins that we directly analyzed after fixing the cells. We acquired three-dimensional (3D) image stacks of several tens of cells (**Supplementary Table 1**) and deconvolved them (**Fig. 1a**). We extracted positional information of fluorescently labeled endomembranes from each single cell by segmentation analysis using multi-dimensional image analysis[17] and aligned coordinates using characteristic landmarks

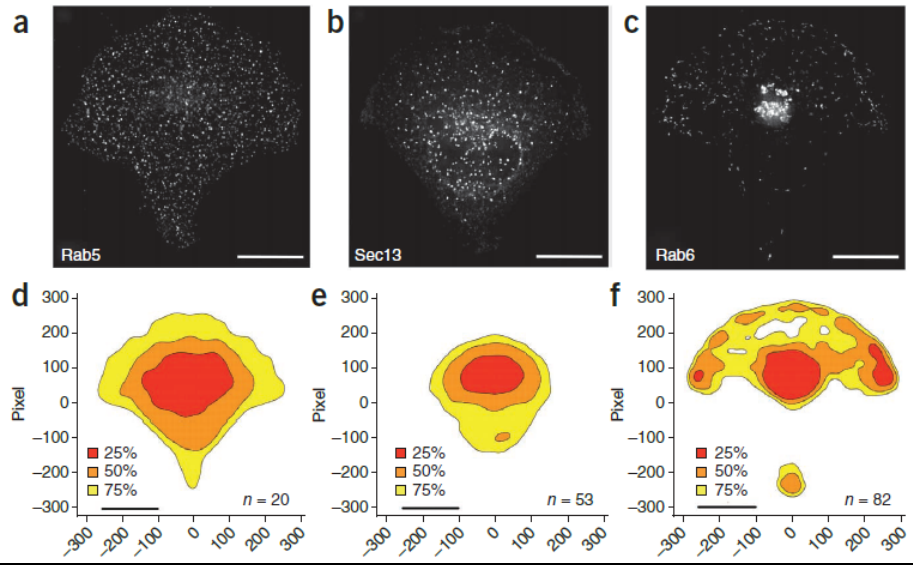

Figure 2 | Analysis of Rab5-, Sec13- and Rab6-positive endomembranes on crossbow-shaped patterns. (**a–c**) Maximum intensity projection of the deconvolved fluorescence of Rab5-positive (**a**), Sec13-positive (**b**) and Rab6-positive (**c**) endomembranes. (**d–f**) The 2D density estimations of Rab5-positive endomembranes from 20 cells (**d**), Sec13-positive endomembranes from 53 cells (**e**) and Rab6-positive endomembranes from 82 cells (**f**). (**g–i**) The 3D density estimations of Rab5-positive endomembranes from 20 cells (**g**), Sec13-positive endomembranes from 53 cells (**h**) and Rab6-positive endomembranes from 82 cells (**i**). Scale bars, 10 μm.

Lastly, in comparison to previous work[16], our 3D analysis provided additional spatial information about the 3D organization of

Schauer K, Duong T, Bleakley K, Bardin S, Bornens M, Goud B 2010 Probabilistic density maps to study global endomembrane organization. Nat Methods 7: 560-566. doi: 10.1038/nmeth.1462. PMID: 20512144

Cool music video: https://www.youtube.com/watch?v=SZkBJnFx5yY

Wow: Nathan in Bin Wu's lab is imaging *for* hours live cell single mRNA (MS2-GFP) translation to single protein molecule(s) (i.e. Red FP), by TIRF

20170926 JHU G.I. Seminar: Bin Wu described an experiment by a graduate student in the Wu lab http://wu.med.jhmi.edu/people , Nathan Livingston, that is a "wow!" experiment setup enabling multiple hours timelapse imaging. Asked Bin (or Nathan) for details, or wait for their publication.

Bin also described that he and his lab now make single molecule RNA probe sets 'in lab' for $30 per probe set (equivalent amount to LGC Biosearch's $800 per probe set or RNAscope branched DNA products from biotechne/ACDbio and ThermoFisher/Affymetrix/Panomics).

Disclosure: Prof. Bin Wu, JHU = my supervisor.

Oxygen (3O2) to Singlet Oxygen (1O2) … specific laser wavelengths direct excitation of monomol and dimol

Blazquez-Castro (2017) review discusses that oxygen molecules can be directly excited by specific wavelengths. I note that 633 nm is a "classic" confocal microscope laser lines, and is also close to the 627 nm transition (see figure below) … recently supplanted by 642 or 638 nm laser lines, such as our Leica SP8 confocal microscope: 405 nm (50 mW), 488 nm (20 mW), 552 nm (20 mW), 638 nm (30 mW). I note from their 2015 "DAB" paper, that it is possible fluorescent Tyramide Signal Amplification (TSA, see earlier sections) or "click tyrosine" might be usable as an alternative to DAB. If doable, this could enable mass spec proteomics of the "laser spot" illumination on the cell.

Abstract:

Molecular oxygen (O2) displays very interesting properties. Its first excited state, commonly known as singlet oxygen (1O2), is one of the so-called Reactive Oxygen Species (ROS). It has been implicated in many redox processes in biological systems. For many decades its role has been that of a deleterious chemical species, although very positive clinical applications in the Photodynamic Therapy of cancer (PDT) have been reported. More recently, many ROS, and also 1O2, are in the spotlight because of their role in physiological signaling, like cell proliferation or tissue regeneration. However, there are methodological shortcomings to properly assess the role of 1O2 in redox biology with classical generation procedures. In this review the direct optical excitation of O2 to produce 1O2 will be introduced, in order to present its main advantages and drawbacks for biological studies. This photonic approach can provide with many interesting possibilities to understand and put to use ROS in redox signaling and in the biomedical field.

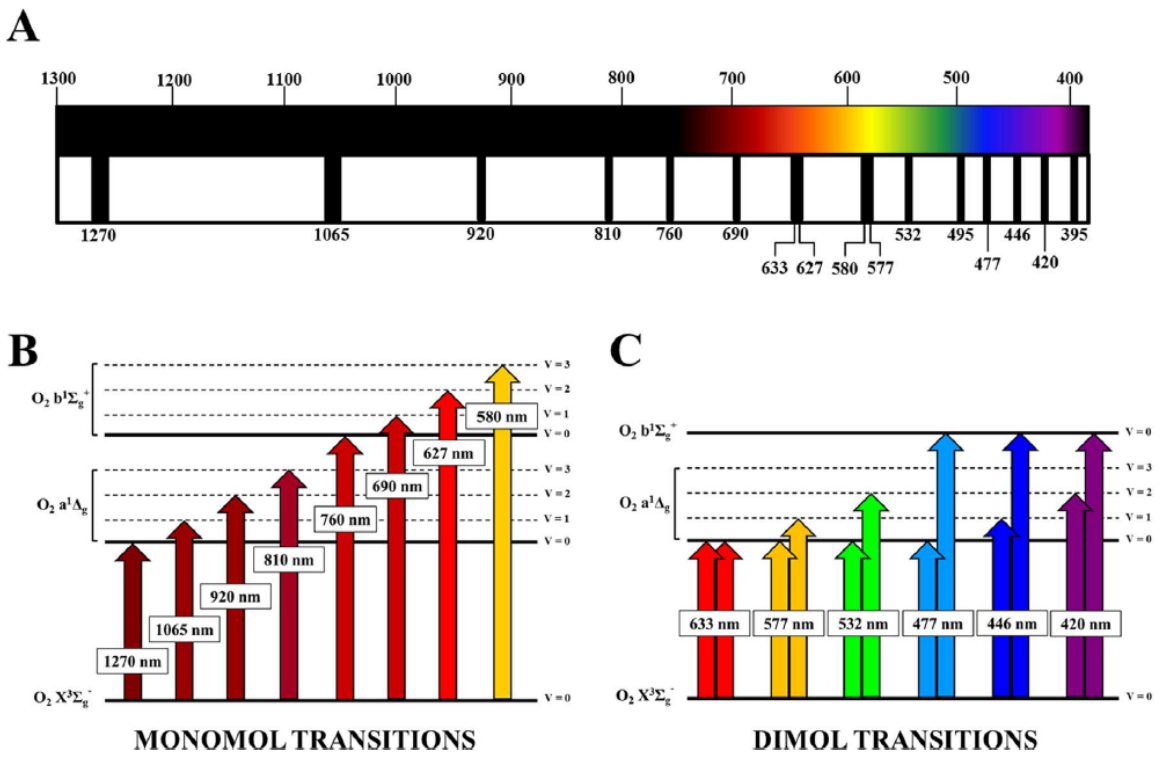

Fig. 4. Oxygen absorption bands and electronic transitions in the optical range (visible-infrared). (A) The O_2 absorption bands (black stripes) between 1300 nm and 390 nm are displayed in the spectral range covering the near-infrared and visible. The number under each transition indicates the peak wavelength, and the stripe width roughly represents the bandwidth for each transition. Both monomol and dimol transitions are plotted. All numbers refer to nanometers. (B) Monomol O_2 transitions represented in a Jablonski diagram. The peak wavelength for each transition is indicated. The arrows connect the initial level (fundamental) and the final levels, along with vibrational excitation (V > 0) in case this occurs. (C) Dimol O_2 transitions (Jablonski diagram), where two $^1O_2$ molecules are produced (double arrows) after single photon absorption. The peak wavelength for each transition is indicated. Some dimol transitions shown in (A) have not been represented here. Data based on [35,99–104,107].

Blázquez-Castro A 2017 Direct 1O2 optical excitation: A tool for redox biology.Redox Biol 13: 39-59. doi: 10.1016/j.redox.2017.05.011. Review. PMID: 28570948

A couple of additional papers:

Stockert JC, Blázquez-Castro A. 2016. Establishing the subcellular localization of photodynamically-induced ROS using 3,3'-diaminobenzidine: A methodological proposal, with a proof-of-concept demonstration. Methods 109: 175-179. doi: 10.1016/j.ymeth.2016.04.031. PMID: 27154745

Bregnhøj M, Blázquez-Castro A, Westberg M, Breitenbach T, Ogilby PR 2015. Direct **765 nm** Optical Excitation of Molecular Oxygen in Solution and in Single Mammalian Cells. J Phys Chem B 119 : 5422-9. doi: 10.1021/acs.jpcb.5b01727. PMID: 25856010

Resolution Blues

https://www.youtube.com/watch?v=T2zc6jpmtFA = Dinah Washington - Resolution Blues (1947)

20170927W update: Maybe I should commission a song, “Resolution Ultras” for ultraviolet fluorescence. See also Richard Levensons “MUSE Microscopy”, using ultraviolet (ex. 280 nm) to just excite surface, currently

typically visible emission, but could be BUV395, BUV395 direct + tandem emission (former for resolution, latter for 'address label', see below), and other UV emitting fluorophores.

Multiplex meets Resolution: BV, SB, BUV's "blues" for resolution, tandems for address labels, 21plex and more

In the section below, "Abbe&Nyquist ➔ Supper-Abbe&Nyquist" we discussed increasing resolution by using shorter wavelength than the "standard" 500 nm (or 520 or 546 nm) wavelength. Here we briefly discuss multiplexing with "blues" resolution.

Below is a graph showing "21plex" by combining BD Biosciences Brilliant Violets (BV) and Brilliant Ultraviolets (BUVs), thermoFisher/eBiosciences SuperBrights (SBs) and my (hopes for) NIRvana Sciences (which will hopefully become "tandem" dyes on BV, BUV, and/or SB, for now could be excited directly).

➔My thinking is the "base polymer" BUV395, BV421, SB436, can be used for best spatial resolution, since their emission maxima are much less than "standard" calculation (500 or 520 or 546 nm) AND the tandems can be used for address labels. I note that of course if only need one, just use the base polymer! I also note that most confocal microscopes shortest excitation wavelength is 405 nm, which is longer then BUV395's excitation curve (left most dotted line in upper graph below), so BUV's should be used for "widefield" experiments with appropriate light source (or buy our confocals a UV laser! … or use our multiphoton microscope).

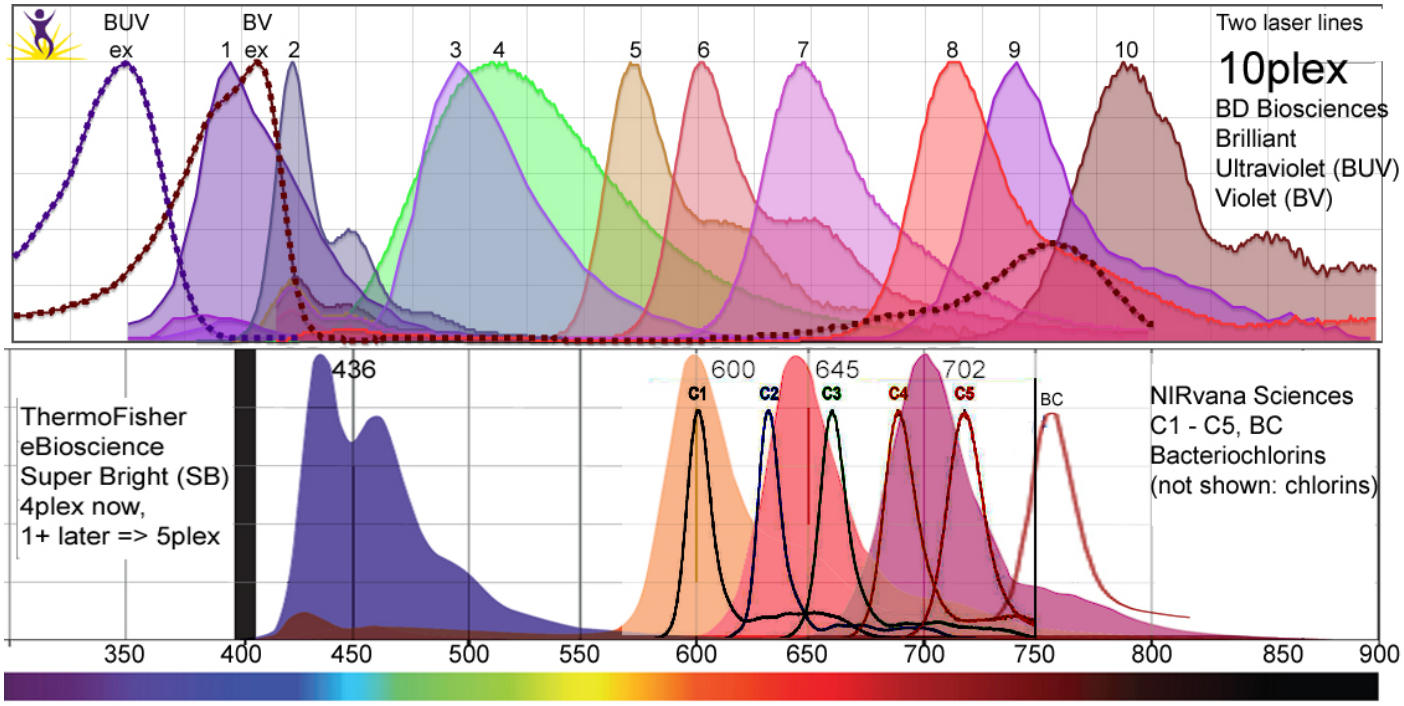

Some more thoughts (for me to try some day … no need for you to wait for me):

- BUV395 … might be excitable with 405 nm laser of 'typical' point scanning confocal microscope. By no means ideal since missing the excitation peak (collect 410-~450 nm), but could be 'better than nothing' if a BUV is what you have (BV or SB would make a lot more sense).
- Acquire peak and tail (with, say equal photons collected for each), then do math: "Tip" = Peak – Tail. This is the fluorescence optical equivalent of "unsharp masking" (a.k.a. "no neighbors deblurring") and could be extended to 3D volumes ("nearest neighbors deblurring").

The Abbe/Airy/Rayleigh XY resolution equation for microscope objective lenses is:

Dxy = 0.61 * Lambda / NA

To which I take the Nyquist Sampling Theorem for a sine wave, that 2.3 data points are needed to obtain the waveform (assuming not being tricked by a multiple), to 2D images, such that hypotenuse, sqrt 2 = 1.414, and 10% more oversampling to take advantage of quantitative spatial deconvolution (see Goodwin 2014):

George's recommended Pixel size ~ dxy / (1.1 * 2.3 * 1.414) ~ 0.6 * Lambda / (NA * 3.6)

Denominator for 1.40 NA lens is therefore 1.4 * 3.6 = 5.0.

Denominator for 1.45 NA lens is therefore 1.4 * 3.6 = 5.22 … for example, Olympus 150x/1.45NA "TIRF" lens, which I note can be used as a widefield objective lens, and may benefit from use of #0 coverglass (~120 um thick, so gain 50 um working distance compared to #1.5 nominally 170 um coverglass … if refractive index match perfectly, then no TIRF).

For high quality oil immersion objective lens (and please, match the refractive index of immersion oil and mounting medium ex. 1.518 oil and ~1.518 Prolong Gold or newer Prolong Diamond mounting media, see also TDE):

McPixel for Widefield fluorescence microscopy 500 vs 400 nm emission (BUV395)

(objective lens, "optovar" magnification changer, C-mount or other camera mount magnification):

McPixel(WF, 500 nm) = 500 / 5 = 100 nm recommended pixel size.

McPixel(WF 400 nm) = 400 / 5 = 80 nm recommended pixel size … ex: BV421, SB436, BUV395 fluorescence emission.

Confocal Microscopy: 0.5 Airy Unit ➔ sqrt(2) better than widefield

Confocal microscopy is typically used with pinhole size of 1.0 Airy unit. This leads to resolution equivalent to widefield, plus the advantage of rejecting most of the out of focus light (assuming zero scattering in the specimen, which degrades performance … scattering is minimized by refractive index matching everything).

Confocal microscopy with infinitely small, that is approaching ZERO pinhole size, provides theoretically the best resolution, except for the practical issue of collecting ZERO photons. Many confocal microscopes allow going to 0.2 Airy unit pinhole size, but still typically not very useful.

A reasonable compromise is 0.5 Airy units, which I strongly urge use of quantitative deconvolution on GPU (as does Leica & SVI for HyVolujtion2, see below).

McPixel(Confocal 0.5 A.U., 500 nm) = (500 / 5) / sqrt(2) = 70 nm recommended pixel size.

McPixel(Confocal 0.5 A.U., 400 nm) = (400 / 5) / sqrt(2) = 56 nm recommended pixel size (I suggest simplify to 50 nm.

***

Leica & SVI HyVolution2: 40nm XY pixel size (1.4NA lens)

Leica and SVI (Huygens deconvolution software, developed HyVolution2, combining Leica SP8 confocal microscope, pinhole 0.5 Airy unit with 1.4 NA objective lens, and Huygens GPU deconvolution. Their recommended pixel size is:

HyVolution2 (1.4 NA lens, Lambda = 500 nm???) ~ 40 nm XY pixel size.

This is probably assuming 500 nm wavelength, but might be calculated for 550 nm, so I'll suggest:

HyVolution2 (1.4 NA lens, Lambda = 400 nm) ~ 36 nm XY pixel size … maybe ~32 nm (if standard assumes 550 nm).

Acknowledgment: Prof. C.D. Mintz, Anesthesiology, purchased a Leica SP8 confocal microscope with HyVolution2, that is being managed by our imaging core (delivered 9/2017).

***

Andor SRRF-Stream: Nyquist sampling, or over-sample, please

There are also specialty applications, such as Andor's SRRF-Stream, a GPU implementation of super-resolution radial fluctuation (SRRF, gustafsson et al 2016) that requires use of Andor "blemish free" (grade 0) EMCCD (and may avoid use of sCMOS because raw sCMOS sensor data have various 'issues' that would mess up calculations).

SRRF-Stream

http://www.andor.com/srrf-stream

http://www.andor.com/pdfs/learning/SRRF_Stream_Technical_Note.pdf

requires 2.3x Nyquist sampling, or higher, to minimize potential artifacts (PALm, STORM, etc, also benefit from correct sampling). Their tech note mentions ok results with modest oversampling.

The EMCCD, iXon Life of iXon Ultra, has 13 um pixel size (one model has 16 um pixel size). A typical 100x/1.4 NA objective lens and 1x C-mount (lensless C-mount) results in a magnification to the camera of 100x, so that

camera pixel 13 um (which is 13,000 nm) corresponds to 130 nm "at the specimen".

This combination is under-sampled with respect to Nyquist, which is likely to lead to artifacts (i.e. "starry commas"). So, need more mag!

I suggest either:

100x objective lens * 2x "mag changer" = 200x mag … so 65 nm pixel size.

150x objective lens * 1.6x "mag changer" = 240x mag … so 54 nm pixel size

150x objective lens * 2x "mag changer" = 300x mag … so 43 nm pixel size

I believe only Olympus offers a 150x lens, which is 1.45 NA (nice!), and discussed briefly above (refractive index match for fixed cells, #0 coverglass, etc).

I see especially opportunity to get more info from the specimen by using shorter emission wavelength, such as "the blues": BV421, SB436, BUV395. I also see opportunity to multiplex with "the blues" for resolution, and tandems (BV570, etc) for "address labels".

Note: 100x2x is a tiny field of view, typically 4 HEK293A (A for Adherent) cells when plated at modest cell density ("sub-confluent"). So, 150x2x is going to be an even smaller field of view, potentially just ONE mammalian cell. This suggests to me:

- Optimize illumination field of view for "just" that cell(s).
- Enable (Andor and/or partners like Olympus on FV3000RS) efficient acquisition of many cells by "scouting" at modest magnification and resolution where cells are (i.e. 100x lens, 1x mag confocal imaging with RS = Resonant Scanner + ZDC Zero Drift Compensation location of correct focal plane).
- Be able to switch light path and acquisition between host microscope (i.e. FV3000RS) and SRRF-Stream (Andor EMCCD, with mag changer in optimal location(s) for best performance SRRF-Stream).
- "SRRF-Stream and TIRF" (pronounced "surf 'n turf" https://en.wikipedia.org/wiki/Surf_and_turf): The EMCCD in standard mode or for more resolution, SRRF-Stream, can be used with TIRF excitation. Some of Olympus 100x and 150x objective lenses are "high NA" TIRF lenses, 1.45 NA or higher is needed for through objective lens excitation (very high NA lenses usually have very short working distances: evaluate use of #0 and #1 coverglasses to extend working distance when doing widefield or confocal imaging with these lenses).. I note that prism or lightguide excitation enables use of concentional (i.e. 1.40NA oil or ~1.3NA silicone oil objective lenses).

Acknowledgment: we thank Jim Belsky, Andor, for demo of SRRF-Stream, 9/2017.

//

Historically, over-sampling has been problematic … now "over-sample can be great"

Historically bad because of photobleaching and "time is money" (2x data in 2x time), now with stable fluorophores, better microscopes, GPU deconvolution, spectral unmixing (and/or spectral phasors), I suggest "over-sampling can be great".

//

Goodwin PC. Quantitative **deconvolution** microscopy. Methods Cell Biol. 2014; 123:177-92. doi: 10.1016/B978-0-12-420138-5.00010-0. PMID: 24974028

Gustafsson N, Culley S, Ashdown G, Owen DM, Pereira PM, Henriques R 2016. Fast live-cell conventional fluorophore nanoscopy with ImageJ through super-resolution radial fluctuations. Nat Commun 7: 12471. doi: 10.1038/ncomms12471. PMID: 27514992.

More Fluorescent Proteins Expression Optimizations … also applies to other proteins

20170927 additions:

Bin Wu's (Miskolci et al 2016) Rac1 and Rac2 FP biosensor paper cites Whitlow linker (Whitlow 1993), along with cpFP comparisons to enhance FRET dynamic range (see the paper):

- Whitlow, M., B. A. Bell, S. L. Feng, D. Filpula, K. D. Hardman, S. L. Hubert, M. L. Rollence, J. F. Wood, M. E. Schott, D. E. Milenic, et al. 1993. An improved linker for single-chain Fv with reduced aggregation and enhanced proteolytic stability. Protein Eng. 6: 989–995.
- Miskolci V, Wu B, Moshfegh Y, Cox D, Hodgson L. 2016 Optical Tools To Study the Isoform-Specific Roles of Small GTPases in Immune Cells. J Immunol 196: 3479-93. doi: 10.4049/jimmunol.1501655. PMID: 26951800/

20171006 addition: avoid GC rich regions of RNA, since ZAP can target such mRNAs for degradation by RNA exosome complex degradation pathway.

http://www.nature.com/nature/journal/v550/n7674/index.html

Stephen P. Goff 2017 Evolution: Zapping viral RNAs**. Nature**

Matthew A. Takata, Daniel Gonçalves-Carneiro, Trinity M. Zang, Steven J. Soll, Ashley York ***+ et al.*** CG dinucleotide suppression enables antiviral defence targeting non-self RNA **Nature**

Vertebrate genomes contain fewer CG dinucleotides than would be expected by chance, and this pattern is mimicked by many viruses; HIV-1 derivatives mutated to contain more CG dinucleotides are targeted by the human antiviral protein ZAP, suggesting that CG suppression has evolved in viruses to evade recognition.

20170919 additions: include intron(s), sfGFP-fusion worked (EGFP-fusion did not), Go FISH!

- include an intron(s) in your expression construct. This made a big improvement for Prof. Frank Bosmans, expression of NaV1.9 sodium ion channel (JHU DDRCC seminar).
    - GM reminder: including an intron deliberately is a good idea (most human protein coding genes include at least one intron); conversely, “cryptic” splice sites are (almost always) bad, for examples, truncated and/or frame shifts often induce “nonsense mediated decay” of the specific mRNA. Good to run and analyze Northern blot(s) to determine if your mRNA is the right length.
- Fluorescent protein fusion: Frank Bosman was able to express sfGFP-NaV1.9 as a fusion protein. sf = SuperFolder (which may not longer be ‘state of the art’ but it worked).
- Go FISH! … This is 2017, you can do single molecule RNA FISH to evaluate expression. Usual result will be “one dot in cytoplasm = one mRNA molecule”. Can also see “transcriptional bursts” from one or both gene loci (assuming diploid cell in G0/G1). smFISH is compatible with most antibodies.

See also my earlier codon and expression optimization tips (below). I summarize Pontes-Quero 2017 tips as:

- Full Kozak sequence is good (ATG is methionine; your protein may or not require its standard 2nd amino acid).
- WPRE = Woodchuck (hepatitis virus) posttranscriptional regulatory element, improves performance.
- Insulators on each side you each gene (expression cassette).
- Improved membrane tag … the De Paola reference leads to an even earlier paper on MARCKs and related family members. *Caveat emptor!* Probably Lck based plasma membrane tag is fine, but your time and money

(or your time and your bosses money). I note that “membrane tag” is sloppy terminology, should (probably) be “plasma membrane tag”. There afre plenty of places in a human cell to target fluorescent protein(s) too.

- Pontes-Quero switched from mKate2 red fluorescent protein to TFP1 (mTFP1, monomeric Teal flujorescent protein … “Teal” and “cyan” fluorescent proteins are similar color).
- See also www.jcat.de and similar web sites for codon optimization, and my earlier sections (search for jcat) on optimizations, including codons and avoiding RNA splicing.

Pontes-Quero et al 2017 text (page 811):

During the development of iMb2-Mosaic and iChr2-Mosaic constructs, we overcame some of the limitations of previous ifgMosaic constructs.

First, when the ORF coding the fluorescent protein and the gene of interest is large and contains one or two 2A peptide sequences, expression of the functional genes and FPs is relatively low due to the reported 2A-peptide-induced translation pause and ribosomal skipping step (Sharma et al., 2012; Trichas et al., 2008). We overcame this problem by including several genetic elements that overall significantly increased the expression of the ifgMosaic ORFs. For instance, we

- ⇨ introduced in all ORFs the full consensus KOZAK sequence (gccaccATGgcg) (Kozak, 1987), and the
- ⇨ WPRE element (Lee et al., 2005), which increases protein levels by increasing mRNA translation and stability (Figures 7A and 7B).

Second, we included four insulators flanking the transcriptional units, for higher expression of the CAG promoter.

Third, the membrane tag in the first-generation ifgMosaic constructs was substituted with an improved membrane tag (De Paola et al., 2003) to increase signal intensity at the membrane and decrease the signal in the cytoplasm (Figure 7B). This is especially important when an iMb-Mosaic is combined with an iChr-Mosaic, in which the separation of nuclei and membrane signals is crucial (Figure 7C, 7E, and S6C). And

fourth, we noticed that the endogenous fluorescence of some proteins, such as Kate2, is reduced when they contain tags that target them to the membrane or nucleus or when they contain the 2A peptide in the C-terminal position (Figure 1E). To circumvent this problem, we used instead Mb2-HA-**Tfp1**-2A, which is a brighter blue-green (teal) FP and more compatible with the other FPs in the Dual ifg2Mosaic system (Figures 7B–7E and S6). We next analyzed the frequency of recombination obtained in Dual ifg2Mosaic ES cells transfected with Cre-expressing plasmids and in mice carrying the Cdh5-CreERT2 allele and pulsed once with tamoxifen. This analysis revealed that the relative recombination ratios depend on the level of Cre expression or induction, the genetic distance between LoxP sites, and the nature of the DNA sequence of the mosaic construct used (Figure 7E and S6A).

Pontes-Quero S, Heredia L, Casquero-García V, Fernández-Chacón M, Luo W, Hermoso A, Bansal M, Garcia-Gonzalez I, Sanchez-Muñoz MS, Perea JR, Galiana-Simal A, Rodriguez-Arabaolaza I, Del Olmo-Cabrera S, Rocha SF, Criado-Rodriguez LM, Giovinazzo G, Benedito R. Dual ifgMosaic: A Versatile Method for Multispectral and Combinatorial Mosaic Gene-Function Analysis. Cell. 2017 Aug 10;170(4):800-814.e18. doi: 10.1016/j.cell.2017.07.031. PMID: 28802047

WPRE:

Earliest reference to WPRE in PubMed:

Woodchuck hepatitis virus contains a tripartite posttranscriptional regulatory element.
Donello JE, Loeb JE, Hope TJ.
J Virol. 1998 Jun;72(6):5085-92. PMID: 9573279

CaliCube 3D printed filter cube … tom DiMatteo, EpiTechnology web link

CaliCube is very cool, because:

1. A way to calibrate a fluorescence microscope excitation source
2. A way to check the quality -- i.e. how badly messed up the lamp or liquid light guide is – of the fluorescence excitation light source
3. One of the first metal 3D printed parts I have seen for light microscopes.

https://tom-dimatteo.squarespace.com/purchase-2/

MPEF-FAIM to image fluorescent drug binding to target (ex. PARPi-BODIPY)

News 20170901:

Our FV1000MP does not currently have this capability (hint: a modest financial contribution from you might be able to add it; or please help us purchase a modern MPEF microscope with MP-FAIM capability, such as Olympus FV-MP) -- Ralph Weissleder et al published a terrific article on using multiphoton excitation fluorescence anisotropy (MP-FAIM) to image and quantify fluorescent conjugated drug binding specifically to the target protein ("receptor"). In this paper they used PARPi-BODIPY, with the unlabeled PARPi as a competitive inhibitor to block binding (and lots of other controls). They have separately published BRAF(V600E)i-BODIPY (Mikula et al 2017) and other fluorescent drug ligands.

Measurement of drug-target engagement in live cells by two-photon fluorescence anisotropy imaging.
Vinegoni C, Fumene Feruglio P, Brand C, Lee S, Nibbs AE, Stapleton S, Shah S, Gryczynski I, Reiner T, Mazitschek R, Weissleder R.
Nat Protoc. 2017 Jul;12(7):1472-1497. doi: 10.1038/nprot.2017.043.
PMID: 28686582
http://www.nature.com/nprot/journal/v12/n7/full/nprot.2017.043.html

The ability to directly image and quantify drug-target engagement and drug distribution with subcellular resolution in live cells and whole organisms is a prerequisite to establishing accurate models of the kinetics and dynamics of drug action. Such methods would thus have far-reaching applications in drug development and molecular pharmacology. We recently presented one such technique based on fluorescence anisotropy, a spectroscopic method based on polarization light analysis and capable of measuring the binding interaction between molecules. Our technique allows the direct characterization of target engagement of fluorescently labeled drugs, using fluorophores with a fluorescence lifetime larger than the rotational correlation of the bound complex. Here we describe an optimized protocol for simultaneous dual-channel two-photon fluorescence anisotropy microscopy acquisition to perform drug-target measurements. We also provide the necessary software to implement stream processing to visualize images and to calculate quantitative parameters. The assembly and characterization part of the protocol can be implemented in 1 d. Sample preparation, characterization and imaging of drug binding can be completed in 2 d. Although currently adapted to an Olympus FV1000MPE microscope, the protocol can be extended to other commercial or custom-built microscopes.
PMID: 28686582 DOI: 10.1038/nprot.2017.043

Refractive Index Matching Reagent to Add for Live Cell Imaging … should be especially good with Olympus Silicone Oil Objective Lenses (optimized for R.I. 1.405) … R.I. matching fixed cells

GM summary for this section: refractive index (R.I.) matching the “mounting medium” (live cell culture media or fixed cell mounting media) and the objective lens immersion medium, greatly improves fluorescence microscopy data.

- Live cells: the cells R.I. is ~1.4, so dry lens (ex. 40x/0.95NA, R.I. 1.0), water immersion (ex. 60x/1.2NA, R.I. 1.33), standard oil immersion (ex. 40x/1.4NA, R.I. 1.518) are not ideal. Olympus Silicone Oil lenses (R.I. 1.405) would be ideal, if the live cell culture media is R.I. matched – see Boothe et al 2017 below.
    - Note: we do not currently own an Olympus Silicone Oil objective lens (may be possible to evaluate a lens from John Gibas, Olympus Imaging Center at JHU).

➔ "It's alive!" -- Consider using
    - DMEMgfp (Evrogen),
    - Opti-Klear (Marker Gene Technologies), or
    - Prolong Live https://www.thermofisher.com/order/catalog/product/P36975?SID=srch-srp-P36975

- Fixed cells: for optimal imaging use the 40x/1.4NA (R.I. 1.518) objective lens (our Zeiss LSM510META confocal microscope). Consider using TDE (Staudt 2007, Stan Vilas has improved protocol online or ask GM), or Prolong Gold (P36941) or newer Prolong Diamond (P36962 for "with DAPI").
    - https://www.thermofisher.com/order/catalog/product/P36941?SID=srch-srp-P36941
    - https://www.thermofisher.com/order/catalog/product/P36962?SID=srch-srp-P36962
- General reagents: see molecular Probes / ThermoFisher "Microscopy Reagents" section https://www.thermofisher.com/search/browse/category/us/en/59201/Microscopy+Reagents

//

➔ Boothe 2017 OptiPrep=Iodixanol enables R.I. matching cells & tissues (i.e. organoids) … original MRI contrast agent

"Commercially available under the brand name Optiprep™, Iodixanol is optically clear and displays a high refractive index of 1.429 as a 60% stock solution, likely at least in parts due to its high density."

Commentary:

Fadero TC, Maddox PS. Live imaging looks deeper. Elife. 2017 Sep 4;6. pii: e30515. doi: 10.7554/eLife.30515. PMID: 28869747 Abstract: "Iodixanol provides an easy and affordable solution to a problem that has limited resolution and brightness when imaging living samples."

Research paper:

Boothe T, Hilbert L, Heide M, Berninger L, Huttner WB, Zaburdaev V, Vastenhouw NL, Myers EW, Drechsel DN, Rink JC. A tunable refractive index matching medium for live imaging cells, tissues and modelorganisms. Elife. 2017 Jul 14;6. pii: e27240. doi: 10.7554/eLife.27240. PMID: 28708059

In light microscopy, refractive index mismatches between media and sample cause spherical aberrations that often limit penetration depth and resolution. Optical clearing techniques can alleviate these mismatches, but they are so far limited to fixed samples. We present Iodixanol as a non-toxic medium supplement that allows refractive index matching in live specimens and thus a substantial improvement of the live-imaging of primary cell cultures, planarians, zebrafish and human cerebral organoids.

KEYWORDS: cell biology; developmental biology; stem **cells**; zebrafish

PMID: 28708059 DOI: 10.7554/eLife.27240

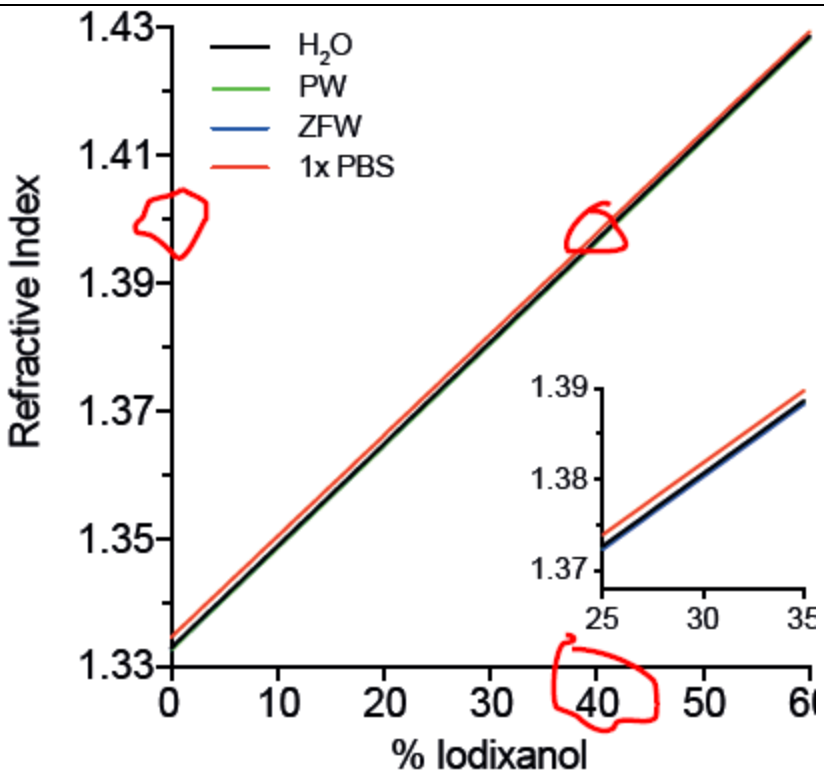

(red circles by GM).

Is the refractive index of the sample known?

Yes

No

Dilute Iodixanol to match RI

Determine tissue RI by phase contrast imaging
Loss of contrast indicates RI match

$$RI_{(media)} \approx 0.0016 \bullet c_{(\%\ Iodixanol)} + 1.333$$

$$c_{(\%\ Iodixanol)} \approx \frac{RI_{(media)} - 1.333}{0.0016}$$

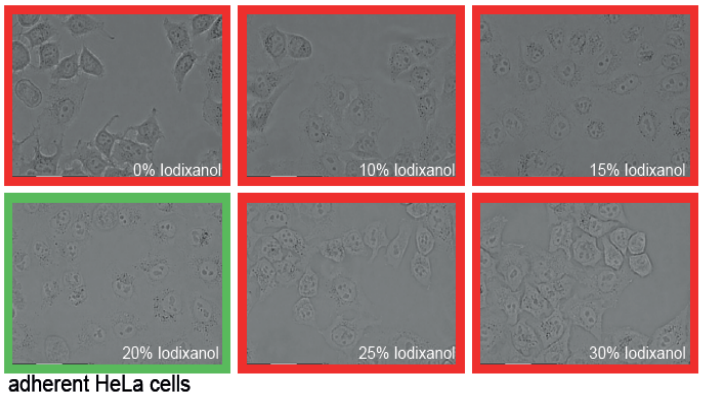

adherent HeLa cells

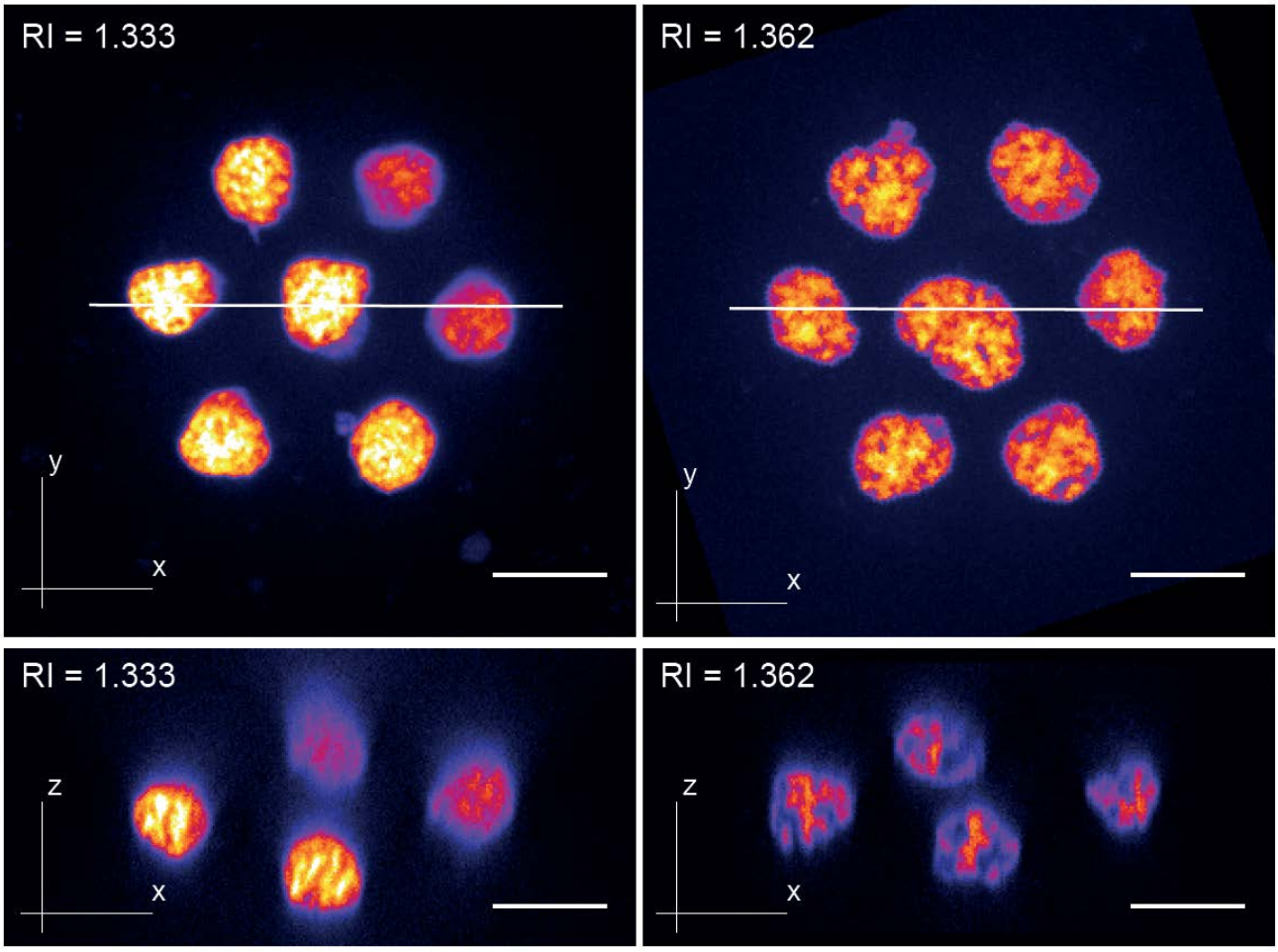

Above: Fig 3, supplemental fig … cerebral organoids, standard tissue culture R.I. 1.33 vs optimized RI 1.362 (optimized for this specimen). {GM note: gut organoids, aka enteroids, may be more complicated in having a lumen closer to R.I. 1.34}.

➔ R.I. matching fixed cell and tissue specimens to high NA oil immersion objective lens (R.I. 1.518):

Staudt T, Lang MC, Medda R, Engelhardt J, **Hell** SW. 2,2'-thiodiethanol: a new water soluble mounting medium for high resolution optical microscopy. Microsc Res Tech. 2007 Jan;70(1):1-9. PMID: 17131355

The use of high numerical aperture immersion lenses in optical microscopy is compromised by spherical aberrations induced by the refractive index mismatch between the immersion system and the embedding medium of the sample. Especially when imaging >10 micro m deep into the specimen, the refractive index mismatch results in a noticeable loss of image brightness and resolution. A solution to this problem is to adapt the index of the embedding medium to that of the immersion system. Unfortunately, not many mounting media are known that are both index tunable as well as compatible with fluorescence imaging. Here we introduce a nontoxic embedding medium, 2,2'-thiodiethanol (TDE), which, by being miscible with water at any ratio, allows fine adjustment of the average refractive index of the sample ranging from that of water (1.33) to that of immersion oil (1.52). TDE thus enables high resolution imaging deep inside fixed specimens with objective lenses of the highest available aperture angles and has the potential to render glycerol embedding redundant. The refractive index changes due to larger cellular structures, such as nuclei, are largely compensated. Additionally, as an antioxidant, TDE preserves the fluorescence quantum yield of most of the fluorophores. We present the optical and chemical properties of this new medium as well as its application to a variety of differently stained cells and cellular substructures.

PMID: 17131355 DOI: 10.1002/jemt.20396

http://onlinelibrary.wiley.com/doi/10.1002/jemt.20396/abstract

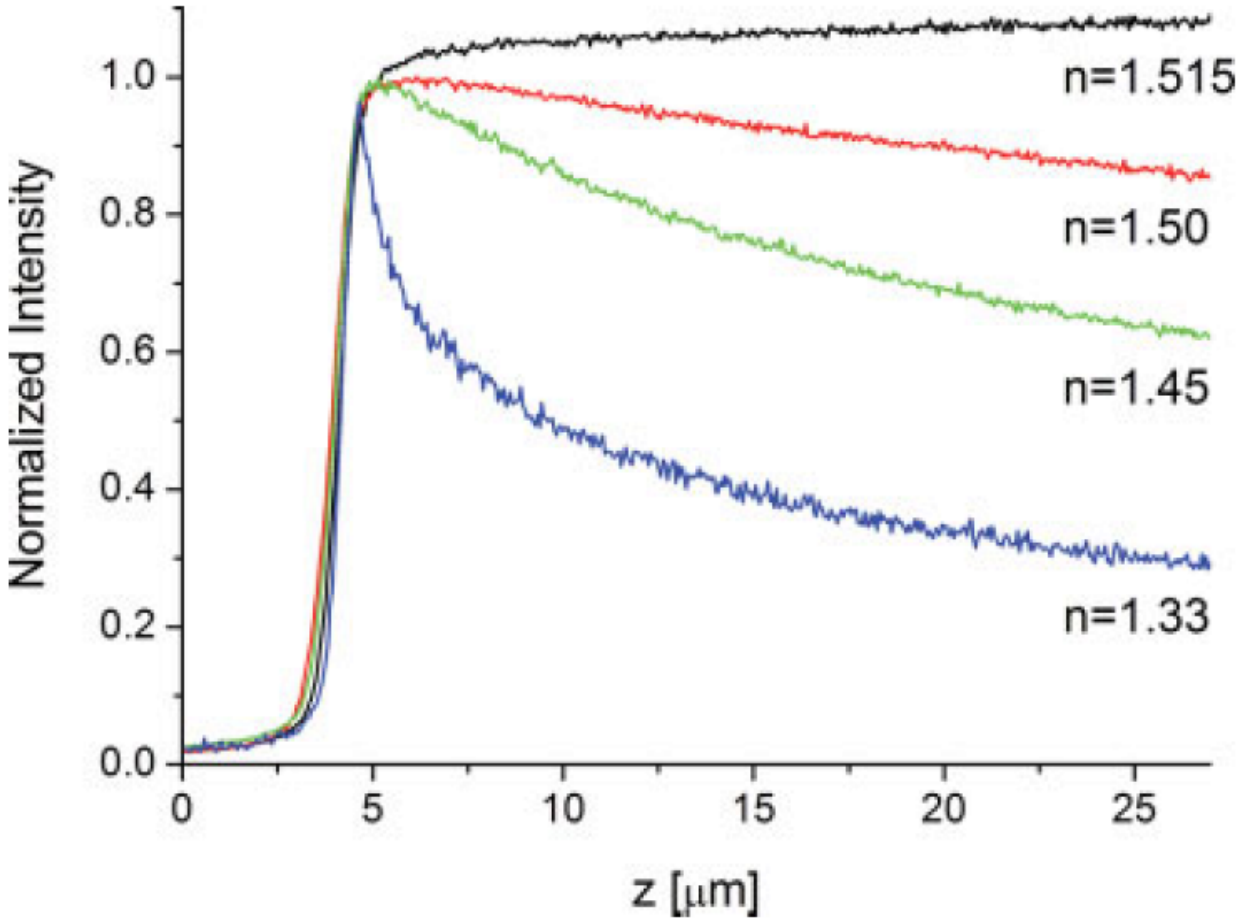

Fig. 6. Confocal axial (z-) scans at the interface of a dye solution with the glass coverslip using an oil immersion lens of 1.46 NA, $\alpha = 75°$. The coverslip is located at $z = 4.0$ μm. At positions $z < 4$ μm is glass and dye solution at $z > 4$ μm. The curves correspond to four different refractive indices set by using different TDE concentrations, as indicated. The deeper the beam is focused into the sample, the fewer photons are collected due to spherical abberations introduced by refractive index mismatch. In case of matching refractive index the signal is constant along the optic axis.

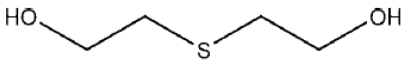

2,2´-Thiodiethanol

Fig. 2. TDE (2,2′-thiodiethanol) is a nontoxic glycol derivative which, owing to the sulfur atom, exhibits a large polarizability and hence a high refractive index. It is soluble in water at any concentration.

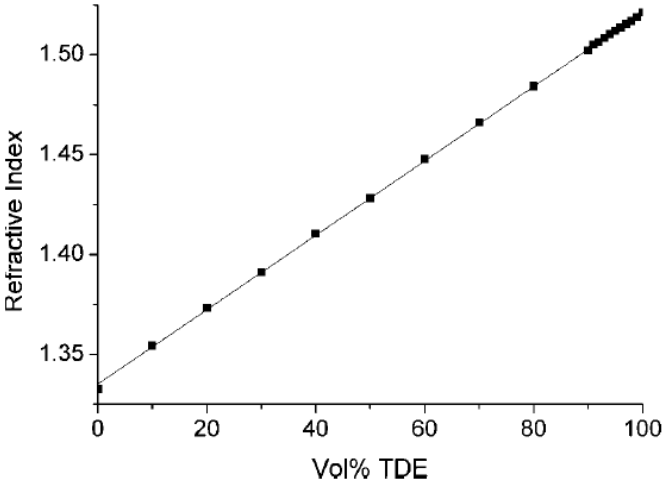

Fig. 3. TDE (2,2′-thiodiethanol) is miscible with water in any proportion. The refractive index of the solution can be precisely tuned to any value between 1.333 (water) and 1.521. The latter is even slightly larger than that of immersion oil.

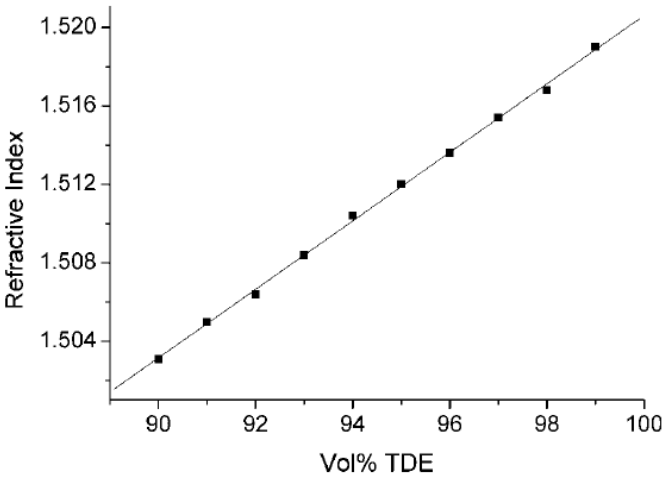

Fig. 4. TDE allows a precise setting of the refractive index by adjusting the water content. For use with an oil immersion lens, a TDE concentration of 97% in water was employed.

Darmstadt, Germany). Absorption spectra were measured with a Cary 4000 UV–VIS spectrophotometer (Varian, Darmstadt, Germany).

Refractive Index

The refractive index of the mounting medium was measured with an AR200 digital hand-held refractometer (Reichert, NY) as a n_D^{23} value (refractive index at 589 nm and 23°C). The refractive index of a standard immersion oil is typically specified as $n_e = 1.518$ (refractive index at 546 nm).

Ce3D: Optical Clearing for 3D Histo-Cytometry

- See also “Histo-Cytometry”, Zellkraftwerk, etc, in earlier section for additional references.
- GM note: Germain recommends spectral unmixing, then spatial deconvolution … I recommend “joint processing” (‘JSUNSD’), per Hoppe et al 2008 Biophys J, Scott and Hoppe 2016 PLoS One … not commercially available as of mid-2017, I am hopeful this will become available “soon”).

Li W, **Germain** RN, **Gerner** MY. Multiplex, quantitative cellular analysis in large tissue volumes with clearing-enhanced 3D microscopy (C_e3D). Proc Natl Acad Sci U S A. 2017 Aug 14. pii: 201708981. doi: 10.1073/pnas.1708981114. PMID: 28808033

Organ homeostasis, cellular differentiation, signal relay, and in situ function all depend on the spatial organization of cells in complex tissues. For this reason, comprehensive, high-resolution mapping of cell positioning, phenotypic identity, and functional state in the context of macroscale tissue structure is critical to a deeper understanding of diverse biological processes. Here we report an easy to use method, clearing-enhanced 3D (C_e3D), which generates excellent tissue transparency for most organs, preserves cellular morphology and protein fluorescence, and is robustly compatible with antibody-based immunolabeling. This enhanced signal quality and capacity for extensive probe multiplexing permits quantitative analysis of distinct, highly intermixed cell populations in intact C_e3D-treated tissues via 3D histo-cytometry. We use this technology to demonstrate large-volume, high-resolution microscopy of diverse cell types in lymphoid and nonlymphoid organs, as well as to perform quantitative analysis of the composition and tissue distribution of multiple cell populations in lymphoid tissues. Combined with histo-cytometry, C_e3D provides a comprehensive strategy for volumetric quantitative imaging and analysis that bridges the gap between conventional section imaging and disassociation-based techniques.

KEYWORDS: *histo-cytometry; immune system; quantitative microscopy; tissue clearing*
PMID: 28808033 DOI: 10.1073/pnas.1708981114

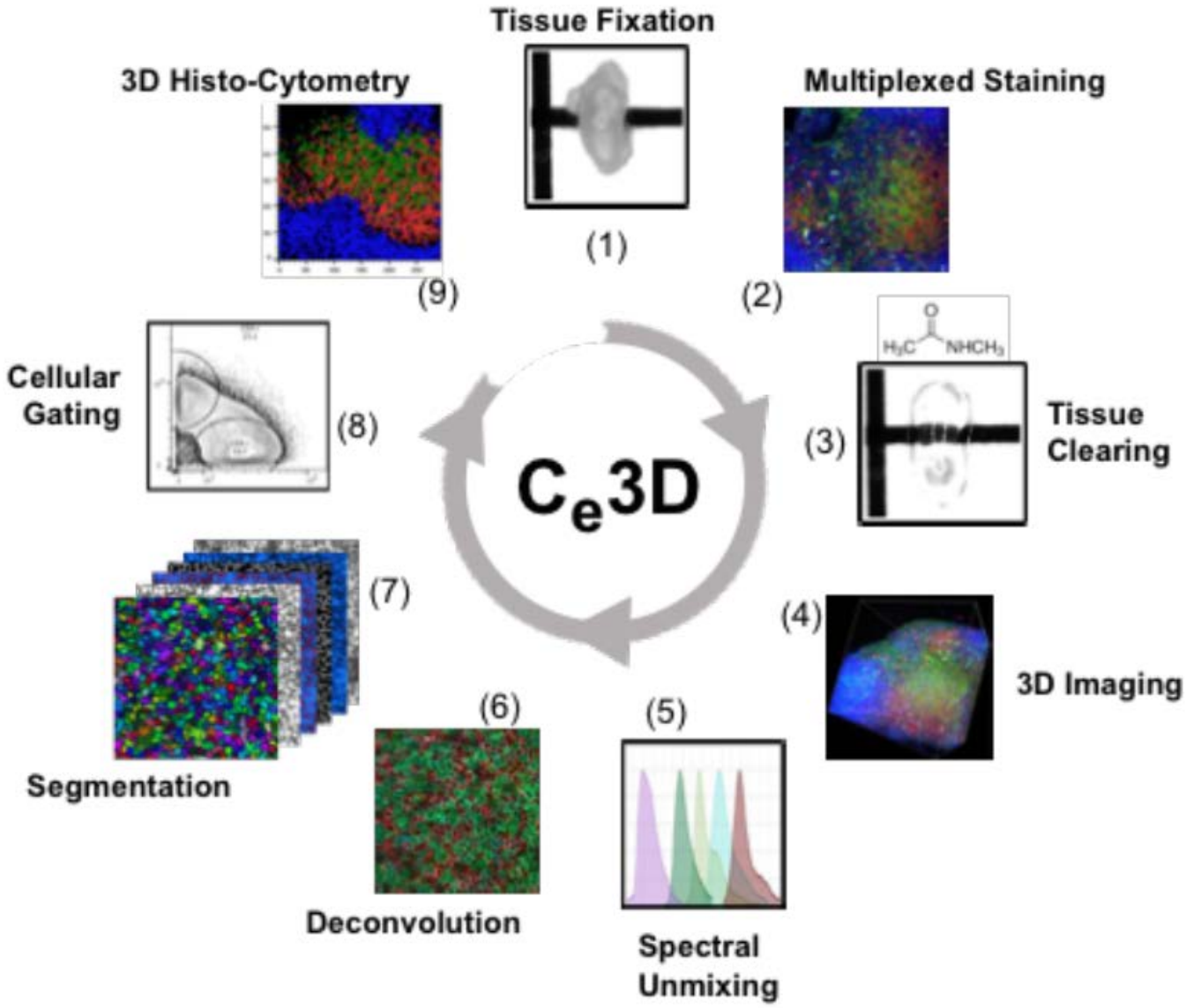

Figure S10. Ce3D pipeline for tissue clearing, imaging and quantitative Histo-Cytometry.
(1) Tissues are fixed,
(2) stained with various fluorophore-conjugated antibodies,
(3) optical cleared and
(4) imaged.
(5) Spectral unmixing to compensate for fluorophore spillover into neighboring detectors is performed.
(6) Deconvolution is performed to improve image quality and quantitative accuracy.
(7) Images are segmented into individual cell objects, with the objects' statistics then exported into graphing software for
(8) population phenotypic gating and
(9) quantitative image Histo-Cytometry.

Germain et al also summarize optical clearing reagents/protocols (no surprise: their's is best in their hands, and they have a patent application).

Method	Transparency	Antibody Staining	Fluorescent Proteins Tested	Fluorophores tested	Antibodies tested	Volume Change	Ease of Use	Clearing Tim
C_e3D	strong	+++	GFP, YFP, CFP, DsRED, TdTomato	>25	30	minor shrinkage	+++	++
ScaleS	strong	+	YFP	~5	N/A	no change	-	+
AbScale	strong	++	None	~5	<5	no change	-	+
Scale	intermediate	-	YFP, DsRed	<5	<5	expansion	++	+
CUBIC	strong	+/-	mKate2, mCherry, GFP, YFP	<5	<5	expansion	+	++
SeeDB	weak	-	YFP	<5	<5	no change	++	+
ClearT/T2	weak	+/-	GFP	<5	<5	minor shrinkage	+++	++
CLARITY	strong	+/-	GFP, YFP, TdTomato	DAPI	5-10	expansion	+	+
PACT	strong	+/-	GFP, YFP	~5	5-10	expansion	++	+
3DISCO	strong	+++	GFP, CFP, YFP (rapid quenching)	<5	<5	shrinkage	+++	+++
iDISCO	strong	+++	TdTomato	~5	28	shrinkage	++	+++

Table 1. Comparison of the various tested tissue-clearing methods with Ce3D. Different parameters desirable for imaging of cleared tissues were compared based on previously published results (P) and empirical observations during direct testing (T).

Multiphoton Excitation Optimization of Fluorescent Protein(s) … Codon Optimization Tip

Molina et al 2017 report on optimizing fluorescent proteins for multiphoton excitation fluorescence (MPEF, also known as 2-photon excitation) with Ti:Sapphire laser (tuning range 690-1040 nm, approximately 345-540 nm with respect to 1-photon excitation … our Spectra-Physics MaiTai DeepSee is one of these lasers).

Blue-Shifted Green Fluorescent Protein Homologues Are Brighter than Enhanced Green Fluorescent Protein under Two-Photon Excitation.

Molina RS, Tran TM, **Campbell** RE, Lambert GG, Salih A, Shaner NC, Hughes TE, Drobizhev M.
J Phys Chem Lett. 2017 Jun 15;8(12):2548-2554. doi: 10.1021/acs.jpclett.7b00960. Epub 2017 May 25.
PMID: 28530831

Fluorescent proteins (FPs) are indispensable markers for two-photon imaging of live tissue, especially in the brains of small model organisms. The quantity of physiologically relevant data collected, however, is limited by heat-induced damage of the tissue due to the high intensities of the excitation laser. We seek to minimize this damage by developing FPs with improved brightness. Among FPs with the same chromophore structure, the spectral properties can vary widely due to differences in the local protein environment. Using a physical model that describes the spectra of FPs containing the anionic green FP (GFP) chromophore, we predict that those that are blue-shifted in one-photon absorption will have stronger peak two-photon absorption cross sections. Following this prediction, we present 12 blue-shifted GFP homologues and demonstrate that they are up to 2.5 times brighter than the commonly used enhanced GFP (EGFP).

PMID: 28530831 PMCID: PMC5474692 DOI: 10.1021/acs.jpclett.7b00960

Results: Four proteins stand out in terms of their 2PA cross sections and brightness: eqFP486 (GenBank Accession AF545829), dTFP0.2,28 amFP486/K68M,27,31 and a new hybrid mutant that we call **Rosmarinus (GenBank Accession KY931461).** Their respective 2PA, 1PA, and emission spectra are presented in Figure 2. Notably, the 2PA spectrum of each of them is blue shifted from double the wavelength of the 1PA spectrum due to enhancement of the vibronic 0−1 transition, as described in our model. This shift, as well as alkaline titration experiments (showing no change of the absorption spectrum before the onset of denaturation), suggests that the chromophore is present in the anionic state in these proteins. For the neutral chromophore, the 1PA and 2PA spectra coincide.29,32 While eqFP486 is the brightest ($\sigma 2,max\phi$ = 100 GM), Rosmarinus is a more efficient folder (see the Methods section) and is similarly bright ($\sigma 2,max\phi$ = 95 GM).

Table 1. 1PA, Fluorescence, and 2PA Properties of FPs Described in this Letter, Ordered by 2P Brightness (last column)[a]

protein	1PA peak (nm)	emission peak (nm)	φ^b (±10%)	ε^c (M^{-1} cm^{-1}) (±1%)	2PA peak (nm)	$\sigma_{2,max}{}^d$ (GM) (±13%)	$\sigma_{2,max}\varphi^e$ (GM) (±16%)
eqFP486	445	486	0.81	49 900	856	125	100
Rosmarinus	437	482	0.85	45 000	852	110	95
amFP486/K68M	458	489	0.93	51 500	862	94	87
dTFP0.2	461	489	0.83 (0.68)[28]	45 000 (60 000)[28]	869	100	85
meleCFP	453	486	0.86 (0.74)[24]	47 400 (47 400)[24]	857	90	77
meffCFP	465	490	0.80 (0.55)[24]	61 000 (88 600)[24]	872	92	74
Tam1	452	486	0.82	46 300	866	81	66
efasCFP	462	490	0.88 (0.77)[24]	57 000 (40 333)[24]	867	73	64
EG-4	438	485	0.88	46 000	853	70	62
dsFP483	439	483	0.76 (0.46,[23] 0.78[41])	46 000 (23 900)[23]	856	78	59
KCyG4219	457	488	0.83 (0.80)[25]	38 000 (21 100)[25]	862	69	57
amFP486	455	486	0.75 (0.24,[23] 0.71[27])	49 200 (40 000)[23]	861	75	56
EGFP	489	510	0.76 (0.61)[42]	58 300 (55 000)[42]	911	54	41[f]
mNeonGreen	506	517	0.78 (0.80)[26]	116 000 (116 000)[26]	944	29	23

[a]All photophysical parameters are presented per single mature chromophore. [b]Fluorescence quantum yield. Relative errors of measurements are shown in parentheses. [c]Extinction coefficient. [d]2PA maximum cross section. [e]2P brightness. [f]The value of 41 GM presented here for the 2P brightness of EGFP corresponds to that reported by Blab et al.[43] but does not match the value of 30 GM previously obtained by Drobizhev et al.[29] This is likely due to the difference in the measured extinction coefficient used to evaluate the chromophore concentration in the 2PA cross section measurement. The value of 46 000 M^{-1} cm^{-1} published in Drobizhev et al.[29] was based on fluorescence lifetime measurements with 400 nm excitation and the Strickler–Berg equation relating the extinction coefficient and radiative lifetime. However, 400 nm light causes fluorescence of the transient anionic I* state, not the steady anionic B* state, whose lifetimes differ by a factor of 1.26, that is, 3.4 vs 2.7 ns.[44] This led to an underestimation of the extinction coefficient and 2PA cross section by the same factor in Drobizhev et al.[29]

➔ Codon Optimization: Rosmarinus MPEF-optimized Cyan FP is not mammalian codon optimized … likely will get better expression in human and mouse cells by optimizing expression

Also: no cryptic mRNA splice sites, no sequence specific RNA binding protein binding sites, at DNA level no transcription factor binding sites. See earlier in this document for more on codon optimization.

A useful "first pass" for optimization is the free web tool, www.jcat.de

Rosmarinus DNA and protein sequences are in GenBank ("NCBI Nucleotide"),

https://www.ncbi.nlm.nih.gov/nuccore/KY931461

```
CDS             1..684
/note="Rosmarinus"
/codon_start=1
/transl_table=11
/product="cyan GFP-like fluorescent protein"
/protein_id="ARU07555.1"
/translation="MSVIKSVMKIKLHMDGIVNGHKFMITGEGEGKPFEGTHTIILKVKEGGPLPFAYDILTTAFQYGNRVFTKYPK
DIPDYFKQSFPEGYSWERSMTFEDQGVCTVTSDIKLEGDYFTYDIRFHGVNFPAGGPVMQKKTLRWEPSTENMYVRDGVLVGEVERT
LLLEGNKHHRCNFRTTYKAKKEVVLPEYHFVDHRIEILGHDKDYNNVVVYENAVARQQASTLPSKAK"
```

```
ORIGIN
        1 atgtcagtga taaagagcgt catgaaaatt aagctgcata tggacggcat cgtgaacggt
       61 cacaaattca tgatcaccgg tgaggggaa ggcaagccat ttgaggggac tcataccatt
      121 atcctgaagg tgaaggaagg aggaccactg cctttcgcat atgatatcct cactacagcc
      181 tttcagtacg gcaatcgggt cttcacaaaa tatcccaagg atattcctga ctacttcaaa
      241 cagtcattcc cggagggcta cagttgggag cggtccatga cctttgagga tcagggcgtg
      301 tgtaccgtga cctctgacat caaactggaa ggagactatt tcacctacga tatcaggttt
      361 cacggagtca atttccccgc cggcggtccc gtcatgcaga aaaagactct gcggtgggaa
      421 ccaagcaccg agaacatgta cgtgcgagac ggcgtgctgg taggcgaggt ggagagaact
      481 ctgctgctgg agggcaataa acatcaccgc tgtaacttca gaacaactta caaagcaaag
      541 aaagaagtag tcctgccaga ataccacttt gttgaccacc ggatagagat cttggggcat
      601 gacaaggact ataacaatgt ggttgtgtat gaaaacgcag tggctcggca acaggcctct
      661 accctgccaa gcaaggcgaa gtag
```

The DNA sequence can be pasted into jcat.de and/or other codon optimization tools, for jcat, human codon usage, 'not optimal' (all 1.0 would be optimal in a simplistic sense):

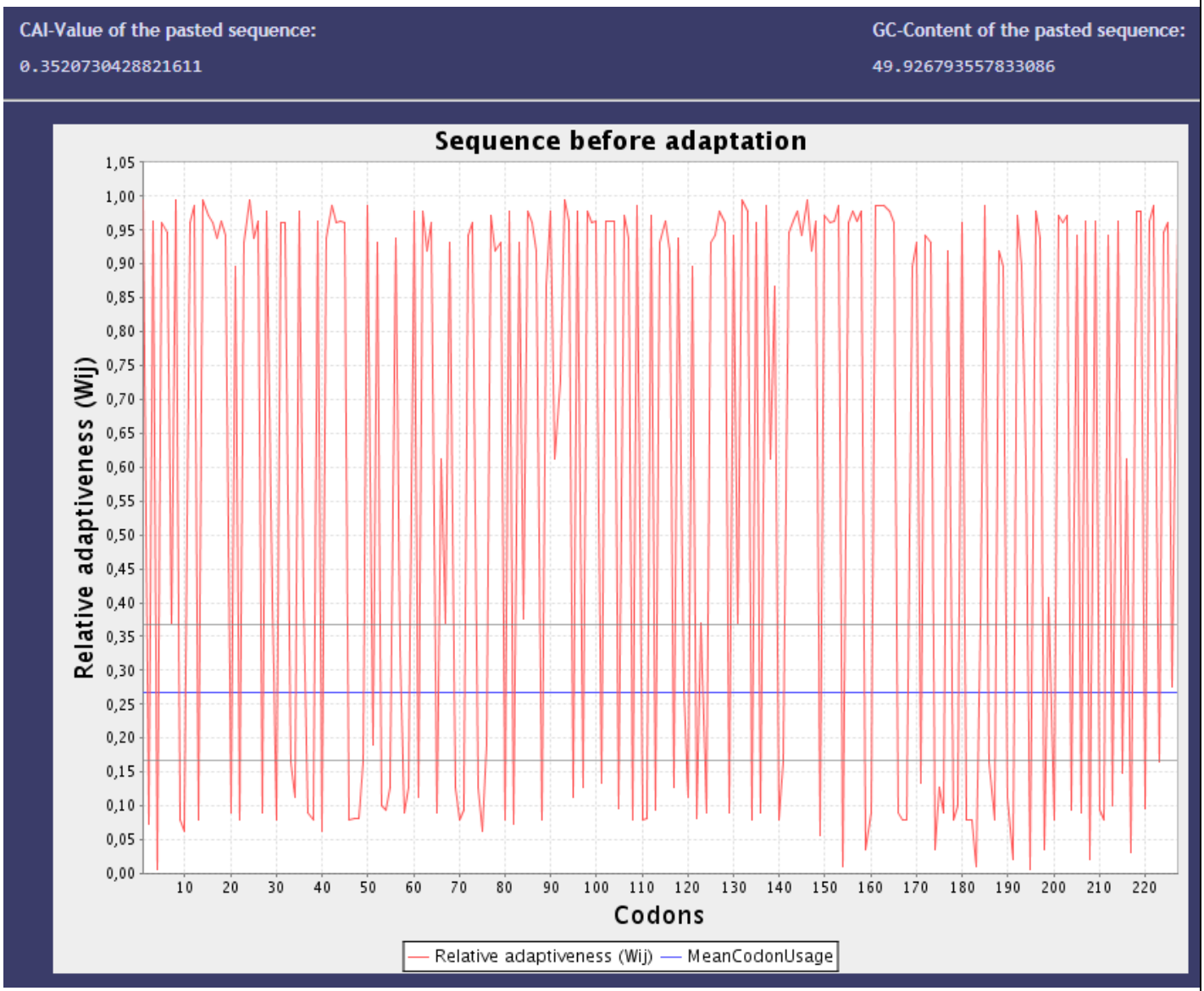

Jcat.de recommends:

Improved DNA:

```
ATGAGCGTGATCAAGAGCGTGATGAAGATCAAGCTGCACATGGACGGCAT      50
CGTGAACGGCCACAAGTTCATGATCACCGGCGAGGGCGAGGGCAAGCCCT      100
TCGAGGGCACCCACACCATCATCCTGAAGGTGAAGGAGGGCGGCCCCCTG      150
CCCTTCGCCTACGACATCCTGACCACCGCCTTCCAGTACGGCAACCGCGT      200
GTTCACCAAGTACCCCAAGGACATCCCCGACTACTTCAAGCAGAGCTTCC      250
CCGAGGGCTACAGCTGGGAGCGCAGCATGACCTTCGAGGACCAGGGCGTG      300
TGCACCGTGACCAGCGACATCAAGCTGGAGGGCGACTACTTCACCTACGA      350
CATCCGCTTCCACGGCGTGAACTTCCCCGCCGGCGGCCCCGTGATGCAGA      400
AGAAGACCCTGCGCTGGGAGCCCAGCACCGAGAACATGTACGTGCGCGAC      450
GGCGTGCTGGTGGGCGAGGTGGAGCGCACCCTGCTGCTGGAGGGCAACAA      500
GCACCACCGCTGCAACTTCCGCACCACCTACAAGGCCAAGAAGGAGGTGG      550
TGCTGCCCGAGTACCACTTCGTGGACCACCGCATCGAGATCCTGGGCCAC      600
GACAAGGACTACAACAACGTGGTGGTGTACGAGAACGCCGTGGCCCGCCA      650
GCAGGCCAGCACCCTGCCCAGCAAGGCCAAG
```

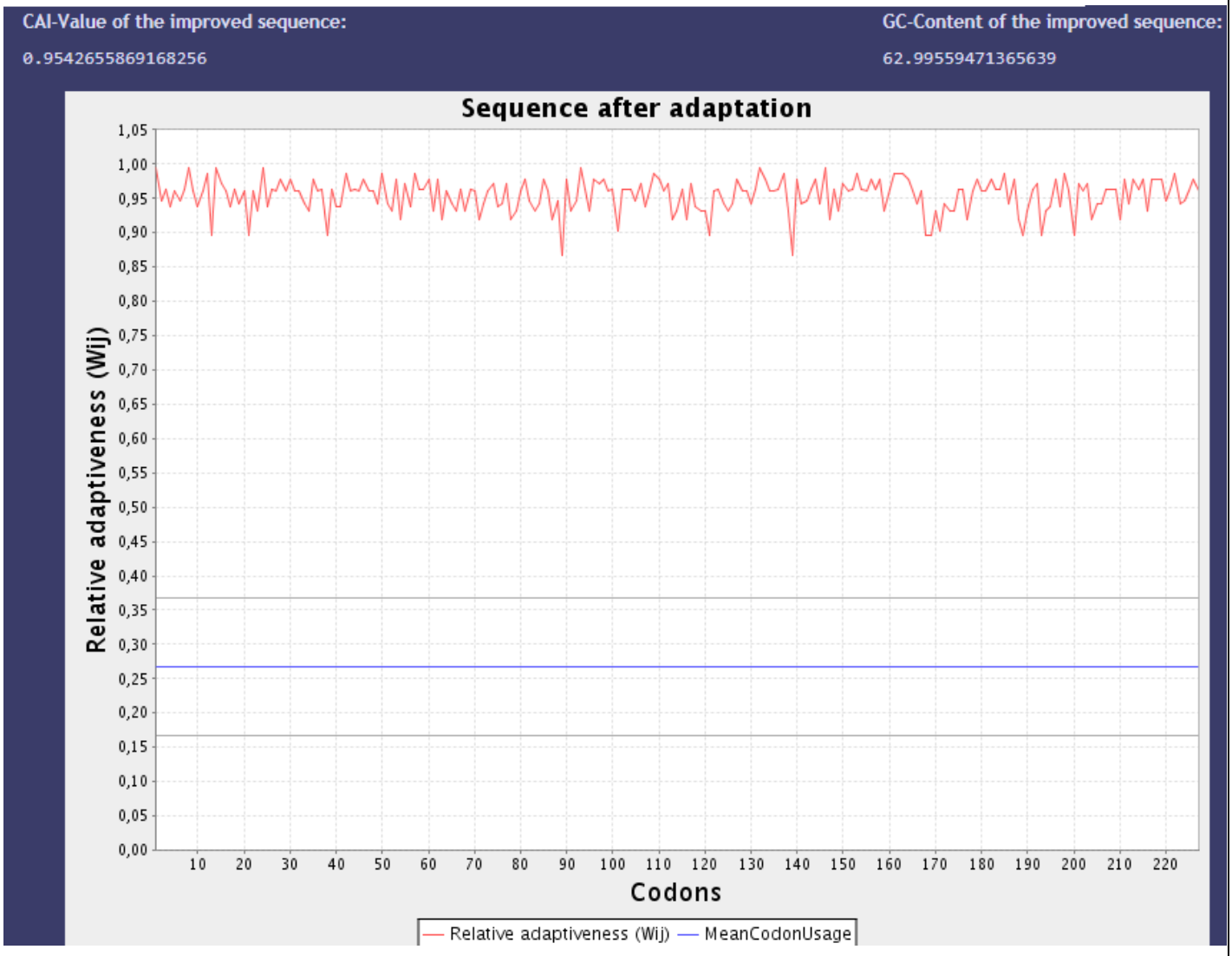

Note especially change in GC content and that all codons are now >0.90.

Is this the DNA sequence you should order from GeneArt or other company … for example, Sean Yu's Epoch Life Sciences (http://www.epochlifescience.com … a boutique molecular biology company, able to handle complicated gene constructs, such as synthetic tandem repeats)?
Answer: up to you. Your time, your money, so *caveat emptor* ("Let the buyer beware").

**

➔ **miRFP670, brightest near infrared fluorescent protein (NIRFP), also not human codon optimized**

DNA sequence is at https://www.ncbi.nlm.nih.gov/nuccore/1053308058

Publication is:

How to Increase Brightness of Near-Infrared Fluorescent Proteins in Mammalian Cells.
Shemetov AA, Oliinyk OS, Verkhusha VV.
Cell Chem Biol. 2017 Jun 22;24(6):758-766.e3. doi: 10.1016/j.chembiol.2017.05.018. PMID: 28602760
Numerous near-infrared (NIR) fluorescent proteins (FPs) were recently engineered from bacterial photoreceptors but lack of their systematic comparison makes researcher's choice rather difficult. Here we evaluated side-by-side several modern NIR FPs, such as **blue-shifted smURFP and miRFP670, and red-shifted mIFP and miRFP703.** We found that among all NIR FPs, miRFP670 had the highest fluorescence intensity in various mammalian cells. For instance, in common HeLa cells miRFP703, mIFP, and smURFP were 2-, 9-, and 53-fold dimmer than miRFP670. Either co-expression of heme oxygenase or incubation of cells with heme precursor weakly affected NIR fluorescence, however, in the latter case elevated cellular autofluorescence. Exogenously added chromophore substantially increased smURFP brightness but only slightly enhanced brightness of other NIR FPs. mIFP showed intermediate, while monomeric miRFP670 and miRFP703 exhibited high binding efficiency of endogenous biliverdin chromophore. This feature makes them easy to use as GFP-like proteins for spectral multiplexing with FPs of visible range.
KEYWORDS: 5-ALA; IFP; biliverdin; firefly luciferase; heme oxygenase; iRFP; in vivo imaging; near infrared; phytochrome; smURFP
PMID: 28602760 PMCID: PMC5519290 DOI: 10.1016/j.chembiol.2017.05.018

Got GFP and Fluorescein (or Alexa Fluor 488)? Consider (i) changing colors with anti-fluorescein (or anti-GFP), (ii) amplifying signal with tyramide signal amplification (TSA) (or "click tyrosine"). Also useful for generally weak signal.

Anti-fluorophore (anti-hapten) and anti-FP antibodies, nanobodies

Anti-fluorescein (sometimes called "anti-FITC", but your specimen does not have any "ITC" in it) has been around for a long time. There are commercial antibodies to (some example web links to products included below):

- Fluorescein
  Alexa Fluor 488
  => https://www.thermofisher.com/antibody/product/Alexa-Fluor-488-Antibody-Polyclonal/A-11094
- Cy3
- Cy5 or Alexa Fluor 647 (very similar chemicals),
- Cy7
- APC (Allophycocyanin)

- PE (Phycoerythrin)
- Fluorescent proteins
    - GFPs (Aequorea based fluorescent proteins)
    - RFPs (Discosoma based fluorescent proteins)
    - See http://www.chromotek.com/products/nano-boosters/ for FP nanoboosters
- More (search online … also see Hapten detection, such as digoxigenin, biotin, dinitrophenol).

Miltenyi Biotec offers several anti-fluorophore on magnetic beads for magnetic cell separation ("MACS"), see

⇨ http://www.miltenyibiotec.com/en/products-and-services/macs-cell-separation/cell-separation-reagents/any-cell-type/anti-cy5-anti-alexa-fluor-647-microbeads.aspx

//

➔ **See "Tag Selector" at Nano-Tag Biotech for Nanobodies (llama, alpaca single domain antibodies), GFP Selector, RFP Selector, BFP Selector … see also "Booster GFP**

http://nano-tag.com/products/bfp-selector

NanoTag Biotechnologies

TagFP Selector

anti-Fluorescent Protein Selector Resins Specificity Chart

Fluorescent Protein	GFP Selector	RFP Selector	TagFP Selector
Sirius	++	–	–
tSapphire	++	–	–
Cerulean	++	–	–
eCFP	++	–	–
mTurquoise2	–	–	–
mTFP (mTeal)	+	–	–
acGFP	+	–	–
EGFP	++	–	–
Emerald GFP	++	–	–
mEGFP (A206K)	++	–	–
mEGFP (L221K)	++	–	–
superecliptic pHluorin	+	–	–
paGFP	+	–	–
superfolder GFP	++	–	–
eYFP	+	–	–
mVenus	++	–	–
Citrine	+	–	–
mOrange2	–	+	–
dsRed1	–	++	–
dsRed2	–	++	–
tdTomato	–	++	–
mRFP	–	+	–
mCherry	–	++	–
mTagBFP	–	–	++
mKate	–	–	++
mTagRFP	–	–	++
mTagRFP657	–	–	++
Dendra2	–	–	–
Dronpa	–	–	–
tdEOS	–	–	–
mEOS3.2	–	–	–

++: strong positive signal; + positive signal; – no signal

NanoTag Biotechnologies GmbH, Rudolf-Wissell-Str. 28a, 37079 Göttingen, Germany
Phone: +49 551 50556-365, E-mail: info@nano-tag.com, Web: www.nano-tag.com

//

GFP-Booster, RFP-Booster from Chromotek (more nanobodies)

http://www.chromotek.com/products/nano-boosters/gfp-booster

GFP-Booster specifically binds to most common GFP derivatives:

eCFP, CFP, mCerulean
eGFP, wtGFP, GFP S65T, AcGFP, TagGFP, tagGFP2, sfGFP, pHluorin
eYFP, YFP, Venus, Citrine

http://www.chromotek.com/products/nano-boosters/rfp-booster/
RFP-Booster specifically binds to most common RFP derivatives:

mRFP, mCherry, mRFPruby, mPlum

//

8plex TSA (tyramide signal amplification)

I am a big fan of tyramide signal amplification (TSA) and have a big section on this below. A recent (2017) paper on 8plex TSA is:

New 8plex TSA (I note that Jim Allison is going to win a Nobel prize for immune checkpoint blockade):

Carstens JL, Correa de Sampaio P, Yang D, Barua S, Wang H, Rao A, **Allison** JP, LeBleu VS, Kalluri R.
Spatial computation of intratumoral T cells correlates with survival of patients with pancreatic cancer.
Nat Commun. 2017; 8: 15095. doi: 10.1038/ncomms15095. PMID: 28447602

Carstens et al 2017 "8plex" TSA.

The exact nature and dynamics of pancreatic ductal adenocarcinoma (PDAC) immune composition remains largely unknown. Desmoplasia is suggested to polarize PDAC immunity. Therefore, a comprehensive evaluation of the composition and distribution of desmoplastic elements and T-cell infiltration is necessary to delineate their roles. Here we develop a novel computational imaging technology for the simultaneous evaluation of eight distinct markers, allowing for spatial analysis of distinct populations within the same section. We report a heterogeneous population of infiltrating T lymphocytes. Spatial distribution of cytotoxic T cells in proximity to cancer cells correlates with increased overall patient survival. Collagen-I and αSMA^{+} fibroblasts do not correlate with paucity in T-cell accumulation, suggesting that PDAC desmoplasia may not be a simple physical barrier. Further exploration of this technology may improve our understanding of how specific stromal composition could impact T-cell activity, with potential impact on the optimization of immune-modulatory therapies.
PMID: 28447602 PMCID: PMC5414182 DOI: 10.1038/ncomms15095

There are some technical details I would do differently, such as not "strip" the antibodies (I recommend crosslink the antibodies&HRP polymer to the specimen: much of the tyramide covalently links to these molecules), use Biocare's

PeroxAbolish (see Takahashi … Ichii papers), and "spectral confocal" microscopy (i.e. Olympus FV3000RS or Leica SP8, not our core's ancient Zeiss LSM510META).

As noted in this section header, I am intrigued by the potential of the new (2017) "click tyrosine" reagent(s) to greatly improve efficiency of labeling (see 20170730 sub-section for abstract):

Click tyrosine

Sato et al 2017 Horseradish-Peroxidase-Catalyzed Tyrosine Click Reaction. Chembiochem 18: 475-478. doi: 10.1002/cbic.201600649.
Sato S[1], Nakamura K[1], Nakamura H[1].

Sato 2017 abstract and figure 1:

The efficiency of protein chemical modification on tyrosine residues with *N*-methylluminol derivatives was drastically improved by using horseradish peroxidase (HRP). In the previous method, based on the use of hemin and H_2O_2, oxidative side reactions such as cysteine oxidation were problematic for functionalization of proteins selectively on tyrosine residues. Oxidative activation of *N*-methylluminol derivatives with a minimum amount of H_2O_2 prevented the occurrence of oxidative side reactions under HRP-catalyzed conditions. As probes for HRP-catalyzed protein modification, *N*-methylluminol derivatives showed much higher efficiency than tyramide without inducing oligomerization of probe molecules. Tyrosine modification also proceeded in the presence of β-nicotinamide adenine dinucleotide (NADH, H_2O_2-free conditions).

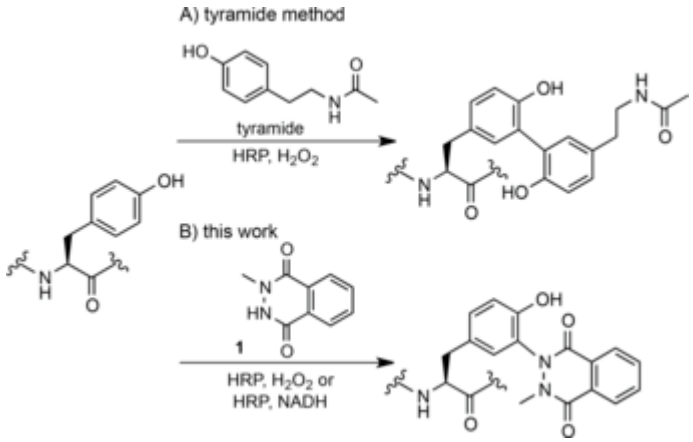

Concept of this work: A) tyramide method, B) this work. Tyrosine modification by using *N*-methylluminol derivatives and HRP.

I expect APEX2 to work as well as HRP for Sato et al's beta-luminol, Cy3-beta-luminol and similar fluorophore-beta-luminol's. Sato et al tested (at least briefly) several HRP substrates, but an 'expanded screen' may identify better molecules.

➔ **interesting "click tyrosine" reagents would be Biotin-linker-fluorophore-beta-luminol's with HRP or APEX2 to detect happen or fluorophore primary antibodies (and go "20plex")**

Because the biotin would facilitate mass spectrometry proteomics AND the various fluorophores would serve as "mass spec tags" of different molecular weights AND enable imaging of the same cells or tissues.

//

Fun historical note: In graduate school in 1982, I was a student in Prof. Ed Voss immunochemistry class at UIUC. Many of Ed's publications involved anti-fluorescein antibodies and each Immunochemistry class student "made" anti-fluorescein antibodies, both rabbit polyclonals and mouse monoclonals (ok, the rabbit and mouse made the antibodies, we made the KLH-fluorescein immunogen, mixed with adjuvant, and injected the animals). The class purified and characterized "our" antisera and mAbs using spectrofluorimetry and other methods (semester long class). My first experience with immunofluorescence and DAPI counterstain was in this class, imaging fluorescent "ANCA" antibodies (anti-nuclear antisera from a patient sera) and DAPI counterstain. My highlight of this chemistry class was finding a mitotic cell on our group's slide (another highlight was discussing with Ed his injecting fish with fluorescein and lighting up their blood vessels, a precedent for our PubMed 24052350 and 26307258 and especially Yiwen Li and Rong Wen's 2008 Nature Protocols "vessel painting" 18846097 paper.

Addgene 2017 Fluorescent Proteins 101 – A Desktop Resource – eBook (161 pages)

Now (8/2017) available online at

https://cdn2.hubspot.net/hubfs/306096/Fluorescent%20Protein%20eBook/Addgene%20Fluorescent%20Protein%20eBook%20Final.pdf

Also in S:\Image Core Manuals on our image data transfer server.

Multiplex immunofluorescence and/or single molecule RNA FISH (optionally: DNA FISH)

I briefly (for me) summarize multiplexing cells and/or tissue section multiplexing. See also Proximity Ligation (APEX2 reagent), EMARS and BioID (mass spectrometry proteomics related to tyramide signal amplification).

Disclosure: I am an inventor on 3 patents for "spectral pathology (SPY)", from my time at Applied Spectral Imaging (ASI) – all now expired (last one issued in 2000, writing August 2017). ASI had previously developed and commercialized spectral karyotyping (SKY), 5plex DNA FISH probes to light up all 24 human chromosomes by combinatorial labeling (simultaneous green, orange, red, NIR2, NIR2 fluorescence), plus DAPI for DNA counterstain (inverse G-banding).

Commercial multiplexing:

- Spectral Pathology ("SPY"). Tsurui 2000 (7plex 3+2+2 exposures with different filter cubes, on SKY system).
- ToposNomos, http://www.toposnomos.com, based on Walter Schubert (2006) 100plex (50 cycles of 2plex).
- Zellkraftwerk (newer name & web site), ChipCytometry, www.zellkraftwerk.com, www.chipcytometry.com, based on Christian Hennig (CEO) method (60+ cycles of 1plex, ~15 min per cycle). See http://www.chipcytometry.com/publications.phtml
- MultiOmyx (Gerdes et al), developed by GE Global R&D, spun off to NeoGenomics. See especially Gerdes 2013; a few additional references: Herring et al 2017 (also scRNAseq), McKinley 2017; Santagata 2014 (GM is a coauthor of this 11plex paper with GE GR&D prototype); Nelson 2013.
- Histo-Cytometry, 6plex on confocal microscope, Gerner … Germain (2012, 2015).
- Multiplex by sequential (4plex * N cycles) Bolognesi 2017 (also discusses interplay between antigen retrieval options and antibody stripping options).
- Opal multiplex tyramide signal amplification: PerkinElmer.
- Simultaneous RNA and Protein (not comprehensive)
- Single molecule RNA FISH … see smFISH discussed in other section(s).

- 120plex FISH (Valm 2016) sequential laser lines, spectral confocal detector.

Ancillary techniques:

- Expansion Microscopy (ExM) / Iterative Expansion Microscopy / Expansion Pathology (ExPath) (primarily Ed Boyden's lab – discussed elsewhere in this document)
- Improved antigen retrieval (Vollert 2015; keep an eye on www.teomics.com), see also Bolognesi 2017.

References (not comprehensive)

Spectral Pathology ("SPY")

Tsurui H, Nishimura H, Hattori S, Hirose S, Okumura K, Shirai T. Seven-color fluorescence imaging of tissue samples based on Fourier spectroscopy and singular value decomposition. J Histochem Cytochem. 2000 May;48(5):653-62. PMID: 10769049

Levenson R, Beechem J, McNamara G. Spectral imaging in preclinical research and clinical pathology. Anal Cell Pathol (Amst). 2012;35(5-6):339-61. doi: 10.3233/ACP-2012-0062. Review. PMID: 22475632

MultiOmyx (NeoGenomyx)

Herring CA, Banerjee A, McKinley ET, Simmons AJ, Ping J, Roland JT, Franklin JL, Liu Q, **Gerdes** MJ, Coffey RJ, Lau KS. Unsupervised Trajectory Analysis of Single-Cell RNA-Seq and Imaging Data Reveals Alternative Tuft Cell Origins in the Gut. Cell Syst. 2017 Nov 7. pii: S2405-4712(17)30449-0. doi: 10.1016/j.cels.2017.10.012. [Epub ahead of print] PMID: 29153838

McKinley ET, Sui Y, Al-Kofahi Y, Millis BA, Tyska MJ, Roland JT, Santamaria-Pang A, Ohland CL, Jobin C, Franklin JL, Lau KS, Gerdes MJ, Coffey RJ. Optimized **multiplex** immunofluorescence single-cell analysis reveals tuft cell heterogeneity. JCI Insight. 2017 Jun 2;2(11). pii: 93487. doi: 10.1172/jci.insight.93487. PMID: 28570279 [60plex]

Santagata S, Thakkar A, Ergonul A, Wang B, Woo T, Hu R, Harrell JC, **McNamara** G, Schwede M, Culhane AC, Kindelberger D, Rodig S, Richardson A, Schnitt SJ, Tamimi RM, **Ince** TA. Taxonomy of breast cancer based on normal cell phenotype predicts outcome. J Clin Invest. 2014 Feb;124(2):859-70. doi: 10.1172/JCI70941. PMID: 24463450

Nelson DA, Manhardt C, Kamath V, Sui Y, Santamaria-Pang A, Can A, Bello M, Corwin A, Dinn SR, Lazare M, Gervais EM, Sequeira SJ, Peters SB, Ginty F, Gerdes MJ, Larsen M. Quantitative single cell analysis of cell population dynamics during submandibular salivary gland development and differentiation. Biol Open. 2013 Apr 18;2(5):439-47. doi: 10.1242/bio.20134309. PMID: 23789091

Gerdes MJ, Sevinsky CJ, Sood A, Adak S, Bello MO, Bordwell A, Can A, Corwin A, Dinn S, Filkins RJ, Hollman D, Kamath V, Kaanumalle S, Kenny K, Larsen M, Lazare M, Li Q, Lowes C, McCulloch CC, McDonough E, Montalto MC, Pang Z, Rittscher J, Santamaria-Pang A, Sarachan BD, Seel ML, Seppo A, Shaikh K, Sui Y, Zhang J, Ginty F. Highly multiplexed single-cell analysis of formalin-fixed, paraffin-embedded cancer tissue. Proc Natl Acad Sci U S A. 2013 Jul 16;110(29):11982-7. doi: 10.1073/pnas.1300136110. PMID: 23818604

Zellkraftwerk/ChipCytometry

Hennig C, Ilginus C, Boztug K, Skokowa J, Marodi L, Szaflarska A, Sass M, Pignata C, Kilic SS, Caragol I, Baumann U, Klein C, Welte K, Hansen G. **High-content cytometry and transcriptomic biomarker profiling of human B-cell activation.** Journal Allergy Clin Immunolo. 2013.

ToposNomos (MLEC/MELK)

Schubert W, Bonnekoh B, Pommer AJ, Philipsen L, Böckelmann R, Malykh Y, Gollnick H, Friedenberger M, Bode M, Dress AW. Analyzing proteome topology and function by automated multidimensional fluorescence microscopy. Nat Biotechnol. **2006** Oct;24(10):1270-8. PMID: 17013374. Commentary: PMID: 17033657

Histo-Cytometry, Ce3D (NIH)

Gerner MY, Torabi-Parizi P, **Germain** RN. Strategically localized dendritic cells promote rapid T cell responses to lymph-borne particulate antigens. Immunity. 2015 Jan 20;42(1):172-85. doi: 10.1016/j.immuni.2014.12.024. PMID: 25607462

Gerner MY, Kastenmuller W, Ifrim I, Kabat J, **Germain** RN. **Histo-cytometry**: a method for highly multiplex quantitative tissue imaging analysis applied to dendritic cell subset microanatomy in lymph nodes. Immunity. 2012 Aug 24;37(2):364-76. doi: 10.1016/j.immuni.2012.07.011. PMID: 22863836

Li W, **Germain** RN, **Gerner** MY. Multiplex, quantitative cellular analysis in large tissue volumes with clearing-enhanced 3D microscopy (C_e3D). Proc Natl Acad Sci U S A. 2017 Aug 14. pii: 201708981. doi: 10.1073/pnas.1708981114. PMID: 28808033

Multiplex by sequential (4plex * N cycles) Bolognesi 2017

Bolognesi MM, Manzoni M, Scalia CR, Zannella S, Bosisio FM, Faretta M, Cattoretti G. Multiplex Staining by Sequential Immunostaining and Antibody Removal on Routine Tissue Sections. J Histochem Cytochem. **2017** Aug;65(8):431-444. doi: 10.1369/0022155417719419. PMID: 28692376

CyTOF ➔ Imaging CyTOF (Fluidigm Helios 3rd gen CyTOF) / MIBI / MIBI-ToF

Garry Nolan lab, MIBI (and MIBI-ToF, unpublished as of 20170802; GM attended talks by Garry in 2016) https://web.stanford.edu/group/nolan/technologies.html

Bodenmiller approach (Giesen 2014) commercialized by Fluidigm on their Helios 3rd generation mass cytometer ($800K for CyTOF flow cytometer + $200K for imaging add on).

Angelo M, Bendall SC, Finck R, Hale MB, Hitzman C, Borowsky AD, Levenson RM, Lowe JB, Liu SD, Zhao S, Natkunam Y, Nolan GP. Multiplexed ion beam imaging of human breast tumors. Nat Med. 2014 Apr;20(4):436-42. doi: 10.1038/nm.3488. PMID: 24584119

Levenson RM, Borowsky AD, Angelo M. Immunohistochemistry and mass spectrometry for highly multiplexed cellular molecular imaging. Lab Invest. 2015 Apr;95(4):397-405. doi: 10.1038/labinvest.2015.2. Review. PMID: 25730370

Bodenmiller B. Multiplexed Epitope-Based Tissue Imaging for Discovery and Healthcare Applications. Cell Syst. 2016 Apr 27;2(4):225-38. doi: 10.1016/j.cels.2016.03.008. Epub 2016 Apr 27. Review. PMID:27135535

Schüffler PJ, Schapiro D, Giesen C, Wang HA, **Bodenmiller** B, Buhmann JM. Automatic single cell segmentation on highly multiplexed tissue images. by **mass cytometry**. **Cytometry A**. 2015 Oct;87(10):936-42. doi: 10.1002/cyto.a.22702. PMID: 26147066

Giesen C, Wang HA, Schapiro D, Zivanovic N, Jacobs A, Hattendorf B, Schüffler PJ, Grolimund D, Buhmann JM, Brandt S, Varga Z, Wild PJ, Günther D, **Bodenmiller** B. Highly multiplexed imaging of tumor tissues with subcellular resolution Nat Methods. 2014 Apr;11(4):417-22. doi: 10.1038/nmeth.2869. PMID: 24584193

Simultaneous RNA and Protein (references are a limited selection of published options)

➔ MERFISH, FISSEQ and similar methods are beyond the scope of this section.

Frei AP, Bava FA, Zunder ER, Hsieh EW, Chen SY, **Nolan GP**, Gherardini PF. Highly multiplexed simultaneous detection of RNAs and proteins in single cells. Nat Methods. 2016 Mar;13(3):269-75. doi: 10.1038/nmeth.3742. PMID: 26808670 "PLAYR (proximity ligation assay for RNA)"

120plex FISH (sequential laser lines, spectral confocal detector)

Valm AM, Oldenbourg R, **Borisy** GG. Multiplexed Spectral Imaging of 120 Different Fluorescent Labels. PLoS One. 2016 Jul 8;11(7):e0158495. doi: 10.1371/journal.pone.0158495. PMID: 27391327

Expansion Microscopy (ExM) / Iterative Expansion Microscopy / Expansion Pathology (ExPath)

➔primarily Ed Boyden's lab – discussed elsewhere in this document.

http://expansionmicroscopy.org/

http://syntheticneurobiology.org/contacts

Zhao Y, Bucur O, Irshad H, Chen F, Weins A, Stancu AL, Oh EY, DiStasio M, Torous V, Glass B, Stillman IE, Schnitt SJ, Beck AH, **Boyden** ES. Nanoscale imaging of clinical specimens using **pathology**-optimized **expansion** microscopy. Nat Biotechnol. 2017 Jul 17. doi: 10.1038/nbt.3892. [Epub ahead of print] PMID: 28714966

Chozinski TJ, Halpern AR, Okawa H, Kim HJ, Tremel GJ, Wong RO, **Vaughan** JC. **Expansion** microscopy with conventional antibodies and fluorescent proteins. Nat Methods. 2016 Jun;13(6):485-8. doi: 10.1038/nmeth.3833. PMID: 27064647

Improved antigen retrieval (hopefully improvements)

➔ hopefully will be commercialized by www.teomics.com (founded by some of Vollert 2015 authors).

Vollert CT, Moree WJ, Gregory S, Bark SJ, Eriksen JL. Formaldehyde scavengers function as novel antigen retrieval agents. Sci Rep. 2015 Nov 27;5:17322. doi: 10.1038/srep17322. PMID: 26612041

Expression optimization: codon usage, codon diversification (for tandem repeats), avoid splicing to death, knock in to endogenous gene, multimerization, localization

I was discussing with Prof. Bin Wu, JHU, expression optimization, and mention a few items here.

➔Do not assume that the DNA sequence published, and sent to addgene, is optimal in any way.

- Codon usage: generally want to use the codons of highly expressed proteins, such as human cytoplasmic actin (beta-actin or human muscle actin).

- No guarantee that high expression level is due to highly efficient protein translation. Could be high mRNA levels, high protein stability (low degradation rate), away from proteases, reactive oxygen species, present in perfect pH (whatever that is), no proteases.
- Codon diversification (for tandem repeats): tandem repeats, such as TALENs, ZFNs, and VNTR containing proteins (latter including MUC1, MUC4), and also tandem FPs, can be unstable in E.coli and retroviruses (and other constructs). Diversification can sometimes help. Bin Wu mentioned <70% homology as being good for improved stability of the tandem repeat gene(s).
- Avoid 'splicing to death': See Rabinovich 2008 (below).
- Knock in to endogenous gene … to get reasonable expression … typically C-terminus (3' end) is targeted. N-terminal (5' end) can work. When neither works, "try the middle" (at a couple of positions). I note that 'standard' FP's have N- and C-terminus close together on one end of the barrel, so an FP can be a relatively innocuous addition (2.4 diameter barrel, 4 nm long).
- Multimerization: 6xYFP is 6x brighter than YFP: see Steven S. Vogel, "V6" (VVVVVV) in addgene.com (pres comm: Steve has made "V8").
- Localization: the smaller the volume a given number of fluorescent proteins are, the brighter the voxels are. I suggest for "quasi 1D" the nucleolus (NoLS Nucleolar Localization Signal); Plasma membrane ("2D") can be preferable to "cytosolic" (3D).

Avoid splicing to death … check for and eliminate cryptic splice sites (and alternative start sites):

Visualizing fewer than 10 mouse T cells with an enhanced firefly luciferase in immunocompetent mouse models of cancer.

Rabinovich BA, Ye Y, Etto T, Chen JQ, Levitsky HI, Overwijk WW, **Cooper LJ**, Gelovani J, Hwu P.
Proc Natl Acad Sci U S A. 2008 Sep 23;105(38):14342-6. doi: 10.1073/pnas.0804105105. Epub 2008 Sep 15.
PMID: 18794521

Table S1. Comparison of ffLuc and effLuc expression in cell lines representative of multiple mouse and human tissues

Brian R Promega

Tissue	Origin	effLuc (p/s/c)	ffLuc (p/s/c)	Fold difference: Intensity	Fold difference: Sensitivity
		Mouse			
Mouse T cells	OT-I	2,206.9 ± 229	38.9 ± 3.9	56.7 ± 0.6	100–110
EL4	Thymoma	456.8 ± 30	10.5 ± 1	43.5 ± 1.21	30–33
Wehi	Pre-B lymphoma	495.0 ± 41	15.9 ± 3.3	32.7 ± 4.1	48–52
P815	Mastocytoma	184.7 ± 14	19.7 ± 1.5	9.4 ± 0.68	14–16
SSCVII	Squamous cell carcinoma	1020.4 ± 153	128.3 ± 28	7.8 ± 0.4	17–20
3T3	Fibroblastoma	2,421 ± 91	32.6 ± 0.18	74.2 ± 2.41	100–110
MCA205	Fibrosarcoma	7,862.7 ± 856	252.5 ± 40	32.1 ± 2.5	39–43
CT26	colon carcinoma	2,361.1 ± 99.8	23.2 ± 1.65	103.0 ± 11.58	110–120
B16	Melanoma	1,399.6 ± 55	6.8 ± 0.8	212.1 ± 23	250–350
		Human			
Human T cells	PBMC	691.1 ± 54	61.3 ± 4.5	11.2 ± 0.3	10–12
Jurkat	T cell lymphoma	935.2 ± 63	3.8 ± 0.9	269.1 ± 24	>400
JM1	B cell lymphoma	175.4 ± 4	1.6 ± 0.18	108.3 ± 9.4	270–290
K562	Chronic myeloid leukemia	888.5 ± 45	42.5 ± 4.4	21.4 ± 1.9	19–22
293	Embryonic renal carcinoma	8,220.6 ± 298	300.5 ± 38	28.0 ± 2.59	37–40
Mel624	Melanoma	4,777.3 ± 159	140.6 ± 16	35.0 ± 3.6	38–42

Mouse and human cell lines (as indicated) were transduced at equivalent MOIs using VSV.G pseudotyped retrovirus. (Mouse T cells were transduced with ecotropic retrovirus). The table reports the observed signal intensity [photons per second per cell (p/s/c)], the fold difference in intensity and sensitivity for effLuc versus ffLuc. Note that the cell lines were not transduced to generate the highest possible signal intensities (i.e. higher MOIs or lentiviral substitution) and are thus not reflective of the highest obtainable with effLuc. Rather, v-ffLuc and v-effLuc were used at the same MOI (0.5) to facilitate intensity and sensitivity comparisons.

Vitaly Boyko on fluorescent proteins: likes mApple (yellow-orange)

mApple is one of Roger Tsien's lab "mFruit" fluorescent proteins, originating from DsRed / mRFP family.

GM notes:

- see also my notes below on T145L and other photostabilizing mutations for EGFP, EYFP and other Aequorea FPs.
- The in vitro (spectrofluorimeter) performance of an FP and "in vivo" (live cells, tissues, organisms) do not correlate very well, so *caveat emptor* ("let the buyer beware") and when possible evaluate a couple of candidates. It is possible to detect "GFP" (Aequorea based FPs, such as EGFP) and "RFP" (DsRed/mRFP1/mCherry based FPs, from Discosoma, with many genetic modifications) with appropriate antibodies or nanobodies. See also "Got GFP and Fluorescein" section, which also mentions use of tyramide signal amplification to greatly boost the signal.

mScarlet may also be useful as a far-red FP.

➔**See http://www.fpvis.org/FP.html for Kurt Thorn's nice interactive graph and tables on fluorescent proteins.**

Vitaly Boyko on coverglass cleaning: 70% EtOH, then 100% EtOH ("anhydrous" EtOH, so use new bottle each month)

Vitaly Boyko (New York), likes to clean coverglasses using 70% EtOH (i.e. "standard lab" 70% Ethanol, though I suggest double distilled or deionized H2O, not tap water, since the point is to clean the glass, not rub dirty water on it), then 100% EtOH.
➔Vitaly specifically uses "fresh" 100% EtOH, that is really anhydrous, not contaminated with water absorpbed from the air. Vitaly ensures this by opening a new bottle of 100% EtOH every month (presumably the previous bottle could be moved to "general lab supplies" … or better, mixed with ddH2O to make clean 70% EtOH).
Vitaly Boyko on Piranha solution: even better than 100% EtOH, but Piranha'd glass is highly charged, kills cells
Vitaly told me Piranha is great at cleaning glass, but results in a highly charged surface that kills cells (that is, human cells). I suggested coating with extracellular matrix or poly-lysine. Vitaly's response was that once the cell(s) digest the ECM, they contact the charged glass and die.

Wikipedia has nice entry discussing the pro's and con's of Piranha (mostly con's!!! Italics mine):
https://en.wikipedia.org/wiki/Piranha_solution
Piranha solution, also known as **piranha etch**, is a mixture of sulfuric acid (H_2SO_4) and hydrogen peroxide (H_2O_2), used to clean organic residues off substrates. Because the mixture is a strong oxidizing agent, it will remove most organic matter, and it will also hydroxylate most surfaces (add OH groups), making them highly hydrophilic (water-compatible).
Many different mixture ratios are commonly used, and all are called piranha. A typical mixture is 3 parts of concentrated sulfuric acid and 1 part of 30% hydrogen peroxide solution; other protocols may use a 4:1 or even 7:1 mixture. A closely related mixture, sometimes called "base piranha", is a 3:1 mixture of ammonium hydroxide (NH_4OH) with hydrogen peroxide.
Piranha solution must be prepared with great care. It is highly corrosive and an extremely powerful oxidizer. Surfaces must be reasonably clean and completely free of organic solvents from previous wash steps before coming into contact with piranha solution. Piranha solution cleans by dissolving organic contaminants, and a large amount of contaminant will cause violent bubbling and a release of gas that can cause an explosion.[1]
Piranha solution should always be prepared by adding hydrogen peroxide to sulfuric acid slowly, never in reverse.[2][3] *Mixing the solution is extremely exothermic. If the solution is made rapidly, it will instantly boil, releasing large amounts of corrosive fumes*. Even when made with care, the resultant heat can bring solution temperatures above 100 °C. It must be allowed to cool reasonably before it is used. The sudden increase in temperature can also lead to violent boiling of the extremely acidic solution. Solutions made using hydrogen peroxide at concentrations greater than 50% may cause an explosion. Once the mixture has stabilized, it can be further heated to sustain its reactivity.[4] The hot (often bubbling) solution cleans organic compounds off substrates and oxidizes or hydroxylates most metal surfaces. Cleaning usually requires about 10 to 40 minutes, after which the substrates can be removed from the solution.

The solution may be mixed before application or directly applied to the material, applying the sulfuric acid first, followed by the peroxide. Due to the self-decomposition of hydrogen peroxide, piranha solution should be used freshly prepared. Piranha solution should not be stored, as it generates gas and therefore cannot be kept in a closed container.[2] As piranha solution reacts violently with many items commonly disposed of as chemical waste if the solution has not neutralised, it must be left in clearly marked containers.
used to clean glassware, though *it is discouraged in many institutions* and it should not be used routinely due to its *dangers*.[6] Unlike chromic acid solutions, *piranha does not contaminate glassware with heavy-metal ions*.

Maximum Intensity Projection in MetaMorph is Process menu → Stack Arithmetic → Sum, or Fiji ImageJ Image Stacks Z-Project

Below is a screenshot of the MetaMorph demo image "Nerve" (after removing plane 16 of 16 and using Stack → Montage) with Stack Arithmetic dialog, "Max" (middle) and "Best Focus" (right) images. Utility of this command, or its Fiji ImageJ equivalent, depends on the information content of your image, both composition (specimen) and singal-to-noise ratio. You can use Metamorph Stack → Keep Planes to keep the most useful planes; typically remove (don't keep!) some of the out of focus planes at top and bottom of your Z-series. The MetaMorph Stack → 3D Reconstruction, "Max", zero degree view is the same as Stack Arithmetic max.

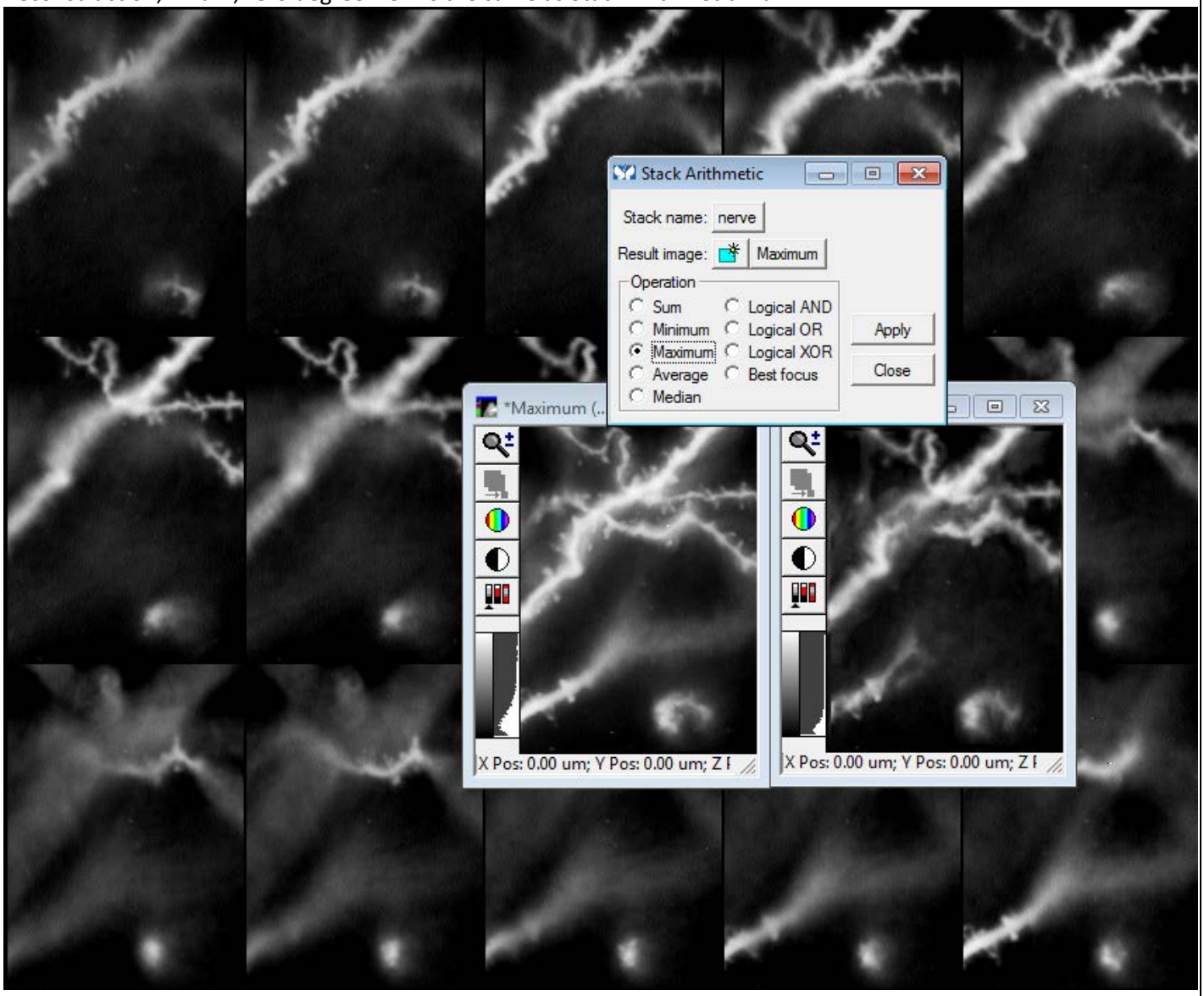

MetaMorph Installation and Updates

Note: GM knows MetaMorph pretty well, having 'celebrated' 25th anniversary of using MetaMorph (May 2017, dated from 1992 AQLM course at MBL, where GM was a consultant/guest of UIC, then moved to West Chester, PA, and formally joined ~July 1992 … was the "voice of MetaMorph and MetaFluor applications and technical support" for 5 years).

MM installers and updaters on the web (part of page contents pasted below).

Quick tip:

URL can be pasted into the address bar of Windows Explorer

ftp://ftp.meta.moleculardevices.com/pub/uic/software

"CDROM" (folder) is MM77 and MM78.

Reminder: follow installer instructions for when USB 'dongle' should be connected or DETACHED during install.

Yes, it is possible to have multiple licenses ('dongles') share one c:\MM or c:\Olympus installation. Use batch files to switch which UICSHELL.INI is in use.

Standard MetaMorph and 'branded' Leica and Olympus MetaMorph's should be installed in separate folders (c:\MM, c:\Olympus, for examples).

If you have an MM license number (often printed on the USB 'dongle'), you can log in through the web portal,

http://www.meta.moleculardevices.com/software/mm/updates/main.php

20170727 update: more MetaMorph/MetaFluor support documents and tutorials at ftp://ftp.meta.moleculardevices.com/support/

http://mdc.custhelp.com/app/answers/detail/a_id/15203/~/metamorph%C2%AE-software-installation-files

MetaMorph® Software installation files

Published 11/09/2010 10:08 AM | Updated **06/30/2014** 01:26 PM | Answer # 15203

How do I access the installation files for the MetaMorph Software Suite of products on the FTP server?

Click on a link below to access the installation files for a specific version of the MetaMorph Software.

ftp://ftp.meta.moleculardevices.com/pub/uic/software/MM78/
ftp://ftp.meta.moleculardevices.com/pub/uic/software/MM77/
ftp://ftp.meta.moleculardevices.com/pub/uic/software/MM76/
ftp://ftp.meta.moleculardevices.com/pub/uic/software/MM75/
ftp://ftp.meta.moleculardevices.com/pub/uic/software/MM71/
ftp://ftp.meta.moleculardevices.com/pub/uic/software/MM70/
ftp://ftp.meta.moleculardevices.com/pub/uic/software/MM63/
ftp://ftp.meta.moleculardevices.com/pub/uic/software/MM50/
ftp://ftp.meta.moleculardevices.com/pub/uic/software/MM46/
ftp://ftp.meta.moleculardevices.com/pub/uic/software/MM45/

Below is a screenshot of accessing FTP form inside Internet Explorer, if needed (see URL above for more information).

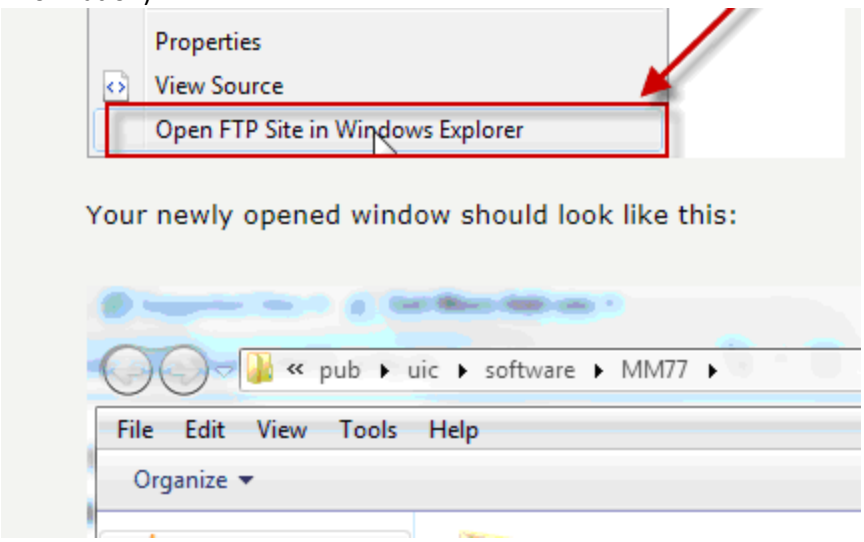

6 Steps to Better Fixed Cell Imaging (Modified from Molecular Probes/Invtirogen/ThermoFisher "5 step" program 2017 PDF)

This is adapted from:
Molecular Probes/Invtirogen/ThermoFisher 2017
Five steps for publication-quality cell imaging the first time
Follow this proven guide to capture the best possible fixed-cell images
(George can send you that PDF).

4 steps directly from Mol Probes:

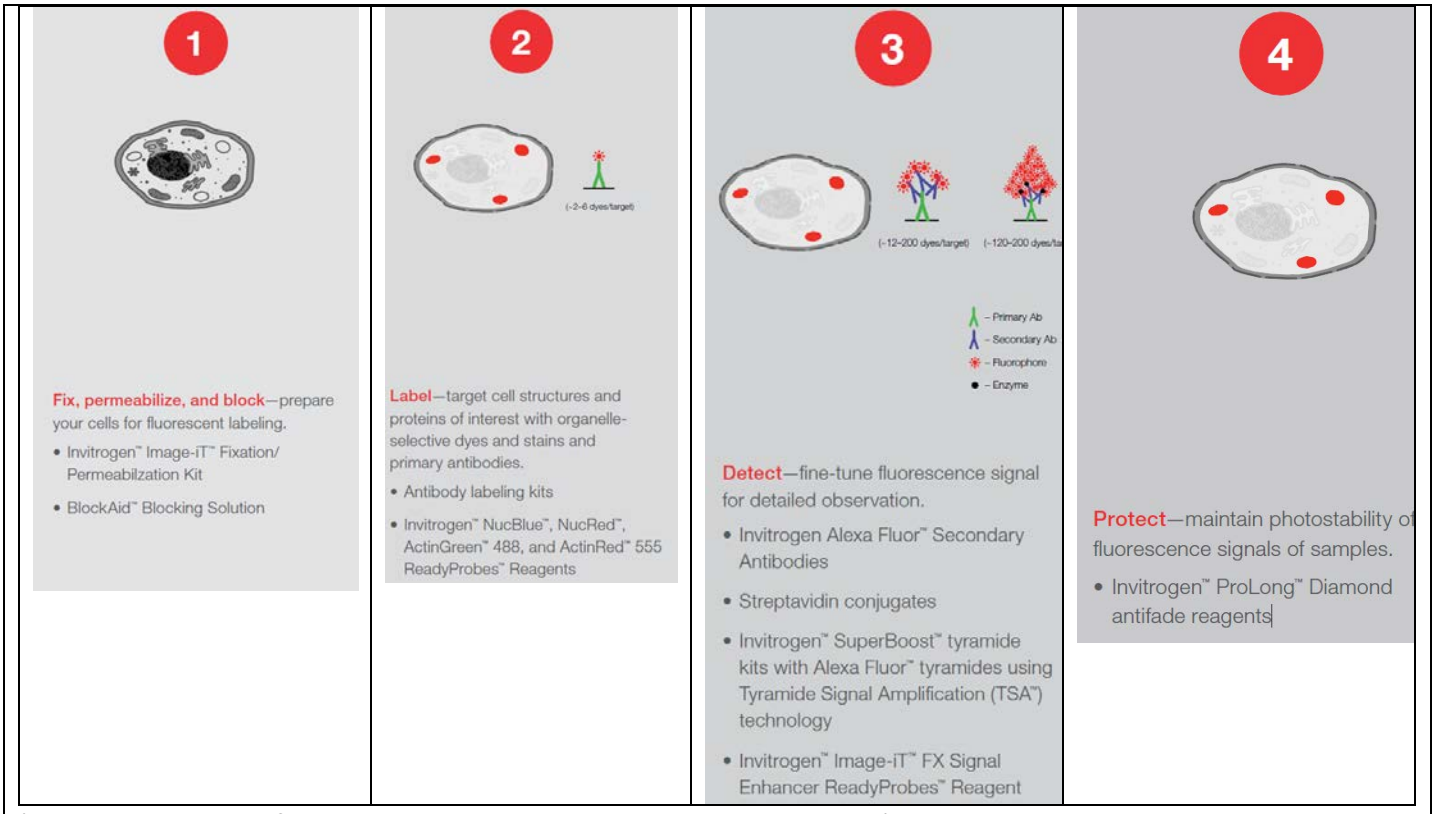

(step 5 involves use of EVOS microscope: not relevant to our image core).
I have a section in this document on tryamide signal amplification (TSA, including SuperBoost option).

My step 5: optimize image acquisition on one of our microscopes.
My step 6: quantitatively deconvolve your image data on Microvolution deconvolution software (MicFac has a license, a couple of buildings away in "Physiology" bldg – would be great if we can find money for a license). I note that Olympus FV3000RS (and maybe VS0120 slide scanner) have Olympus deconvolution software.

PTI RatioMaster Information: Ion imaging and potential excitation spectral scanning

20170712W: I am currently setting up the PTI RatioMaster components of the Zeiss AxioImager upright microscope (now in S972, was hiding in 'back' room for several months). This section provides web links to the company (PTI-NJ, now part of Horiba Jobin Yvon).
Our microscope hardware:

- Zeiss AxioImager (upright fluorescence microscope).
- Fluorescence illuminator: HXP metal halide "arc" lamp (to microscope).
- PTI RatioMaster monochromator (see below).
- MetaMorph Imaging System (acquisition: camera, Zeiss microscope, PTI RatioMaster).
- Photometrics Coolsnap HQ2 scientific grade CCD camera.

➔RatioMaster was designed for use with fluorescence excitation ratiometric imaging, such as:

- Fura-2 for Calcium ions (340, 380 nm)
- BCECF for intracellular pH (pHi) (440, 490 nm)

- Fura-2 *and* BCECF for Ca++ ions and pHi (340, 380, 440, 490 nm)
- SNARF or SNAFL for intracellular pH
- "ROS" indicators
- Fluorescent protein biosensors.

➔RatioMaster may also be useful for excitation spectral scanning ('stay tuned').

PTI Brochure (if download button does not work, try printing to PDF), I pasted summary paragraph below:

http://www.pti-nj.com/brochures/RatioMaster.pdf

PTI's time tested RatioMaster™, offering researchers solid, dependable, sensitive detection for the collection and analysis of ratiometric photometry data for calcium, pH, and intracellular ion imaging!
The RatioMaster™ is a microscope-based ratio spectrofluorometer capable of dynamic ratio fluorescence measurements on a millisecond timescale. A xenon arc lamp provides high intensity, continuous broadband illumination. Alternating excitation wavelengths are selected by a computer-controlled high-speed random access monochromator coupled to a inverted fluorescence microscope with a liquid light guide. Emitted light is collected from the sample and passed through a photometer with a bilateral translatable iris and a viewing eyepiece to a switchable analog/photon counting photomultiplier detector. Analog detection is used when emitted light is relatively intense while low light levels are detected by photon counting. All system functions are under computer control. Data is collected and analyzed by proprietary Windows™ based advanced fluorescence software.

http://www.pti-nj.com/products/Fluorescence-Microscopy/RatioMaster/RatioMaster-TechnicalNotes.html

RatioMaster Technical Notes (PDF downloads)

- Improving Signal-to-Noise Ratios in pH Measurements with BCECF (208 KB PDF)
- Advantages of Using a Scanning Monochromator (300 KB PDF)
- Fluorescence Indicators for Ion Detection (1.09 MB PDF)
  Remote Sampling of Intracellular Calcium Transients on Langendorff-Perfused Mammilian Whole Heart
  In-Situ Calibration on Intracellular $[Ca^{++}]_i$, $[Na^{+}]_i$ and pH_i
  The Effects of Reflector Design and Lamp Orientation

Lamp component

Lamp Power Supply
PTI RatioMaster lamp power supplies are highly-regulated DC units that provides very stable power for xenon, mercury, and mercury/xenon compact arc lamps as well as tungsten-halogen lamps.

Lamp power capacity	75 to 200 watts
Height	100 mm (3.9 inches)
Width	100 mm (3.9 inches)
Length	210 mm (8.3 inches)
Weight	1.9 kg (4.2 pounds)
Window diameter (D)	65 mm

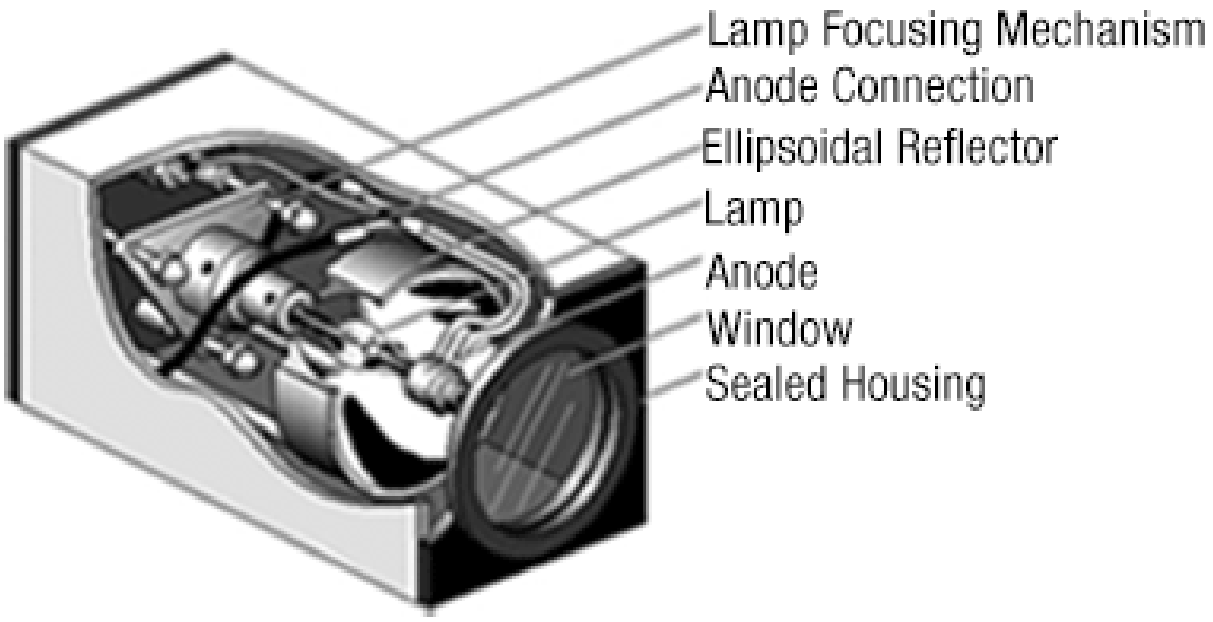

DeltaRAM X Monochromator component

http://www.horiba.com/us/en/scientific/products/fluorescence-spectroscopy/microscopy-mapping/pti-ratiomaster/

DeltaRAM X™ Random Access Monochromator

PTI RatioMaster's exciting new DeltaRAM X™ represents the next bold step in the evolution of light sources. The compact, proprietary (patented) single monochromator design permits the selection of any single wavelength in two milliseconds or less. It is ideally suited for multi-wavelength applications as well as excitation scanning. It is easily controlled via a single low voltage signal line. Includes a 2-meter liquid light guide, for use with most microscopes and other sample handling devices. DeltaRAM X™ delivers powerful excitation wavelength from 250–650 nm under synch-lock computer control. Synch-lock control, locks the DeltaRAM X™ monochromator to the camera exposure or frame readout. The DeltaRAM X™ saves you money by not requiring purchase of additional excitation filters for each dye you wish to use. Synch-lock allows accurate timing to be retained between camera and illuminator.

Systems not synch-locked can be plagued with synchronization problems or latency due to operating events or user clicking events. Try this in another imaging software package, click and drag a window, either the illuminator will stop moving, or images will stop being acquired until the mouse button is released. This does not happen with PTI RatioMaster's sync lock!

Excitation wavelength range	250–650 nm
Optimum scanning range	290–610 nm
Wavelength selection speed	< 2 milliseconds point-to-point
Resolution	< 1 nm
Accuracy	+ 3/-1 nm
Wavelength bandwidth	Adjustable from 0–24 nm
Stray light rejection	> 104
Light delivery	0.5 meter quartz fiber optic bundle

Liquid light guide	2 meter length 2 mm core diameter
Microscope adapter	User specified

PTI DeltaRAM Monochromator information on youtube (links for George)
Installing bulb (for George or PTI Service)
https://www.youtube.com/watch?v=DdgUEQzXndg

Getting bulb focused first time (for George or PTI service): "Focusing Lamps in PTI Arc Lamp Housings"
https://www.youtube.com/watch?v=IJ4pimIBKX0

PTI -- DeltaRAM High Speed Monochromator
https://www.youtube.com/watch?v=o0WZxok3CZg

How about Alexa Fluor 700 to add yet another fluorescence channel?! Owen Schwartz (NIH) likes AF700

Note: best to walk with 2, then 3 and later 4 color immunofluorescence, than get burned going for 5plex up front).

In principle, we can image (see also BD Brilliant's, ThermoFisher SuperBright's and PerkinElmer Opal TSA):

- Alexa Fluor 700 (NIR)
- Alexa Fluor 647 (NIR)
- Alexa Fluor 568 (or Cy3 or Alexa Fluor 555)
- Alexa Fluor 488 (or mClover GFP)
- DAPI (fixed cells) or Hoechst (H33258 or H33342)(live).

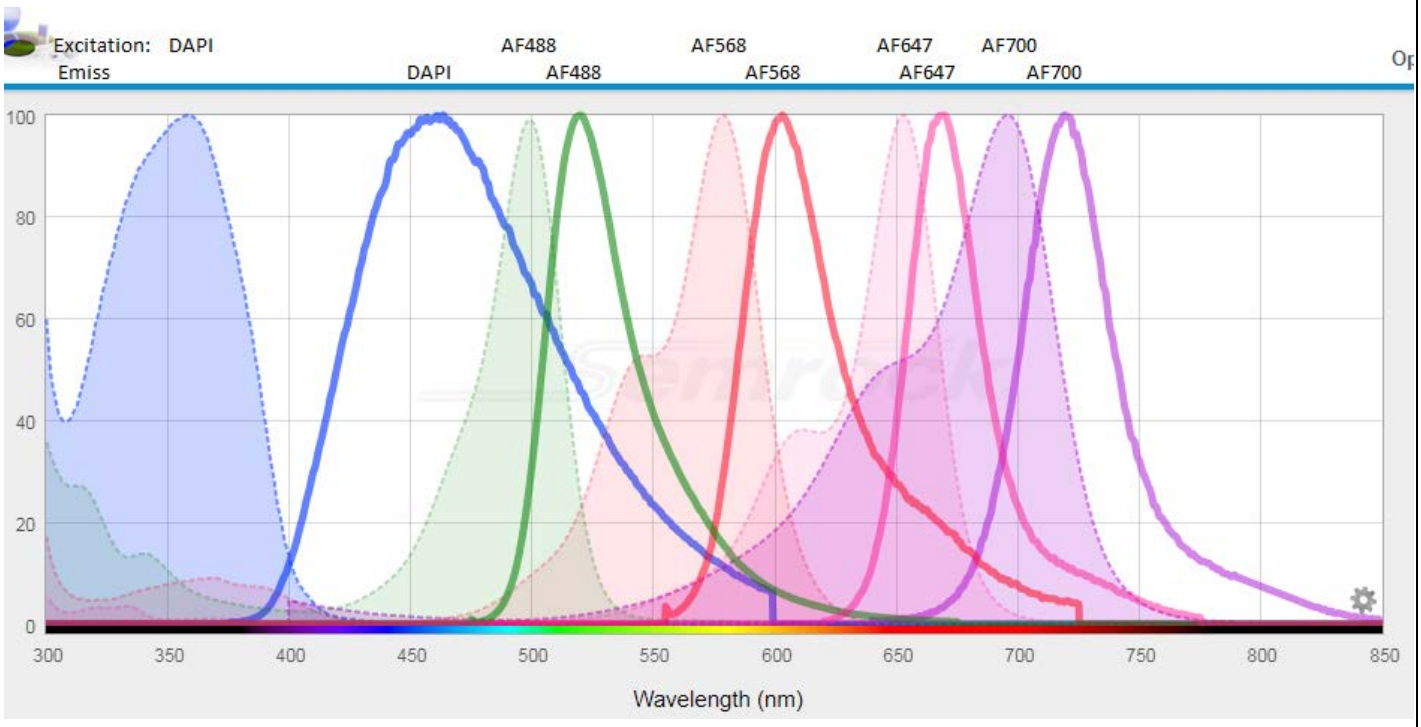

This article by Owen Schwartz (NIH) touts use of a 690 nm laser to excite well the AF700. Since we do not have a 690 nm laser (except for multiphoton!!!), I suggest evaluating 633 nm (or 642 nm on newer) confocal laser lines. We

could – if useful (and especially if a user contributes the $$ for the filter cube) but AF700 optimized filter set(s) for the widefield microscopes.

http://www.imaging-git.com/science/light-microscopy/far-red-laser-confocal-excitation

Schwartz O. 2016 GIT.

(part of essay)

Alexa 700 is bright even with low laser power, while crosstalk from Alexa 633 is minimal. …
To accommodate this, use of the complete bandwidth of the instrument is essential to minimizing crosstalk between the channels. Use of the 700-800 nm portion of the spectrum is of major benefit to this effort.
A number of new far red excitable probes for microscopy have been released in recently years. These include Alexa 700, 750 and 800 from Invitrogen, Silicon Rhodamine (SiR) 700 probes, and others such as Indo-cyanine green. Many of these are already used routinely for flow cytometry, but rarely for microscopy.
To add a longer wavelength laser to our SP8 confocal system, we worked with the development group at Leica Microsystems, Mannheim, Germany. A 690 nm laser proved to be the best compromise given the required mechanical compatibility, and the required excitation range.

PerkinElmer Envision plate reader (Ross Fluorescence Imaging Center has one) – account manager contact info

Matthew L. Reuter, MS
PerkinElmer Inc. | Human Health
Sr. Account Manager for Assay Chemistries and Detection Technologies
Mobile Phone: 443-928-4092
Email: Matthew.Reuter@perkinelmer.com

Brilliant(s)! … BD Biosciences Brilliant BB, BV, BUV fluorophores …. ThermoFisher SuperBright's

GM note: you must use BD's Brilliant's dilution buffer (a tube in every order) when using 2 or more Brilliant's together. If you fail to do this, expect 'brilliant aggregates' (can be great products, so do not let the requirement to use their buffer during labeling to dissuade you). I also note may photobleach faster than (say) Alexa Fluor 488.

https://www.bdbiosciences.com/us/applications/research/multicolor-flow/m/745795/products
Featured Fluorochromes
BD Horizon Brilliant™ Blue 515 Reagents
BD Horizon™ Brilliant Stain Buffer
BD Horizon Brilliant™ Violet BV480
BD Horizon Brilliant™ Ultraviolet Reagents

Lots of colors:

Fluorochrome-Conjugated Antibodies (Excitation Source/Emission Max)
BD Horizon Brilliant™ Ultraviolet 395 (BUV395) (355 nm/395 nm)
BD Horizon Brilliant™ Ultraviolet 496 (BUV496) (355 nm/496 nm)
BD Horizon Brilliant™ Ultraviolet 563 (BUV563) (355 nm/563 nm)
BD Horizon Brilliant™ Ultraviolet 661 (BUV661) (355 nm/661 nm)
BD Horizon Brilliant™ Ultraviolet 737 (BUV737) (355 nm/737 nm)
BD Horizon Brilliant™ Ultraviolet 805 (BUV805) (355 nm/805 nm)

BD Horizon Brilliant™ Violet 421 (BV421) (405 nm/421 nm)
BD Horizon Brilliant™ Violet 480 (BV480) (405 nm/478 nm)
BD Horizon Brilliant™ Violet 510 (BV510) (405 nm/510 nm)
BD Horizon Brilliant™ Violet 605 (BV605) (405 nm/602 nm)
BD Horizon Brilliant™ Violet 650 (BV650) (405 nm/650 nm)
BD Horizon Brilliant™ Violet 711 (BV711) (405 nm/711 nm)
BD Horizon Brilliant™ Violet 786 (BV786) (405 nm/786 nm)

BD Horizon Brilliant™ Blue 515 (BB515) (488 nm/515 nm)

ThermoFisher (eBiosciences component) has a few SuperBright's now (6/2017), may equal Brilliant's at ~20 each by end of 2017.

Micropatterned coverglass (or SBS plate): "morpho clones", cell statistics, endosomes are not generic

CYTOO (www.cytoo.com) is the best known company for buying micropatterned coverglasses or SBS plates, there are other companies and there are now microscope accessories and reagents for "do-it-yourself" micropatterning (the Multiphoton microscope 'has the power' to 'just do it', though maybe not the software).

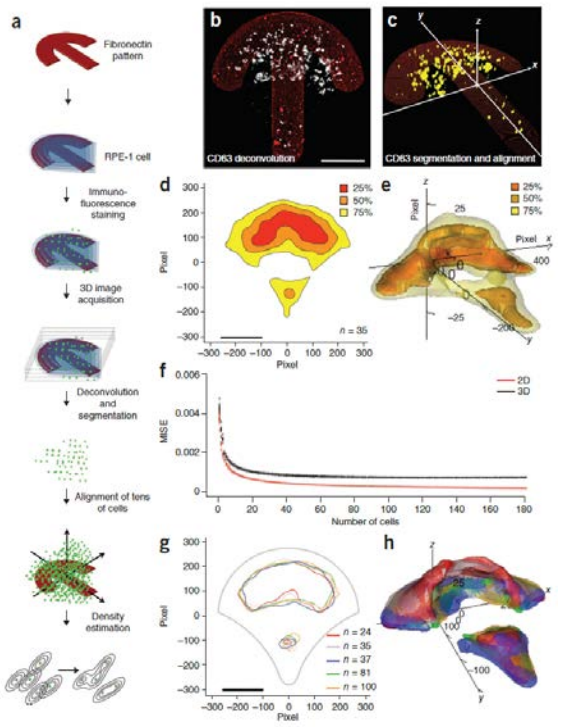

Schauer K et al 2010 - Figure 1 | Analysis of CD63-positive endomembranes from 35 cells on crossbow-shaped patterns. (**a**) Outline of experimental procedure. (**b**) Maximum intensity projection of the deconvolved fluorescence of CD63-positive endomembranes (white) and the fluorescently marked crossbow pattern (red). (**c**) Schematic representation of the segmentation and alignment procedure using the fluorescently marked crossbow pattern. (**d**) The 2D density estimation map with the indicated percentile probability contours representing the smallest regions in which the corresponding percentage of CD63-positive endomembranes were found. (**e**) The 3D density estimation map. For ease of visualization, the height (*z* axis) has been stretched fivefold. (**f**) Estimated MISE for 2D and 3D density estimation as a function of the number of CD63-positive cells analyzed. (**g**) Overlap of the 50% contour of the 2D estimation for five independent experiments. Each color represents an independent experiment using *n* cells. The outer gray outline represents spread of crossbow-shaped cells. (**h**) Overlap of the 50% contour of the 3D estimation for five independent experiments; color-code for independent experiments as in **g**. Scale bars, 10 µm.

➔Micropattern is ideal for studying localization of Rab's and other endosome markers (re: bacteria, bacterial toxin uptake, TLR's, STING, etc, localizations).

Schauer et al 2010 - **Figure 2** | Analysis of Rab5-, Sec13- and Rab6-positive endomembranes on crossbow-shaped patterns. (**a**–**c**) Maximum intensity projection of the deconvolved fluorescence of Rab5-positive (**a**), Sec13-positive (**b**) and Rab6-positive (**c**) endomembranes.

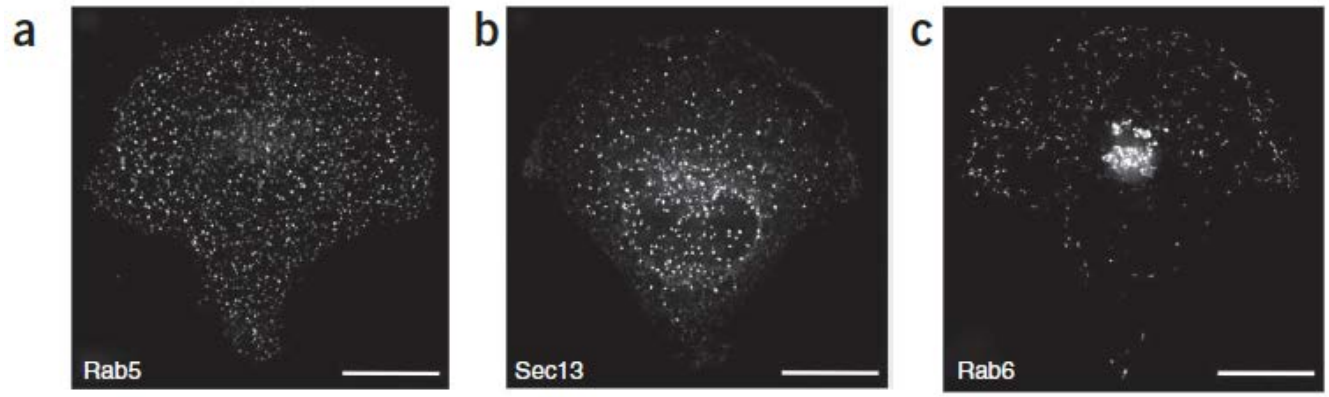

For example, using CYTOO's (www.cytoo.com) micropatterned coverglasses (also available multiwall plates) to make every cell a "morphological clone" ('morpho clone'), with the micropattern imposing 'apical' vs 'basolateral' polarity (maybe). This format would then facilitate imaging (cells in optimal XY flatness for optics) and statistics (morpho clone cells can be 'added' together, unlike random 'splat' tissue culture shapes). J.P. Thierry, coinventor of the CYTOO micropatterns, and a top cell-ECM interaction researcher, hypothesized that the CYTOO coverglasses impose 'bio-realistic' apical-basolateral polarity (whether JP is correct or not in context of intestinal cells can be tested … by you).

Schauer K, Duong T, Bleakley K, Bardin S, Bornens M, Goud B.Probabilistic density maps to study global endomembrane organization.Nat Methods. 2010; 7: 560-6. doi: 10.1038/nmeth.1462. PMID: 20512144
See also: "CELLebrate" https://www.youtube.com/watch?v=SZkBJnFx5yY

"Reflect on this": confocal reflection ('backscatter') mode can help your research

Confocal microscopy is often assumed to be fluorescence microscopy with optical sectioning. However, it can be extremely useful to also image reflected light.

- *Precision focusing coverglass-cell interface for consistency!!!* See Jiang et al 2010 figure below.
- Independent of how intense your fluorescence is. Example: ideal for "proving" your negative control is in focus.
- Enables you to find the correct focus, with optical sectioning.
- Interference reflection contrast microscopy (IRM, sometimes called RICM) shows you "edges" of cells at the coverglass, coverglass-cell interaction sites, especially focal adhesions vs "close contacts".
- Quantitative interference reflection contrast microscopy (qIRM, qRICM) enables you to quantify coverglass-cell interface distances with nanometer accuracy and precision (~5 nm). This can be done with 2 laser lines (dual wavelength qIRM) and an (optional) third wavelength can resolve some ambiguities (see box below discussing Barr, Bunnell 543 and 633 nm image pair.
- Other parts of cells, and other parts of your specimen, reflect light. Interpreting what is what is not trivial.

Barr, Bunnell (2009) Fig 4.23.4: IRM. I note that for a 1.3NA or 1.4NA oil immersion lens, confocal pinhole 1.0 airy unit, the optical slice thickness is ~0.6 um (600 nm).

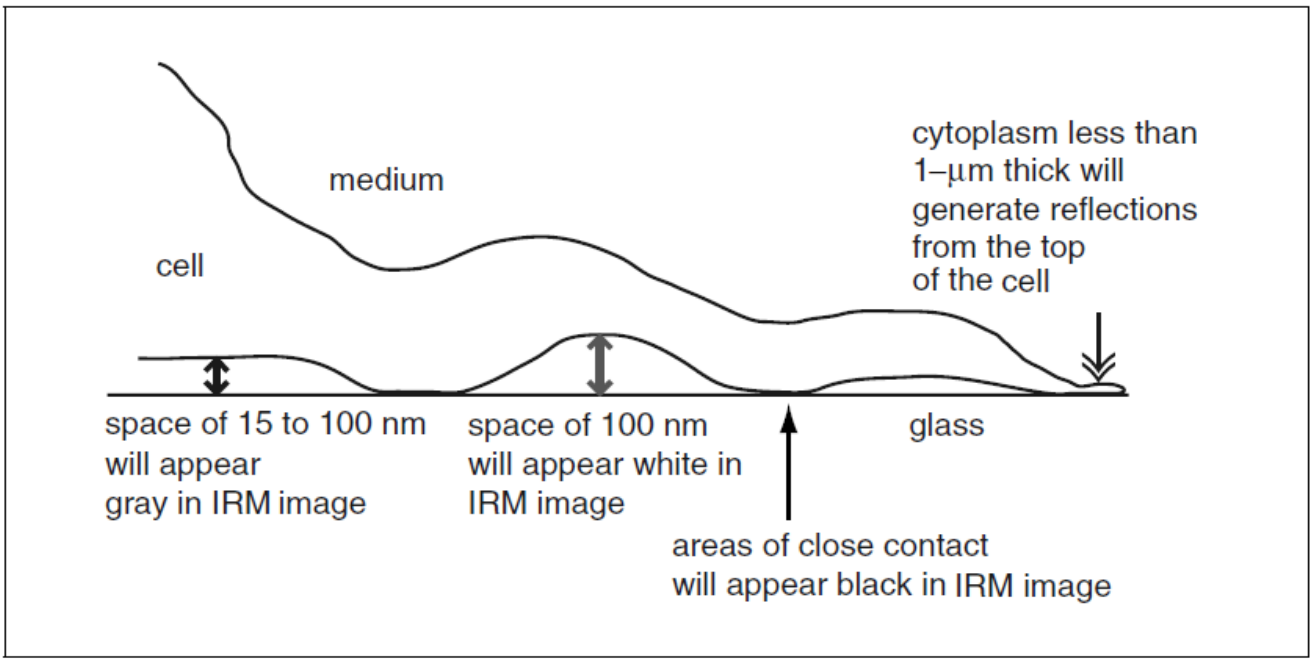

Figure 4.23.4 Gray-level intensities observed in a zero-order IRM images. The size of the gaps between the cell and coverslip have been exaggerated. A cell adhering to the coverslip will generate black areas on an IRM image in areas of close contact where the gap between the cell and coverslip is <15 nm (black arrow). If the gap is between 15 and 100 nm, the IRM image will show shades of gray (double-headed arrow). The brightest areas on the IRM image will come from areas where the cell is ~100 nm from the coverslip (gray double-headed arrow). If the cytoplasm is <1-μm thick (feathered arrow), reflections from the top of the cell will affect the intensity of the IRM image, so it will not be possible to approximate the distance between the cell and the coverslip unless the thickness of the layer of cytoplasm is known.

Two wavelengths example image pair from Barr, Bunnell (2009)

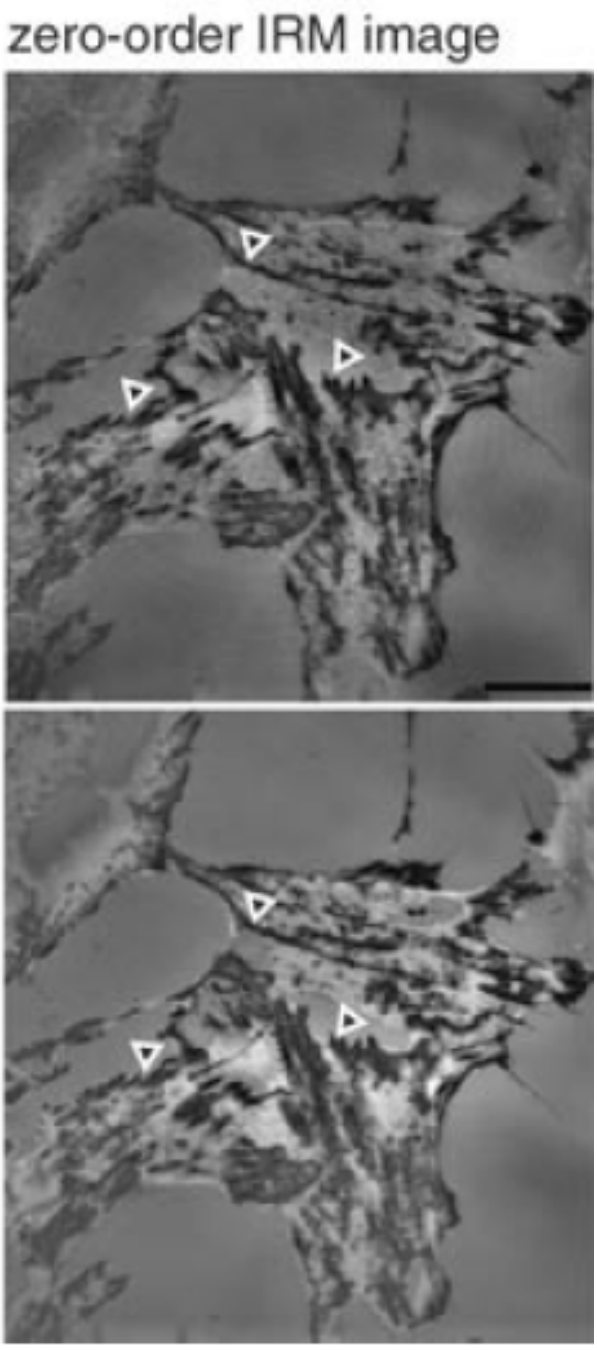

The image pair at left is from Barr, Bunnell (2009), 633 nm (top) and 543 nm (bottom) laser illumination.

The published purpose of the image pair was to illustrate *similarity* at the two wavelengths, especially of the black features (focal adhesion sites). I suggest two wavelengths "further parat but able to get high quality image pair" will be more useful, i.e. 633 nm laser line and 458 (or 476) nm laser lines on our Zeiss LSM510META. The 633 and 405 nm pair would in principle be even better for qIRM calculation (and 405 nm slightly better resolution), but in practice the 510META is not designed to let the user image 405 nm reflected light (one of many Zeiss dumb design features of the 510META).

Ideal qIRM would use 3 wavelengths. This would resolve certain ambiguities in the calculations of distances. My suggested wavelengths: 458nm, 561 nm, 633 nm (assuming 633 nm and the other two are perfectly parfocal).

The Zeiss LSM510META is not a great microscope for qIRM (or anything else in 2017). I suggest accessing a Leica SP5 or SP8 confocal microscope. I discuss SP5 IRM in https://works.bepress.com/gmcnamara/7

Suggestions:

1. get some help from JHU computer science or biomedical engineering student(s) [an undergrad class or a grad student) to program the qIRM calculation(s) in Fiji ImageJ.
2. I realize our main 3D enteroids and 2D monolayers-on-Transwells, are not "IRM friendly". There may still be opportunities to use 'real cells' (human intestinal cells from donors, patients) in single cell IRM and qIRM friendly format(s). For example, using CYTOO's micropatterned coverglasses (see entry in row above) can be very useful 'organizing' endosomes, and other features.

Jiang 2010 Blood, Fig 2C (not shown here: Fig 2E illustrates Dr. Xiaoyu Jiang's "HeLa tetrads" to get 4 granddaughter cells in one oil immersion lens field of view (Zeiss LSM510, yu Jiang's "HeLa tetrads" to get 4 granddaughter cells in one oil immersion lens field of view (Zeiss LSM510, 63x 1.4NA oil immersion, 2x zoom). Cells routinely imaged at 0.0 um (coverglass-cell interface defined by IRM brightest coverglass focal plane), +2.0 um, +4.0 um (pinhole 1 A.U., so ~0.6 um Z optical slices_.

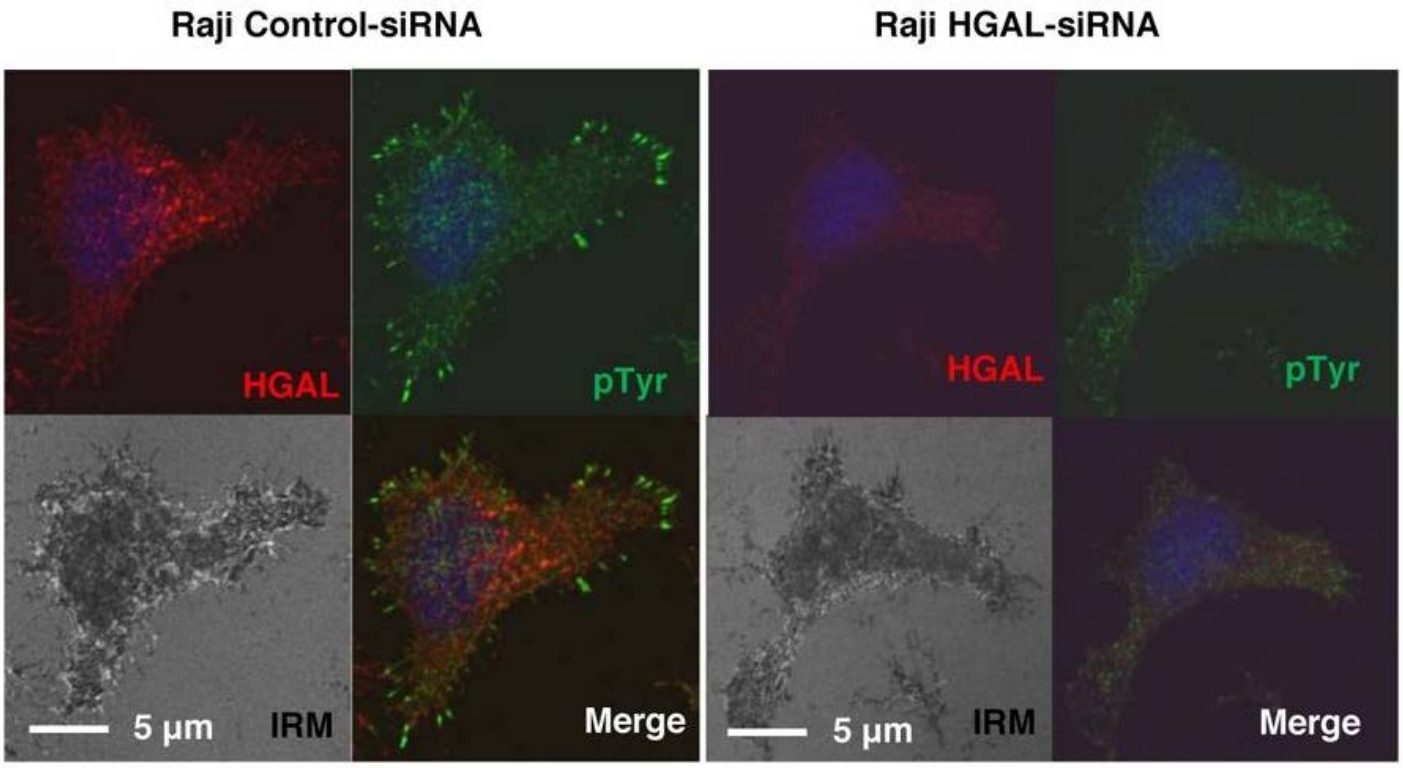

Barr VA, Bunnell SC. Interference reflection microscopy. Curr Protoc Cell Biol. 2009 Dec;Chapter 4:Unit 4.23. doi: 10.1002/0471143030.cb0423s45. PMID: 20013754.

Jiang X, Lu X, McNamara G, Liu X, Cubedo E, Sarosiek KA, Sánchez-García I, Helfman DM, Lossos IS. RhoA signaling pathway.Blood. 2010; 116: 5217-27. doi: 10.1182/blood-2010-04-281568. PMID: 20844236.

Limozin L, Sengupta K. Quantitative reflection interference contrast microscopy (RICM) in soft matter and cell adhesion. Chemphyschem. 2009;10: 2752-68. doi: 10.1002/cphc.200900601. PMID: 19816893

Monzel C, Fenz SF, Merkel R, Sengupta K. Probing biomembrane dynamics by dual-wavelength reflection interference contrast microscopy. Chemphyschem. 2009; 10: 2828-38. doi: 10.1002/cphc.200900645. PMID: 19821476

Schilling J, Sengupta K, Goennenwein S, Bausch AR, Sackmann E.Absolute interfacial distance measurements by dual-wavelength reflection interference contrast microscopy. Phys Rev E Stat Nonlin Soft Matter Phys. 2004; 69(2 Pt 1): 021901. PMID: 14995485
http://www.bio.ph.tum.de/uploads/media/PRE2004.pdf

20170810: Notes on how IRM and reflection contrast can be used to analyze specimen and optical system

Note (testing in image core 8/2017): The Olympus FV3000RS works great for IRM and other reflection contrast; the Zeiss LSM510META works ok. Each can use the 458 nm laser line, 405/488/561/633 “quad” master beamsplitter, and “go through” the “DAPI” emission light path (ex. BP420-480 on the Zeiss). The “RT10/90” (10% reflection, 90% transmission) master beamsplitter also works (and simplifies testing all laser lines).

//

(copy&paste from email).
fun with confocal reflected light, note that qIRM is quantitative Interference Reflection contrast Microscopy:

* 458 nm (also 514 nm, etc) reflection confocal works fine with Quad 405/488/561/633 nm primary dichroic (LSM510, FV3000RS).

* dual wavelength DW-qIRM (DW-RICM), Schilling 2004, enables "absolute" distances from coverglass to underside of cell, on a pixel by pixel basis. Ambiguities (where two cosine waves crossover) can be resolved by either:
  a) phase unwrapping from other pixels (will usually work)
  b) triple (or more!) qIRM = optical data only ... more is better! Plus info can be used as described below.

* Reflection from one (or a couple of) laser line(s)
  a) underside of coverglass (in inverted microscope geometry) = side closest to objective lens.
  b) "upper side" of coverglass (coverglass-mounting medium + cells/tissue).
  e) "top side" of specimen = mounting medium - slide surface (assuming slide or microfluidic chamber, rather than open dish with top far away).
  Payoffs:
  * coverglass thickness (do need to compensate for R.I. of glass). ==> better deconvolution, decide if should buy "0.170" coverglass dishes, or change to another manufacturer.
  * flatness of coverglass, both 'under' and "upper' sides, field per field (re: mattek #1.5 not flat, though I did observe some occasional fields at 40x/1.4NA being practically flat).
  * IRM, discussed above.

* Reflection from every laser line !!! Optional: shrink pinhole to <1.0 Airy unit for better axial resolution.
  a) is the objective "plan apo" with respect to:
    i) "plan" = flat field (may need an "optical flat" for this, and level stage ... can rotate the optical flat 90 degrees and/or other to test).
    ii) "apo" = color corrected at all wavelengths, including NIR (which is technically not color) and UV (expensive!)
  b) is the imaging system flat? "Is it live, or is it Memorex?" is a (somewhat) famous series of ads (see youtube). If the "plan apo" lens(es) is not flat, is it the lens(es) and/or the other optical components? Case in point: Semrock and/or Chroma are encouraging use of 2 mm thick dichroic beamsplitters for TIRF imaging (my advice: check out http://www.tirf-labs.com and consider using Alex Asanov's light guide or prism based TIRF illumiinators, instead of "through objective" TIRF - discussed in online supplemental file of my 2017 CPHG Unit).

Transmission on Confocal: You can acquire on the confocal microscope(s) – transmitted light image

Zeiss LSM510META is “ChD”.

This is comparable to what you see by eye, “TRANS” on the 510META.

In the next section (above) I discuss reflected light confocal imaging (which does have optical sectioning, also has “IRM”).

Confocal Light Microscopy XY Resolution ~214 nm, Z ~600 nm, implies pixel size ~60nm, Z step ~200nm

The XY resolution equation for widefield epi-illumination light microscopy is (definitions below):

Resolution(X,Y) = 0.61 * Lambda / NA

Example (I simplify the equation by ignoring the 0.01 in 0.61):

Resolution(X,Y) = 0.6 * 500 / 1.4 = 214 nm … which I then round to 200 nm.

My recommended “optimal” pixel size: Resolution / ~3.5 … 60 nm

For Z-step size, I am not including the equations (there is more than one to choose from), and simply state that Z resolution on a confocal microscope (at pinhole 1.0 Airy Unit) is ~3x bigger than XY resolution. That is:

(approximate) Resolution (Z, confocal, 1 Airy Unit) = ~600 nm.

You are not required by (any) law to use “optimal” pixel size, or Z-step size, defined by me, Zeiss, or any review. I do encourage you to take the time to think through to understand why the instrument default pixel size – i.e. 512x512 pixels at zoom of 1 – is unlikely to be either “optimal” by some theory or pundit, or more importantly, unlikely to be “best practice” for your experiment(s).

Lambda is wavelength of light, i.e. the emission peak of your fluorophore (a simpler number to obtain than the geometric weighted mean of fluorophore spectra). A convenient alternative when using LSM510 META ChS “band” or a bandpass emission filter is the center wavelength of the bandpass, i.e. 500-550 nm would be 525 nm.

NA is Numerical Aperture of the objective lens, NA = *n* sin (alpha), the ‘collection angle’ of the objective lens (*n* is refractive index of the immersion medium and mounting medium, in principle should be matched, ex. *n* = 1.515 for standard immersion oil for a 1.4 NA objective lens).

Why I like 60 nm XY pixel size (the relatively brief explanation): The ~3.5 is Nyquist sampling theorem (2.3 samples per sine wave) * 1.414 (diagonal of a pixel since XY not sine wave AND/OR use of confocal pinhole 1.0 Airy Unit in theory !!! improves resolution by sqrt(2) = 1.414). I am a big fan of quantitative spatial deconvolution (see earlier section below). When done correctly, deconvolution both “dehazes” the image AND improves resolution by ~10% (Goodwin 2014). The deconvolution software could interpolate from (say) 66 nm to 60 nm pixel size, but I think it much more sensible to acquire with pixel size (and Z-step) at the preferred output dimension.

I also note that ‘confocal’ works great in “reflected light mode”, sometimes called “backscatter mode”. If you are studying cell-coverglass interactions (or cell-very thin extracellular matrix-coverglass), interference reflection contrast microscopy (IRM, also known as RICM) is awesome in providing quantitation of focal adhesions and close contacts. More on quantitative IRM (qIRM) at https://works.bepress.com/gmcnamara/7 (the G.I. dept is much more into cell-matrix-transwell than cell-glass, so I minimize discussion of IRM and qIRM for now). Note: more on IRM above.

Goodwin PC. Quantitative deconvolution microscopy. Methods Cell Biol. 2014;123:177-92. doi: 10.1016/B978-0-12-420138-5.00010-0. PMID: 24974028.

20170726: Vitaly Boyko likes AutoQuant X3 for its linear deconvolution algorithm, which might be "more quantitative" than the algorithms used by Microvolution or SVI Huygens. All three companies now offer GPU processing (ex. NVidia Titan Xp cards) for near instant gratification deconvolution image processing. Whether any software (even if using the nominally same algorithm) is more or less quantitative, is hard to tell.

Multi-Probe Microscopy (2011)

I posted a document online (in 2011)
https://works.bepress.com/gmcnamara/2/
with more or less everything I knew about light microscopy. This was written mostly in 1995-2005, with a few updates through 2011.
Please do not hit the print button.

Apple Mac users networking SMB://networkname is equivalent to Windows PC \\networkname

That is, to connect to a local PC or server, assuming it has a drive or folder that is shared, and that you have login credentials for, the Macintosh address is formatted with forward slashes similar to an http://web address.

Online resources:

https://support.apple.com/en-us/HT204445

- The above web page has lots of great tips, one of which is: "You cannot type spaces as part of a share name when connecting. In place of any space in the share name, use %20 ."

https://users.wfu.edu/yipcw/atg/apple/smb/

George's guide to "the usual color scheme" for Alexa Fluor dyes

The usual colors for an immunofluorescence experiment are:

Blue (Nuclear counterstain)	DAPI	Hoechst 33258 or Hoechst 33342
Green	Alexa Fluor 488	(use AF488) (live cells: Clover3 FP)
Orange	Alexa Fluor 568	Alexa Fluor 555 > Alexa Fluor 546
Red	(none)	Alexa Fluor 594 or Texas Red
Near infrared (NIR)	Alexa Fluor 647	(use AF647)

See also "Tyramide Signal Amplification" section below (3rd from bottom), ~100 fold increase in signal, especially if you are (i) transitioning from DAB/HRP IHC, or (ii) using the Zeiss LSM510META confocal. Be sure to spend the time to re-titer your primary antibody (this can reduce background and save money).

Generally best to go with Blue, Green, Orange, NIR. The spectral unmixing of the Zeiss LSM510 is not very friendly for adding "Red" (AF594 or Texas Red).

DAPI vs Hoechst 33258 or Hoechst 33342 … Traditionally DAPI is used for fixed cell imaging and either Hoechst 33258 or Hoechst 33342 are used for live cell imaging. For live cell imaging, I recommend testing different concentrations of Hoechst (either). My memory is: If 10 mM bottle, dilute 100-fold in (sterile!!!) dH2O [so 100 uM), then dilute that 1000-fold in culture media (so 100 nM). Low laser power (405 nm laser or MP 750nm or try 780nm), moderate to high gain, ok to open pinhole >>1 Airy Unit.

Future: switch to Luke Lavis' Janelia Fluor dyes ("JF" dyes) and/or Abberior dyes (see sections below).

p.s. ok, Alexa Fluor 647 emission is near infrared, not technically a "color", since invisible to most human eyes (with bright enough labeling and right "for eyes" filter set, some people can see AF647 by eye).

Alexa Fluor 647 is very likely superior to Alexa Fluor 633 (G.I. lab has traditionally used AF633-Phalloidin)

Confocal listserv 6/2017 thread discusses comparison of these.

https://lists.umn.edu/cgi-bin/wa?A0=confocalmicroscopy
(login required at the listserv … there is a mirror at "nabble", if you prefer).

https://lists.umn.edu/cgi-bin/wa?A2=confocalmicroscopy;ee164028.1706 (Mon 6/19/2017 message in thread).

Brainbow and Confetti mice → enteroids and monolayers "paint by cell type" (GM suggestion)

The Brainbow and Confetti mice are nice, but how about (we/you!) make human enteroids and epithelial cell monoloayers.

There are lots of fluorescent protein colors available, see
http://www.geomcnamara.com/fluorescent-proteins-photophysics-data (columns sortable).
http://www.fpvis.org/FP.html (graphical interface plus tables by color below).

Color palette spans blue to near infrared. Multimerizing is good: V8 is 8x brighter than Venus (1x).

I suggest generating a **set of Master transcription factor "promoter response elements" ➔ fluorescent protein(s)**, localized to BOTH nucleolus and plasma membrane (dual targeting is not trivial, but is doable). Localizing results in "dimension reduction" so the same number of molecules are more concentrated:

- 1D nucleolus … very bright
- 2D nuclear envelope … 'pretty good' (FP-Lamin A).
- 2D plasma membrane … 'good' brightness.
- 3D nucleosol (FP-NLS nuclear localizing signal) or 3D chromatin (FP-Histone H3B) … 'not as bright' as 1d or 2D.
- 3D cytosol + nucleosol … 'dim'.

A classic example is 6x Hypoxia Response Element (6xHRE) for HIF-1alpha (may also be activated by HIF-2alpha and I note there is a HIF-3alpha, and various isoforms of each may activate or inhibit … also, HIF's require HIF-1beta = ARNT, which also is binding partner for AhR, which binds "DRE's" Dioxin response elements).

Possible approaches:

- Collaborate with thermoFisher/GeneArt/Invitrogen/Molecular Probes to have GeneArt (subsidiary) generate PREs➔FP(s) in DNA plasmid and Lentivirus (or other virus) formats (I am assuming for now we can transfect / transduce our cells of interest, i.e. 3D enteroid stem cells).
- MXS Chaining kit / "Colorful Cell" … generate in lab, collaborate with academic lab that published this, or find money to have a company do it (i.e. ThermoFisher … consider contacting Sean Yu, Epoch Life Sciences, Houston, for hard to clone projects). https://www.ncbi.nlm.nih.gov/pubmed/?term=mxs+chaining and in addgene.org:
- https://www.addgene.org/62449/ "ColorfulCell" (6 colors, each in a different organelle)
- https://www.addgene.org/browse/article/10274/ (MXS-Chaining Kit list).
- Note: I suggest reformatting "ES-Fucci" to use the current "Fucci2" proteins and localize to Nucleolus using NoLS (Nucleolar Localization Signal, also acts as a Nuclear Localization Signal).

Sladitschek HL, Neveu PA 2015 MXS-Chaining: A Highly Efficient Cloning Platform for Imaging and Flow Cytometry Approaches in Mammalian Systems. PLoS One 10: e0124958. doi: 10.1371/journal.pone.0124958. PMID: 25909630

The continuous improvement of imaging technologies has driven the development of sophisticated reporters to monitor biological processes. Such constructs should ideally be assembled in a flexible enough way to allow for

their optimization. Here we describe a highly reliable cloning method to efficiently assemble constructs for imaging or flow cytometry applications in mammalian cell culture systems. We bioinformatically identified a list of restriction enzymes whose sites are rarely found in human and mouse cDNA libraries. From the best candidates, we chose an enzyme combination (MluI, XhoI and SalI: MXS) that enables iterative chaining of individual building blocks. The ligation scar resulting from the compatible XhoI- and SalI-sticky ends can be translated and hence enables easy in-frame cloning of coding sequences. The robustness of the MXS-chaining approach was validated by assembling constructs up to 20 kb long and comprising up to 34 individual building blocks. By assessing the success rate of 400 ligation reactions, we determined cloning efficiency to be 90% on average. Large polycistronic constructs for single-cell imaging or flow cytometry applications were generated to demonstrate the versatility of the MXS-chaining approach. We devised several constructs that fluorescently label subcellular structures, an adapted version of FUCCI (fluorescent, ubiquitination-based cell cycle indicator) optimized to visualize cell cycle progression in mouse embryonic stem cells and an array of artificial promoters enabling dosage of doxycyline-inducible transgene expression. We made publicly available through the Addgene repository a comprehensive set of MXS-building blocks comprising custom vectors, a set of fluorescent proteins, constitutive promoters, polyadenylation signals, selection cassettes and tools for inducible gene expression. Finally, detailed guidelines describe how to chain together prebuilt MXS-building blocks and how to generate new customized MXS-building blocks.

For possible T.F.'s:

Cell lineage transcription factors adapted from text of:

Kanaya T, Ohno H 2014 Mechanisms of M-cell Differentiation. Bioscience of Microbiota, Food and Health Vol. 33: 91–97.
https://www.ncbi.nlm.nih.gov/pubmed/25032083
https://www.ncbi.nlm.nih.gov/pmc/articles/PMC4098651/pdf/bmfh-33-91.pdf (open access).

Kanaya 2014 BMFH - Mechanisms of M-cell Differentiation - Microfold cells - Ohno - RANKL vs OPG=Osteoprotegerin, RANK-TNFRSF11a, Ets SpiB Spi-B TF transcription factor

- Notch(#) → NICD(#) (NICD = Notch intracellular domain) (note: GM curious about fate(s) of extracellular facing "stub" of Notch after cleavage).
- Hes1 (i.e. stem cell marker, downstream of Notch).
- and other Notch pathway players, coolest named protein is "Mastermind".
- Wnt receptor(s) (Frizzled, etc).
- R-spondin receptor(s) … Lgr5, Lgr6.
- Atoh1 (repressed by Hes1 in the intestinal stem cells)

"secretory lineages, including goblet cells, Paneth cells, enteroendocrine cells and tuft cells [40]. Downstream of Atoh1, the specification of the individual secretory cell lineages requires at least one additional transcription factor":

- KLF4 is required for the maturation of goblet cells [41];
- Sox9 is required for the maturation of Paneth cells [42, 43];
- neurogenin3 is required for the maturation of enteroendocrine cells [44].
- SpiB (Spi-B) master T.F. for M-cells (Spi-B is an ets family member).

Other players:

- GP2 (GPI anchored glycoprotein … mature M-cells)
- RANKL = RANK Ligand = TNFSF11 … synthesized by other cells (GALT B-cells?)
- RANK = TNFRSF11a (receptor of RANKL) … on M-cells
- RANK → non-canonical (???) NF-KappaB pathway(s).
- Polymeric Ig Receptor (basolateral surface … gets shed as component of "secretory IgA" (sIgA) at apical surface … IgA(dimer) + J-chain + (part of) pIgA … GM would like to know what happens to "stub".

- "*Ulex europaeus* agglutinin-I (UEA-I), which binds α-1,2 fucosylated residues, has become a classical marker for murine M cells" … lectin UEA-1 and/or enzymes that generate the sugar(s).

Kanaya, Ohno 2014, Table 1:

Table 1. The list of published M-cell markers

Name	References
Annexin A5	[15]
CCL9	[16]
GP2	[2, 17]
Marcksl1	[17]
M-Sec	[19]
PGRP-S	[20]
PrP^c	[21]
Sgne-1	[18]
Umod	[22]

Iterative Expansion Microscopy (expand your specimens, not your mind)

20x higher resolution with the same microscope (~4.5x * 4.5x = 20x).
OK, more practical for some time will be the simpler original Expansion Microscopy, ~4.5x expansion, which still takes your experiments from a limiting XY resolution of ~214 nm, to ~50 nm and Z from ~600 nm to ~150 nm.

http://expansionmicroscopy.org protocols, references.
http://www.extbio.com kits

Chang JB, Chen F, Yoon YG, Jung EE, Babcock H, Kang JS, Asano S, Suk HJ, Pak N, Tillberg PW, Wassie AT, Cai D, Boyden ES
Iterative expansion microscopy.
Nat Methods. 2017 Jun;14(6):593-599. doi: 10.1038/nmeth.4261. Epub 2017 Apr 17.
We recently developed a method called expansion microscopy, in which preserved biological specimens are physically magnified by embedding them in a densely crosslinked polyelectrolyte gel, anchoring key labels or biomolecules to the gel, mechanically homogenizing the specimen, and then swelling the gel-specimen composite by ∼4.5× in linear dimension. Here we describe iterative expansionmicroscopy (iExM), in which a sample is expanded ∼20×. After preliminary expansion a second swellable polymer mesh is formed in the space newly opened up by the first expansion, and the sample is expanded again. iExM expands biological specimens ∼4.5 × 4.5, or ∼20×, and enables ∼25-nm-resolution imaging of cells and tissues on conventional microscopes. We used iExM to visualize synaptic proteins, as well as the detailed architecture of dendritic spines, in mouse brain
circuitry.
DOI: 10.1038/nmeth.4261 PMID: 28417997
https://www.ncbi.nlm.nih.gov/pubmed/28417997
https://www.nature.com/nmeth/journal/v14/n6/full/nmeth.4261.html
Note: see paper and/or http://expansionmicroscopy.org for first generation Expansion Microscopy references.

Click mucus

Click chemistry may enable you to make mucus fluorescent (maybe even in live cultures).

Tachaprutinun A, Pan-In P, Samutprasert P, Banlunara W, Chaichanawongsaroj N, Wanichwecharungruang S.
Acrylate-tethering drug carrier: covalently linking carrier to biological surface and application in the treatment of Helicobacter pylori infection.
Biomacromolecules. 2014 Nov 10;15(11):4239-48. doi: 10.1021/bm5012618. PMID: 25300443
The development of carriers to sustain drugs at stomach surface is an attractive strategy to increase drug bioavailability locally and systematically. So far, the only reported carrier that can form a covalent bond with mucus, the thiolated carrier, relies on a reversible disulfide exchange reaction between thiols on the carrier and disulfide bridges on the mucus. Here we show the design and fabrication of a cellulose carrier with tethering acrylate groups (denoted here as clickable carrier) that, under a nontoxic condition, can efficiently react with thiols on biomaterials in situ through the thermodynamically driven and kinetically probable Michael thiol-ene click reaction. Here we show the attachments of the clickable carriers to a mucin protein, a surface of human laryngeal carcinoma cells, and a surface of a fresh porcine stomach. We also show that the required thiol moieties can be generated in situ by reducing existing cystine disulfide bridges with either the edible vitamin C or the relatively nontoxic tris(2-carboxyethyl) phosphine. Comparing to a control carrier, the clickable carrier can increase some drug concentrations in an ex vivo stomach tissue, and improve the Helicobacter pylori treatment in infected C57BL/6 mice.

Johansson ME, Hansson GC.
Analysis of assembly of secreted mucins.
Methods Mol Biol. 2012;842:109-21. doi: 10.1007/978-1-61779-513-8_6. PMID: 22259132
Studies of assembly and secretion of gel-forming mucins are complex. The pulse-chase methods for mucins described here include metabolic radiolabeling and labeling in animals with azido-GalNAc. The labeled mucins are analyzed by composite agarose-polyacrylamide gel electrophoresis and autoradiography or by mucus-preserving tissue fixation and Click-iT(®) chemistry.
Note: authors used TAMRA-alkyne for fluorescence imaging (would also work for fluorescent gel documentation).

ThermoFisher/Molecular Probes sells “click” fluorophores in many colors.

https://www.thermofisher.com/us/en/home/references/molecular-probes-the-handbook/reagents-for-modifying-groups-other-than-thiols-or-amines/click-chemistry.html

Copper free click chemistry (Copper ions are generally considered toxic to live cells, so “copper free” is the way to go for live cells, and works perfectly well for fixed cells or biochemical experiments – I suggest standardizing on “Copper free” unless the vendor recommends copper).

https://tools.thermofisher.com/content/sfs/manuals/mp10405.pdf

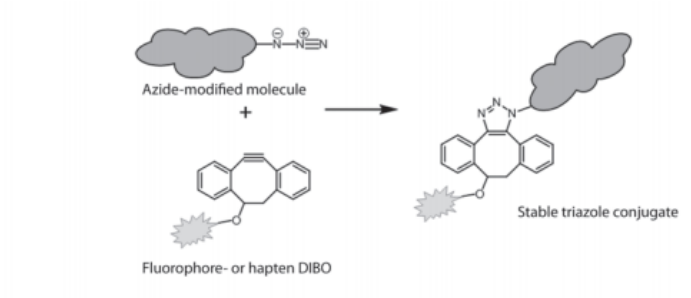

Figure 1. Copper-less click azide/DIBO reaction. The azide and alkyne moieties are interchangeable. The molecule can be labeled with a DIBO and reacted with a fluorophore or hapten-azide.

Table 2. DIBO modified fluorophores and haptens.

Label	Ex/Em*	Cat. no.	Use
Click-iT® DIBO-Alexa Fluor® 488	495/519	C10405	Fluorescent dye or hapten
Click-iT® DIBO-Alexa Fluor® 555	555/565	C10406	Fluorescent dye
Click-iT® DIBO-Alexa Fluor® 594	590/617	C10407	
Click-iT® DIBO-Alexa Fluor® 647	650/655	C10408	
Click-iT® DIBO TAMRA	555/580	C10410	
Click-iT® DIBO-biotin	NA	C10412	Hapten, Avidin binding

*Fluorescence excitation and emission maxima in nm. NA = not applicable.

Table 3. DIBO compounds containing reactive moieties.

Compound	Cat. no.	Reactivity
Click-iT® DIBO-amine	C10411	Carboxylic acids
Click-iT® DIBO-maleimide	C10413	Thiols
Click-iT® DIBO-succinimidyl ester	C10414	Primary amines

*Fluorescence excitation and emission maxima in nm. NA = not applicable.

Epithelial monolayer culture system for real-time single-cell analyses – Two O-rings surrounding filter (Seo 2014)

Physiol Rep. 2014 Apr 22;2(4):e12002. doi: 10.14814/phy2.12002. Print 2014.
Epithelial monolayer culture system for real-time single-cell analyses.
Seo JB[1], Moody M, Koh DS.

Abstract Many epithelial cells form polarized monolayers under in vivo and in vitro conditions.
Typically, epithelial cells are cultured for differentiation on insert systems where cells are plated on a porous filter membrane. Although the cultured monolayers have been a standard system to study epithelial physiology, there are some limits: The epithelial cells growing inside the commercial inserts are not optimal to visualize directly through lenses on inverted microscopes. The cell images are optically distorted and background fluorescence is bright due to the filter membrane positioned between the cells and the lens. In addition, the cells are not easily accessible by electrodes due to the presence of tall side walls. Here, we present the design, fabrication, and practical applications of an improved system for analysis of polarized epithelial monolayers. This new system allows (1) direct imaging of cells without an interfering filter membrane, (2) electrophysiological measurements, and (3) detection of apical secretion with minimal dilution. Therefore, our culture method is optimized to study differentiated epithelial cells at the single-cell and subcellular levels, and can be extended to other cell types with minor modifications.
Keywords: Ca2+ signal; electrophysiology; epithelial culture; imaging; salt secretion
PMID: 24771696 PMCID: PMC4001881 DOI: 10.14814/phy2.12002

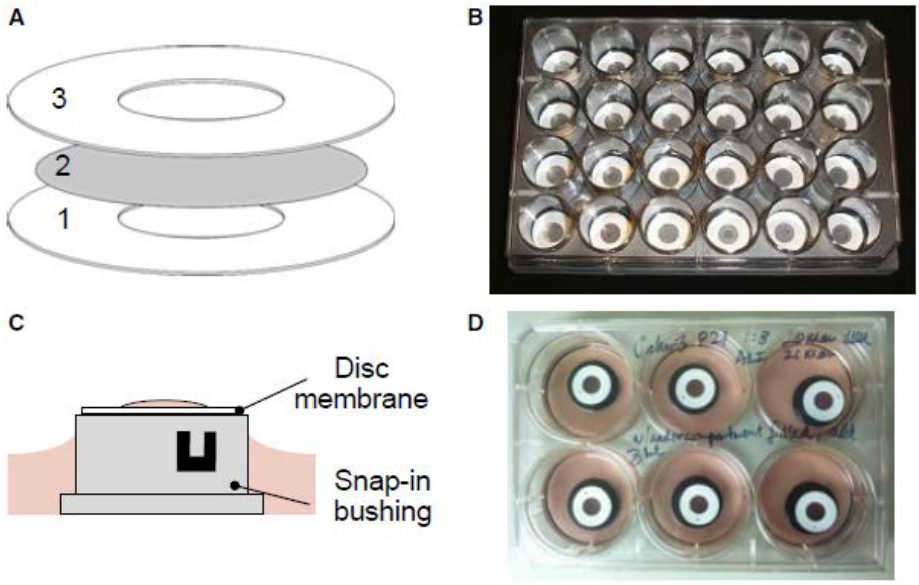

Figure 1. Fabrication of disk membranes and culture method. (A) Disk membrane 'sandwich' construction. Disks comprised three layers: two thin O-rings with a filter membrane in the middle. See Materials and Methods for detailed information. (B) Assembled and coated disk membranes in a standard 24-well plate ready to be used for submerged cell culture. (C, D) Air–liquid interface culture of Calu-3 cells. A schematic diagram for a disk membrane sitting on the top of a nylon snap-in bushing (C) and disk membranes containing confluent Calu-3 cells in a six-well plate (D). First, each well is filled with 4.5-mL culture medium and a bushing (black) is added. It is necessary to take care to exclude bubbles from under the disk membrane. The disk membrane assembly allows serosal retention of approximately 1 mL of culture medium through surface tension. A portion of medium (3.5 mL) is freshly exchanged two or three times per week. Two vents on the sides of the bushing promote free exchange of medium to the basolateral surface of Calu-3 cells.

" Disks comprised three layers: two thin O-rings with a filter membrane in the middle."

Transwell inverted configuration - Wakabayashi (2007)
… may make your imaging more efficient.

➔added 20170614: Corning Costar Snapwell insert uses polycarbonate membrane, may be transparent. Two web links are:

https://catalog2.corning.com/LifeSciences/en-US/Shopping/ProductDetails.aspx?productid=3407(Lifesciences)
Costar® 12mm Snapwell™ Insert with 0.4µm Pore Polycarbonate Membrane, Sterile (Product #3407).

Sigma-Aldrich webpage
http://www.sigmaaldrich.com/catalog/product/sigma/cls3407?lang=en&region=US

//

➔My thinking is this "inverted configuration" could be used with Mattek or other 35mm imaging dishes (ex. one case of 200 sterile dishes, ~$335, https://www.mattek.com/store/p35g-1-5-10-c-case/).

Wakabayashi Y1, Chua J, Larkin JM, Lippincott-Schwartz J, Arias IM.
Four-dimensional imaging of filter-grown polarized epithelial cells.
Histochem Cell Biol. 2007. 127: 463-472.
https://www.ncbi.nlm.nih.gov/pubmed/17308935
https://link.springer.com/article/10.1007%2Fs00418-007-0274-x

Understanding how epithelial cells generate and maintain polarity and function requires live cell imaging. In order for cells to become fully polarized, it is necessary to grow them on a permeable membrane filter; however, the translucent filter obstructs the microscope light path required for quantitative live cell imaging. Alternatively, the membrane filter may be excised but this eliminates selective access to apical and basolateral surfaces. Conversely, epithelial cells cultured directly on glass exhibit different phenotypes and functions from filter grown cells. Here, we describe a new method for culturing polarized epithelial cells on a Transwell filter insert that allows superior live cell imaging with spatial and temporal image resolution previously unachievable using conventional methods. Cells were cultured on the underside of a filter support. Epithelial cells grown in this inverted configuration exhibit a fully polarized architecture, including the presence of functional tight junctions. This new culturing system permits four-dimensional (three spatial dimension over time) imaging of endosome and Golgi apparatus dynamics, and permits selective manipulation of the apical and basolateral surfaces. This new technique has wide applicability for visualization and manipulation of polarized epithelial cells.
PMID: 17308935 DOI: 10.1007/s00418-007-0274-x

Don't forget the popcorn! Supplemental videos at
https://link.springer.com/article/10.1007%2Fs00418-007-0274-x#SupplementaryMaterial

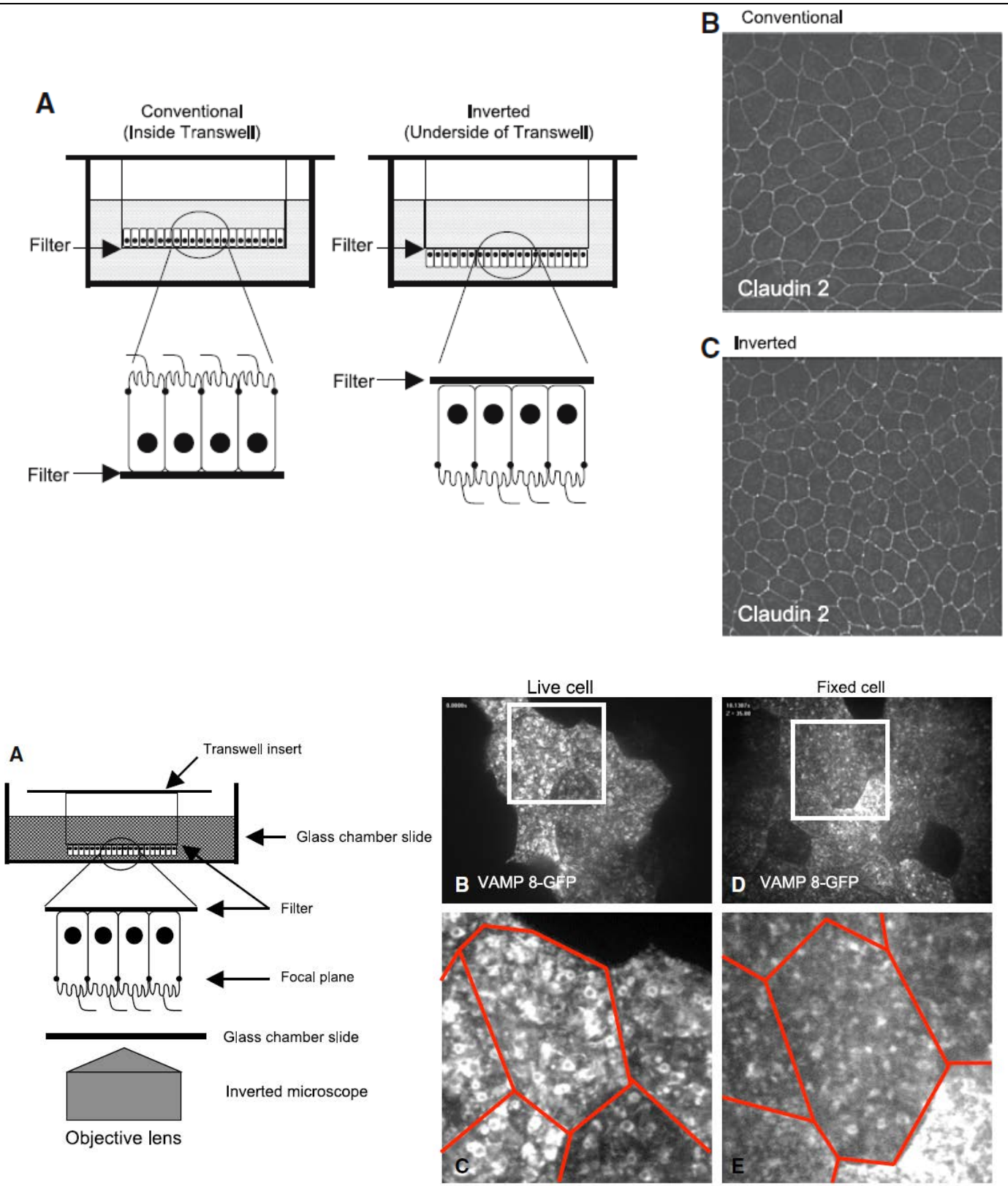

Fig. 4 Live cell imaging of endosome dynamics. **a** Schematic diagram of live cell imaging of MDCK cells grown on the underside of a filter insert. MDCK cells stably expressing VAMP 8-GFP were imaged under live conditions (**b**) and fixed conditions (**d**). **c** *Insert* in **b**. **e** *Insert* in **d**. *Red line* denotes cell boundary. See supplementary movies 1–3

Cell culturing on coverglass vs "imaging dish": Use the dish!

Coverglass:

- Hard to handle
- Easier to flip wrong side up
- Typically culture in a SBS plate (ex. 6-well plate), which costs money and waste a lot of reagents.

Imaging dish:

- Glass bottom ➔ best image quality with full range of objective lenses.
- Fixative easy to handle, can use large volume. “Law of mass action wins”.
- Wash steps: more volume, more wash cycles, are better. Pipet to edge of the plate (not the glass-plastic edge).
- Precious cells and/or reagents? Use smaller imaging area size dish (7 mm, 10 mm, 14 mm, 20 mm, 30 mm available).
- No bubbles! Just drop on the mounting medium (adding a coverglass on top is optional).

My “standard of care” is Mattek 35 mm diameter dish, 20 mm imaging area, “No. 170” coverglass (which means 0.170 mm thick = 170 um thick, more importantly, standard deviation is +/- 5 um).

➔My thinking is these imaging dishes can be used with the “ Transwell inverted configuration may make your imaging more efficient.”

https://www.mattek.com/products/glass-bottom-dishes/

Microwell Diameter

	7 mm	10 mm	14 mm	20 mm	30 mm
35 mm	■	■	■	■	
50 mm			■		■
60 mm				■	■
100 mm					■

For most applications, a 14 mm glass microwell is sufficient. Choose the 20 mm diameter microwell to maximize viewing area, or a 10 mm diameter if your application is cell-limited or to limit media or reagent consumption.

Glass Thickness

	No. 0	No. 1.0	No. 1.5	No. 0.170	No. 2.0 (Grid)
35 mm	■	■	■	■	■
50 mm	■		■		■
60 mm			■		
100 mm			■		

For most applications, No. 1.5 is the preferred coverslip thickness, especially for optimizing image quality with high numerical aperture objectives. The No. 0 coverslip gives you the most working distance and may be useful for thicker specimens.

Coatings: MatTek offers Poly-d-lysine and collagen coated dishes.

Mattek and Nunc Lab-Tek each offer Chambered Cell Culture Slides … I am not a fan, because the coverglass version gives better image quality, but are often broken when trying to take off the top. One option: just leave the chamber on.

https://www.mattek.com/products/chambered-cell-culture-slides-2/
https://www.thermofisher.com/order/catalog/product/154453

Greiner Bio-One offer lots of stuff, as does ThermoFisher (and often significant discount from list when ordering through ThermoFisher/FisherSci, due to University vendor agreement).

Refractive index matching is critical for best results.

Fixed cells: identical refractive index for the cells&mounting medium AND coverglass AND immersion medium, produces optimal results. Since the glass is RI=1.515, and we have immersion oil from Zeiss RI=1.518 ('close enough' to RI of glass), this leaves the cells (presence or absence of lipid membranes) and mounting medium, under YOUR control.

Please note: RI and NA are not the same thing!!!
RI = refractive index, of media and material.

Coverglass and optical glass RI	1.515
oil	1.518
water (or PBS)	1.333
vacuum or air	1.0

NA = numerical aperture, an objective lens specification based on NA = *n* sine(alpha), with *n* being the RI of the media the lens is designed to work with.

Perfect RI matching enables
➔maximum brightness (fluorescence signal) both at the coverglass and 'at distance', see Staudt 2007 Fig 6 below.
Staudt ... Hell 2007 2,2'-thiodiethanol: a new water soluble mounting medium for high resolution optical microscopy. Microsc Res Tech. 70: 1-9.
http://onlinelibrary.wiley.com/doi/10.1002/jemt.20396/pdf

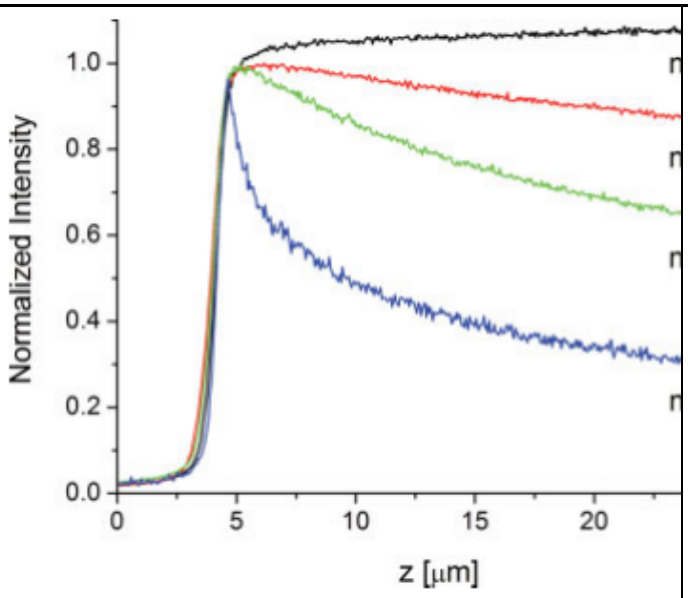

Fig. 6. Confocal axial (z-) scans at the interface of a dye with the glass coverslip using an oil immersion lens of 1.46 75°. The coverslip is located at $z = 4.0$ μm. At positions $z <$ glass and dye solution at $z > 4$ μm. The curves correspond to ferent refractive indices set by using different TDE concentra indicated. The deeper the beam is focused into the sample, t photons are collected due to spherical abberations introduce fractive index mismatch. In case of matching refractive index nal is constant along the optic axis.

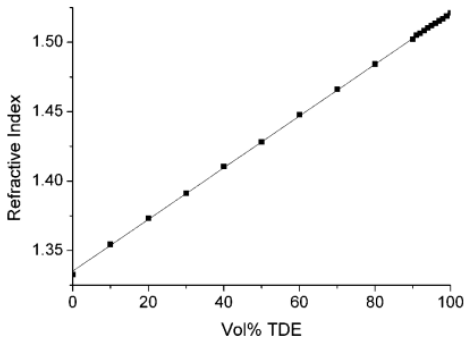

Fig. 3. TDE (2,2′-thiodiethanol) is miscible with water in any proportion. The refractive index of the solution can be precisely tuned to any value between 1.333 (water) and 1.521. The latter is even slightly larger than that of immersion oil.

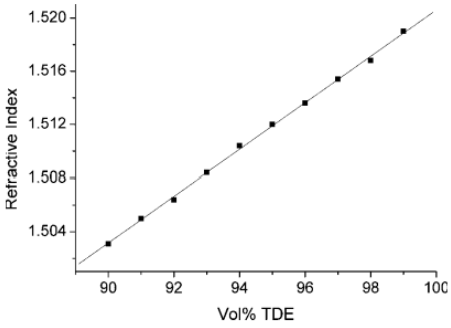

Fig. 4. TDE allows a precise setting of the refractive index by adjusting the water content. For use with an oil immersion lens, a TDE concentration of 97% in water was employed.

Lam 2017 is pretty good, but not perfect (ex. of latter: they do not correctly account for scanning speed)

Super-resolution for everybody: An image processing workflow to obtain high-resolution images with a standard confocal microscope.
Lam F, Cladière D, Guillaume C, Wassmann K, Bolte S.
Methods. 2017 Feb 15;115:17-27. doi: 10.1016/j.ymeth.2016.11.003. PMID: 27826080
http://www.sciencedirect.com/science/article/pii/S1046202316304364 (open access)

******

Live cells: Ask john Gibas, Olympus, about their Silicon oil immersion lenses, for RI matching with live cells (coverglass RI still 1.515, but since parallel to optical path, least critical to RI match).
https://www.olympus-global.com/en/common/pdf/eprecognition_120.pdf

Silicone Immersion Objective UPLSAPO30XS/40XS/60XS/100XS

This silicone immersion objective is one of UIS2 microscope objective for biology.
It has large numerical aperture (30XS:1.05, 30XSIR:1.05, 40XS:1.25, 60XS2:1.3, 100XS:1.35) and it is possible to observe deep part of a living cell by unprecedentedly high resolution when it is used with silicone oil.
Also, it has correction circle that correct aberration by changing cover glass thickness (30XS:0.13-0.19, 30XSIR:0.13-0.19, 40XS:0.13-0.19, 60XS2:0.15-0.19, 100XS:0.13-0.19) and temperature (23-37 degrees).
It can be used for bright-field transmission, fluorescent observation, differential interference contrast and multi-photon.

Want better fluorescent dyes? Luke Lavis (HHMI Janelia Research Campus)
Luke has them (and gives some away).

Luke Lavis – Janelia Fluor's
https://www.janelia.org/open-science/janelia-fluor-dyes
Spectral tuning dyes to match popular laser lines
http://biorxiv.org/content/early/2017/04/14/127613 (2017).
10x improvement in photostability by appending Azetidine ring(s)
https://www.ncbi.nlm.nih.gov/pubmed/25599551
https://www.nature.com/nmeth/journal/v12/n3/full/nmeth.3256.html (Grimm 2015).

Want better fluorescent dyes? Abberior (Stefan Hell's company)
Abberior fluorescent dyes:

- STAR … mostly for fixed cells.
- LIVE (510, 515, 580)
    - LIVE dyes are designed for cell permeability
    - LIVE dyes are optimized for live-cell STED & confocal imaging
    - Conjugates are tested for specific targets: tubulin, actin, lysosomes
        - Actin (jasplakinolide) 50 µg
        - Tubulin (cabazitaxel) 50 µg
- Phospholipids**:** Try the new Abberior dye-labelled phospholipids DOPE, DPPE, C12 Sphingosyl PE (d17:1/12:0) for your membrane labelling experiments!
- Biotin: All Abberior dyes are now available coupled to biotin to be used for fluorescent labelling of avidin/Streptavidin/Neutravidin-conjugated molecules.
- Streptavidin/Neutravidin: Target your biotin-labelled molecule of interest with our new Abberior dye Streptavidin and Neutravidin conjugates.
- Carboxylic acid: Make your own Abberior dye derivatives/conjugates with our carboxylic acids!
- New secondary antibody specificities: We now offer goat anti-rat IgG, goat anti-guinea pig IgG and goat anti-chicken IgY conjugated to all Abberior dyes.

Mounting media (all for fixed cells, may want to permeabilize the cells too)
http://www.abberior.com/shop/Microscopy-Supplies:::8.html

- Abberior TDE Mounting Medium is a specimen mounting medium designed for use in high-resolution fluorescence microscopy
- Abberior Mount Solid is an aqueous mounting medium designed for confocal and superresolution microscopy.
- Abberior Mount Liquid is an aqueous mounting medium designed for 3D confocal and superresolution microscopy.

Figure below: ignore the "down arrows" because these are for STED depletion.
http://www.abberior.com/references/dye-overview/overview-abberior-dyes

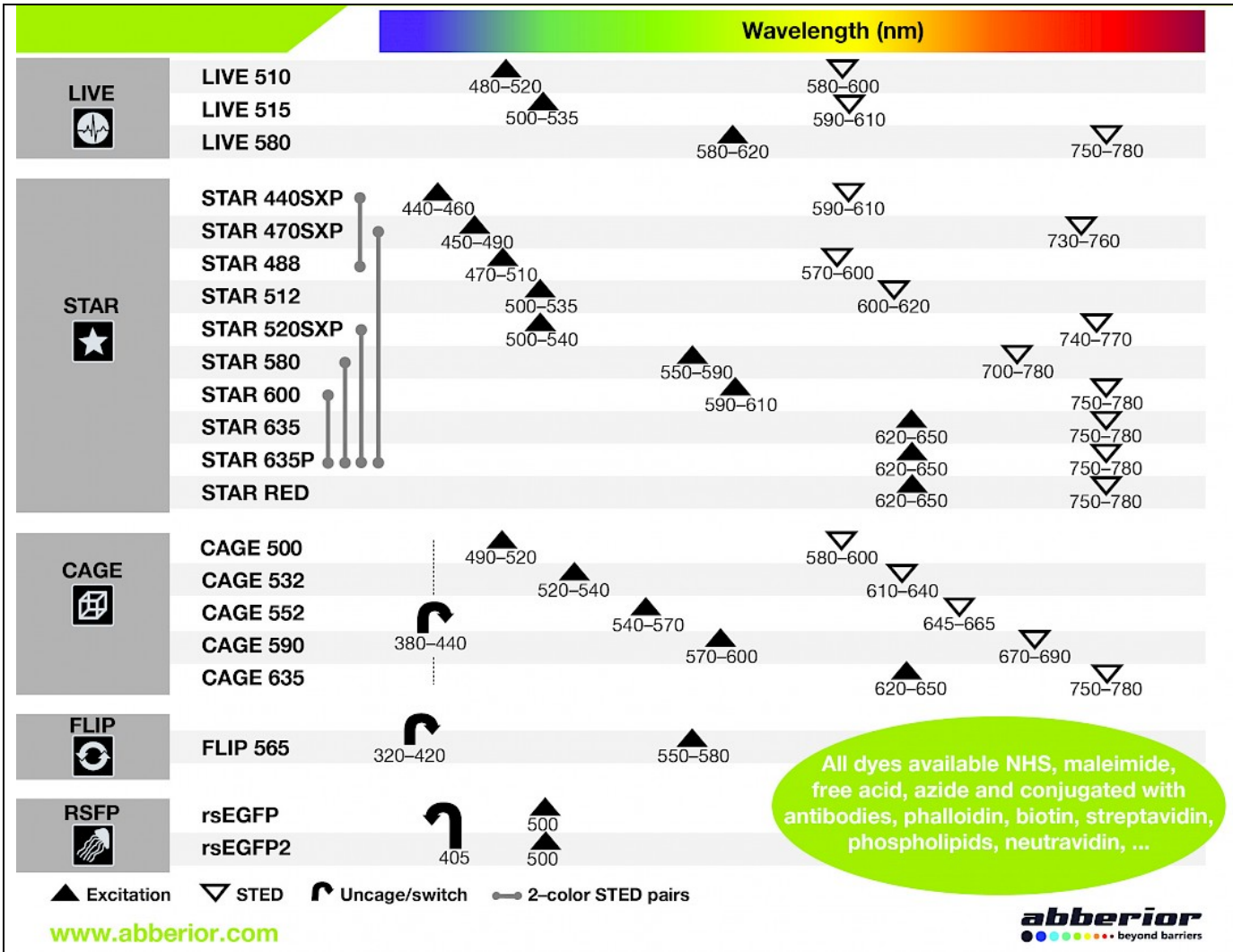

McNamara 2007: Color Balancing Histology Images for Presentations and Publication" (using Photoshop).

home.earthlink.net/~geomcnamara/McNamara2005JoH28n2pp81-88.pdf (JHU I.T. appears to be blocking this web site).

➔ I used to teach classes on "Scientific Imaging with Adobe Photoshop". Contact me if interested (note: I have higher priorities).

See also 20171222 post.

I am a big fan of fluorescent proteins and fluorescent protein biosensors
http://www.geomcnamara.com/**fluorescent-proteins**-photophysics-data

http://www.geomcnamara.com/fluorescent-**biosensors** (newer list than on the poster by olga's lab).

McNamara G, Boswell CA 2007 Thousand Proteins of Light: 15 years of advances in fluorescent proteins.
http://www.formatex.org/microscopy3/pdf/pp287-296.pdf

Please be aware that my FP "knowledge base" is almost entirely by reading literature and listening to seminar speakers, conversations, and emails. I am not a molecular biologist, protein chemist or spectroscopist.

20170719 update: glucose biosensor ('LoogerGlu'), chloride (mCl-YFP)

Loren Looger glucose sensor ("ratiometric"):

The Oscillating Stimulus Transporter Assay, OSTA: Quantitative Functional Imaging of Transporter Protein Activity in Time and Frequency Domains.
Keller JP, Looger LL.
Mol Cell. 2016 Oct 6;64(1):199-212. doi: 10.1016/j.molcel.2016.09.001.
PMID: 27716484

A genetically-encoded YFP sensor with enhanced chloride sensitivity, photostability and reduced ph interference demonstrates augmented transmembrane chloride movement by gerbil prestin (SLC26a5).
Zhong S, Navaratnam D, Santos-Sacchi J.
PLoS One. 2014 Jun 5;9(6):e99095. doi: 10.1371/journal.pone.0099095. eCollection 2014.
PMID: 24901231

20170719 update: increase photostability with any of Y145L (or Y145M), S205V, E222H
S025V is in Zhong 2014 PLoS One, above (also introduced monomeric mutations, either L221K or A206K).

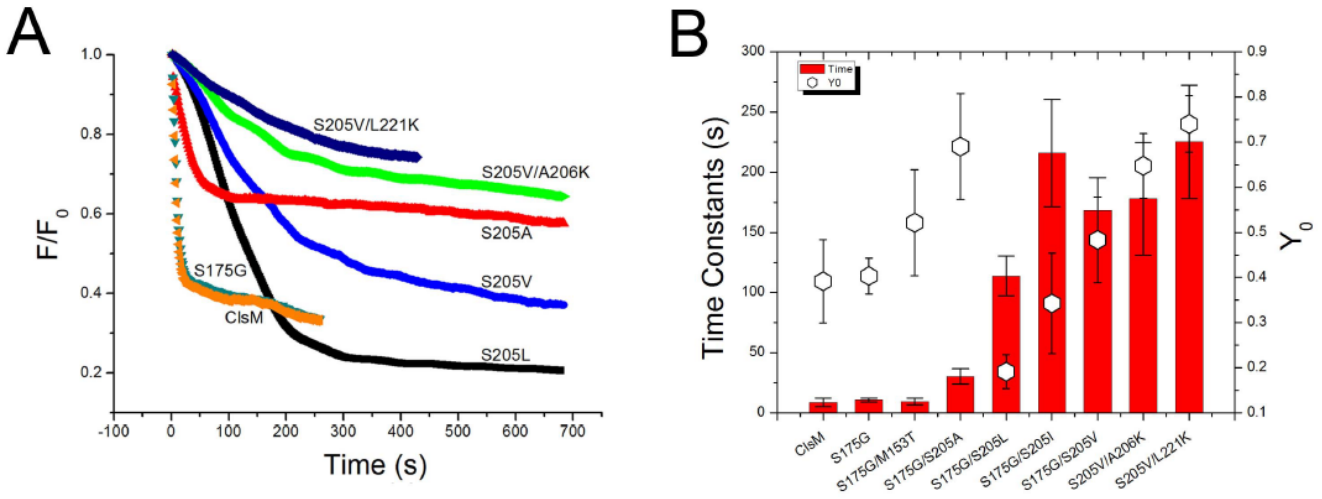

Figure 1. Photobleaching dynamics of YFP chloride sensor mutations. (**A**) Representative traces of some YFP variants photobleached at 430 nm. All variants are based on the EYFP-F46L/Q69K/H148Q/I152L/V163S (**ClsM**). Photobleaching data were fit by a single exponential decay function, $Y = Y_0 + Ae^{-x/t}$, where Y_0 is the constant offset representing the residual fluorescence after photobeaching (R^2 ranged from 0.96–0.99). It is notable that the mutant ClsM-S175G/S205V/A206K (mClY, green curve) has a long time constant of 175 s under our photobleaching conditions, which is much longer than wild-type YFP and **ClsM** each at ~10 s. (**B**) The red columns are the time constants of fluorescence decay during photobleaching, and Y_0 is the constant offset of fluorescence exponential decay by photobleaching, representing the residual fluorescence when photobleaching reached a stable state. The folding mutations of S175G and M153T did not enhance the photostability of **ClsM**, while the mutations of S205 did increase the time constants of fluorescence decay.
doi:10.1371/journal.pone.0099095.g001

E222H (instead of more common E222Q):

Photophysics of EGFP (E222H) Mutant, with Comparisons to Model Chromophores: Excited State pK's, Progressions, Quenching and Exciton Interaction.
Kirk W, Allen T, Atanasova E, Wessels W, Yao J, Prendergast F.
J Fluoresc. 2017 May;27(3):895-919. doi: 10.1007/s10895-017-2025-2. Epub 2017 Feb 20.
PMID: 28217828

Replacement of highly conserved E222 by the photostable non-photoconvertible histidine in GFP.

Auerbach D, Klein M, Franz S, Carius Y, Lancaster CR, Jung G.
Chembiochem. 2014 Jul 7;15(10):1404-8. doi: 10.1002/cbic.201402075. Epub 2014 Jun 11.
PMID: 24919579

Y145L (and Y145M):

Bogdanov 2016 is the most useful of these Y145L/M papers 9in my opinion).

Synthesis and sequence optimization of GFP mutants containing aromatic non-natural amino acids at the Tyr66 position.
Kajihara D, Hohsaka T, Sisido M.
Protein Eng Des Sel. 2005 Jun;18(6):273-8. Epub 2005 May 31.
PMID: 15928004

Theoretical Computer-Aided Mutagenic Study on the Triple Green Fluorescent Protein Mutant S65T/H148D/Y145F.
Armengol P, Gelabert R, Moreno M, Lluch JM.
Chemphyschem. 2015 Jul 20;16(10):2134-9. doi: 10.1002/cphc.201500158. Epub 2015 Apr 27.
PMID: 25916771

Turning On and Off Photoinduced Electron Transfer in Fluorescent Proteins by π-Stacking, Halide Binding, and Tyr145 Mutations.
Bogdanov AM, Acharya A, Titelmayer AV, Mamontova AV, Bravaya KB, Kolomeisky AB, Lukyanov KA, Krylov AI.
J Am Chem Soc. 2016 Apr 13;138(14):4807-17. doi: 10.1021/jacs.6b00092. Epub 2016 Apr 5.
PMID: 26999576

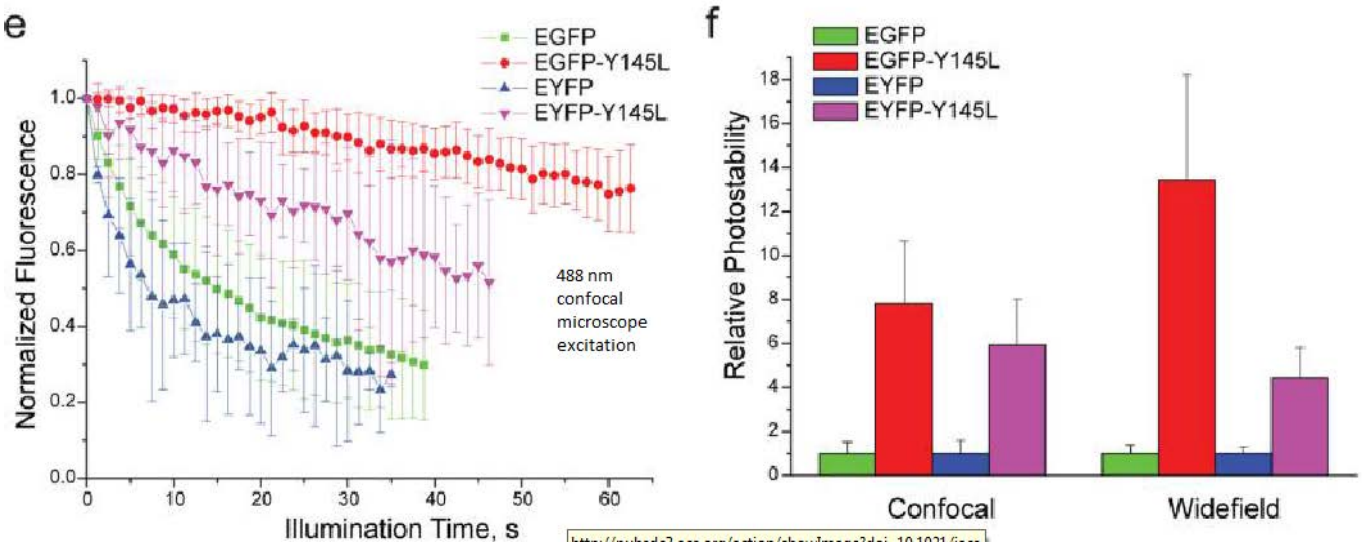

20170728 update: Acharya, Bogdanov … Lukyanov 2017. Excellent review on FP photophysics:

Photoinduced Chemistry in Fluorescent Proteins: Curse or Blessing?
Acharya A, **Bogdanov** AM, Grigorenko BL, Bravaya KB, Nemukhin AV, **Lukyanov** KA, Krylov AI.
Chem Rev. 2017 Jan 25;117(2):758-795. doi: 10.1021/acs.chemrev.6b00238. Epub 2016 Oct 18. Review.
PMID: 27754659

20170719 update: improving photostability by 'better living through chemistry' (DMEMgfp, Opti-Klear)

- DMEMgfp: Evrogen (use its U.S. distributors), see papers for adding Rutin.
- Opti-Klear: Marker Gene Technologies.
  https://www.markergene.com/opti-klear-live-cell-imaging-buffer-5x.html

Influence of cell growth conditions and medium composition on EGFP photostability in live cells.
Mamontova AV, Bogdanov AM, Lukyanov KA.
Biotechniques. 2015 May 1;58(5):258-61. doi: 10.2144/000114289. eCollection 2015 May.
PMID: 25967905

Anti-fading media for live cell GFP imaging.
Bogdanov AM, Kudryavtseva EI, Lukyanov KA.
PLoS One. 2012;7(12):e53004. doi: 10.1371/journal.pone.0053004. Epub 2012 Dec 21.
PMID: 23285248

Cell culture medium affects GFP photostability: a solution.
Bogdanov AM, Bogdanova EA, Chudakov DM, Gorodnicheva TV, Lukyanov S, Lukyanov KA.
Nat Methods. 2009 Dec;6(12):859-60. doi: 10.1038/nmeth1209-859. No abstract available.
PMID: 19935837

I am a big fan of quantitative spatial deconvolution
see
https://www.microvolution.com/gallery
example (of smFISH, discussed next item):

Before deconvolution	After deconvolution, 6 second
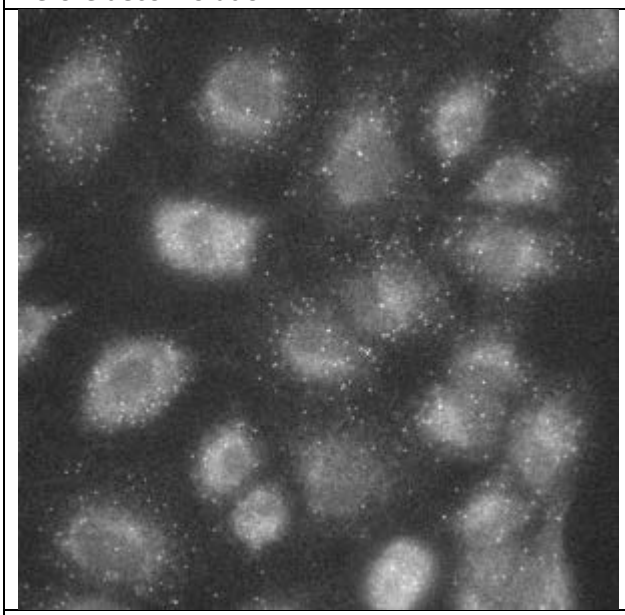	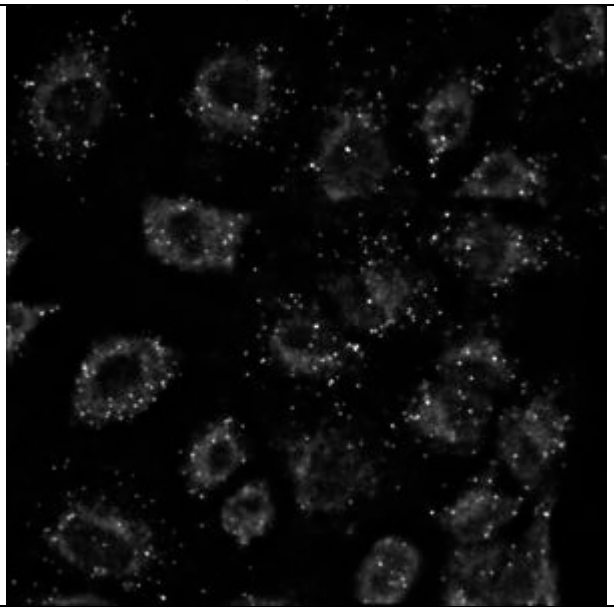

Widefield image of RNA FISH (fluorescence in-situ hybridization), labeling TOP1 (DNA topoisomerase 1).
Single slice of 1024x1024x39 image, deconvolved in 6 seconds.
Image courtesy of: Dane Maxfield, Technical Instruments.

➔**Microvolution**: JHU MicFac image core (Scott Kuo) has a license
https://microscopy.jhmi.edu/Services/SciSoftware.html
I am hoping that in the future (not available currently) that we will be able to “drop and drag” files from the acquisition PCs (ex. LSM510 PC) or server space to Scott’s Microvolution workstation/server, such that your images

can be processed automatically (i.e. read the image settings from the "metadata" in your image files). Please be patient!

2017070W: Zeiss LSM510META Z-series on Microvolution

- under 10 seconds to process >100 Mb dataset.

Left: Zeiss LSM510META (pinhole 1 Airy Unit, etc) Right: after 100 iterations of deconvolution.

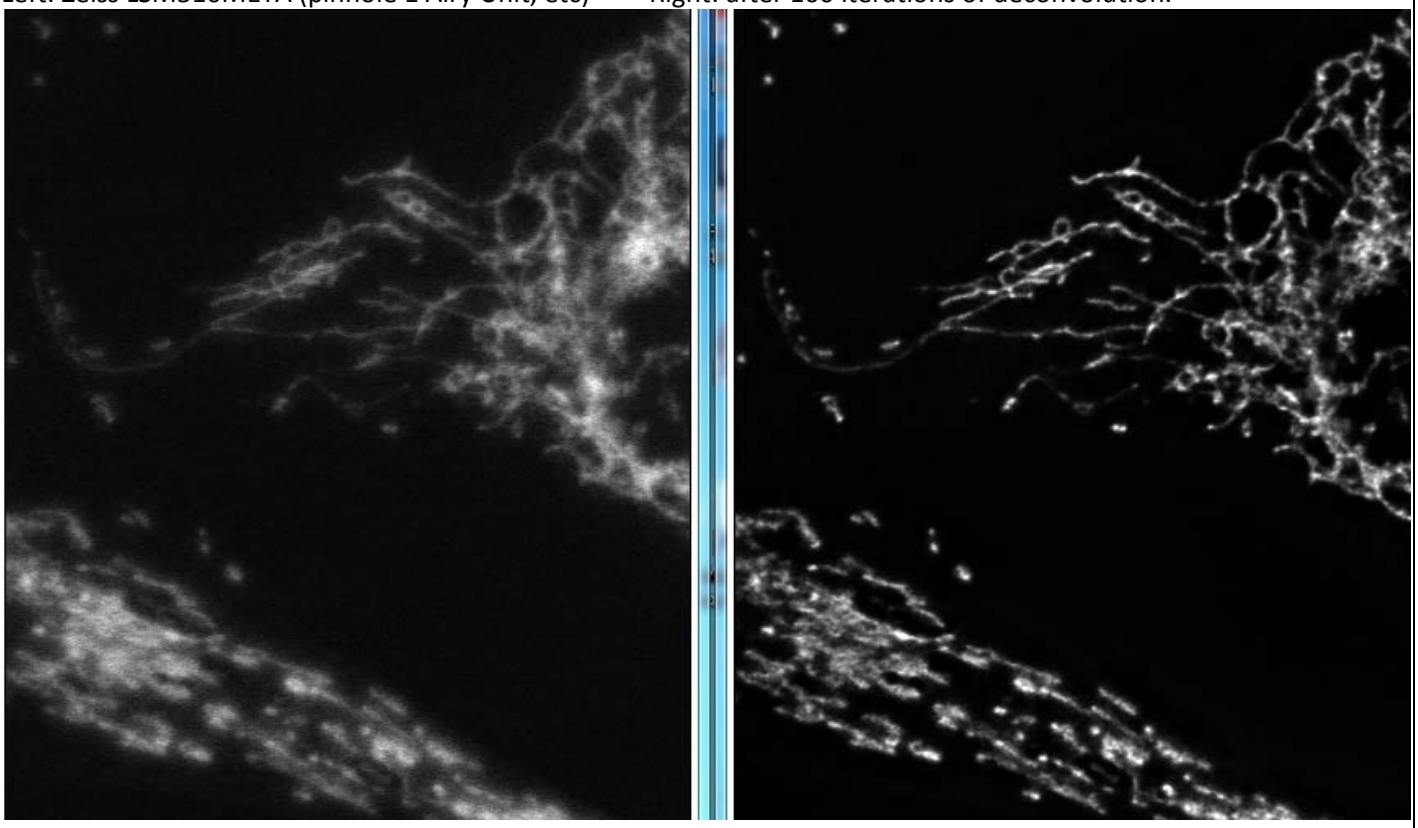

- I compared Zeiss LSM510META 40x/1.4NA oil with 100x/1.4NA oil and widefield with Keyence BZ-X700 microscope equipped with Nikon 100x1.45NA oil immersion lens. Microvolution (100 iterations, with regularization, improved each. 100x/1.40NA shown above (the 40x/1.40NA, 2.5x zoom images were brighter). Specimen is tyramide signal amplification Alexa Fluor 488 mitochondria protein detection (slide made ~2011 in Miami, imaged 7/2017 at JHU).
- I also would like to have "joint" spatial deconvolution and spectral unmixing
  https://www.ncbi.nlm.nih.gov/pubmed/18339754 (2008, open access, was slow)
  https://www.ncbi.nlm.nih.gov/pubmed/27023704 (2016, open access, better speed)

  Microbiome + human cells at high plex: One "payoff" would be to combine with smFISH (and immunofluorescence) for both microbiome (rRNA species identification, mRNA toxin genes expression, immunofluorescence) and human cell info (Lgr5 mRNA smFISH, more FISH), such as
  https://www.ncbi.nlm.nih.gov/pubmed/27391327 (120plex bacteria species)

"smFISH" = Fixed cell single molecule RNA FISH ("smFISH" … mRNA, lncRNA, rRNA)

- I am a big fan of "single molecules FISH". In Houston I used "Stellaris FISH" reagents,
  http://stellarisgallery.biosearchtech.com
  and yes, can multiplex with other smFISH probes
  http://stellarisgallery.biosearchtech.com/Multiplexing/i-XF2zTRr

antibodies
http://stellarisgallery.biosearchtech.com/Immunofluorescence-RNA-FISH/
exon and intron probe sets (intron probesets light up "active transcriptional burst sites" … discovered in 2006 with this method)
http://stellarisgallery.biosearchtech.com/IceFISH/

- An academic expert, Prof. Arjun Raj, is at UPenn, very collaborative, excellent speaker (i.e. invite Arjun to speak here)
  http://rajlab.seas.upenn.edu
  https://sites.google.com/site/singlemoleculernafish/
  Single nucleotide variants (SNVs, a.k.a. polymorphisms, SNP) FISH
  https://www.nature.com/nmeth/journal/v10/n9/full/nmeth.2589.html
- DNA FISH with oligos is also possible, as is with TALE's or CRISPR/Cas9, see https://www.ncbi.nlm.nih.gov/pubmed/28355536 for latter (also fixed, denatured, used smFISH oligos).

➔ Disclosure: GM was an 'advisor' to Marc Beal and Ron Cook at Biosearch, and *may* become an advisor to them at Optical Biosystems, who are developing a new imaging system.

***

Best (in my mind) positive control to start with is Human (*Homo sapiens*) RNA Polymerase 2A

LGC Biosearch – Stellaris DesignReady probe set is available in any of four fluorophores,

http://stellarisgallery.biosearchtech.com/Designready-Probe-Sets/i-gvtbKRH/A

VSMF-2292-5	Stellaris® FISH Probes, Human POLR2A with CAL Fluor® Red 590 Dye	**$849**	1	5 nmol Total
VSMF-2293-5	Stellaris® FISH Probes, Human POLR2A with CAL Fluor® Red 610 Dye	**$849**	1	5 nmol Total
VSMF-2294-5	Stellaris® FISH Probes, Human POLR2A with Quasar® 570 Dye	**$849**	1	5 nmol Total
VSMF-2295-5	Stellaris® FISH Probes, Human POLR2A with Quasar® 670 Dye	**$849**	1	5 nmol Total

I also recommend buying LGC Biosearch's packaged buffers:

https://www.biosearchtech.com/products/rna-fish/stellaris-buffers

CATALOG #	ITEM NAME	PRICE	SIZE/SCALE
SMF-HB1-10	Stellaris® RNA FISH Hybridization Buffer	$225	10 mL
SMF-WA1-60	Stellaris® RNA FISH Wash Buffer A	$65	60 mL
SMF-WB1-20	Stellaris® RNA FISH Wash Buffer B	$55	20 mL

Branched DNA technology:

RNAscope (usually DAB), QuantiGene (DAB or fluorescence), same branched DNA tech (i.p.), different companies. Both with confusing pricing

.

* RNAscope (ACDbio/Biotechne)
* QuantiGene ViewRNA Probe Set (Panomics/Affymetrix/eBioscience/ThermoFisher)

http://cdn.panomics.com/index.php?id=ebio_viewrna-probe-set-catalog&spec=human&catnum=&phrase=polymerase&asse=&sym=POLR2A

QuantiGene ViewRNA "By Request" Probe Set - Custom FISH and CISH Probes

Probes for your new/novel RNA target can be designed and synthesized at no additional cost. Please provide requested information and provide any information on any special design requirements. Allow 1 week for delivery of a "By Request" QuantiGene ViewRNA Probe Set.

Species: human | Catalog Number: | Accession: | Symbol: POLR2A | Contains the Phrase: polymerase | Search | Reset

1

3 records were found

Type	Species	Symbol	Gene Name	Accession	Catalog #
TYPE 6	HUMAN	POLR2A	polymerase (RNA) II (DNA directed) polypeptide A, 220kDa	NM_000937	VA6-11464
TYPE 1	HUMAN	POLR2A	polymerase (RNA) II (DNA directed) polypeptide A, 220kDa	NM_000937	VA1-12326
TYPE 4	HUMAN	POLR2A	polymerase (RNA) II (DNA directed) polypeptide A, 220kDa	NM_000937	VA4-15150

QuantiGene ViewRNA Probe Sets TYPES - FISH and CISH Probes

Target specific probe set TYPE	Fluorescent label excitation	Hybridizes to	Compatible with the following assay formats	Applications
TYPE 1 Probes	550 nm	PreAmp1, Amp1, LP1	HC Screening, ISH Cell, ISH Tissue	CISH/FISH
TYPE 4 Probes	488 nm	PreAmp4, Amp4, LP4	HC Screening, ISH Cell	FISH
TYPE 6 Probes	650 nm	PreAmp6, Amp6, LP6	HC Screening, ISH Cell, ISH Tissue	CISH/FISH
TYPE 8 Probes	All nm	PreAmp8, Amp8, LP8	HC Screening	FISH
TYPE 10 Probes	740 nm	PreAmp10, Amp10, LP10	HC Screening, ISH Cell	FISH

https://www.thermofisher.com/order/genome-database/browse/quantigene-gene-expression/keyword/VA6-11464?searchFormId=ge-quantigene-only&SID=srch-uc-qge-VA6-11464

Assay ID
VA6-11464-VCP

View Assay on Map

Gene	Species	Transcripts	Detection Label	Type	Product Type	Availability	Catalog #
POLR2A	Human	1 RefSeq	Alexa Fluor 647	6	ViewRNA Cell Plus Probe Set	Made to Order	VX-01

M: 440 uL

Price (USD): 341.00

Check your price

View Details

Add To Cart

Gene Transcripts

Gene Symbol	POLR2A
Entrez Gene ID	5430
Gene Name	RNA polymerase II subunit A
Gene Aliases	POLR2, POLRA, RPB1, RPBh1, RPO2, RPOL2, RpIILS, hRPB220, hsRPB1
Chromosome Location	Chr.17: 7484379 - 7514618 on Build GRCh38
Uni Gene	Hs.270017

Interrogated Sequence		Translated Protein
RefSeq	NM_000937.4	NP_000928.1
GenBank mRNA	AK293777.1	-

RNAscope pricing (from a distributor)
https://www.insightbio.com/datasheets/RNAscopePrices.pdf

1 pound = $1.32
467 + 655 + 560 = 1,682 * 1.32 = $2,220

RNAscope Products & Prices

RNAscope Reagents

Please see a list of products and prices for RNAscope in the righthand table. You will need the following items to run the RNAscope assay in your lab:

1. An RNAscope target probe, cat: 300031. Choose from a list of approximately 1000 target probes. If no probe is currently listed for your target of interest, a new probe set up service will be required, cat: 320269. Contact Insight Bio with your target sequence or gene ID and we will arrange for a new probe to be designed in a process that takes 3 weeks, cat:320269.

2. A reagent Kit. Choose from red or brown, single and duoplex chromogenic kits.

3. Positive and negative control probes for your species of interest.

4. A humidifying hybridisation oven such as the Hybez system, which has been shown to work extremely well with RNAsope. Insight Bio can provide the Hybez oven at cost price, on a sale or return basis, allowing you to verify ACD's claims in your own lab on a risk free basis. The RNAscope assay is hugely robust and will work on all tissues and targets with single copy sensitivity.

Insight Biotechnology's PhD level technical Team is happy to discuss how RNAscope can be used to achieve your experimental objectives. Contact us by telephone +44(0)208 385 0303 or email info@insightbio.com.

Special Offer

Until May 31st 2014 Insight Bio is offering complementary probe design with purchase of all reagents required to run a standard RNAscope assay in your lab (excluding the Hybez system). This offer equates to a saving of approximately 30%. Contact Insight Bio's technical team for further information.

INSIGHT BIOTECHNOLOGY

Catalogue No	Category	Product Description	List Price	Academic Price
320269	RNAscope new probe set up	Set up Service	£667	£467
300031	RNAscope 2.0 Target Probe	Target Probe	£600	£420
310030	RNAscope 1.0 Chromogenic Detection Kit	Reagent Kits	£667	£467
310090	RNAscope 1.0 FFPE Reagent Kit	Reagent Kits	£935	£655
310033	RNAscope 2.0 Chromogenic Detection Kit - Brown	Reagent Kits	£800	£560
310034	RNAscope 2.0 Chromogenic Detection Kit - Red	Reagent Kits	£800	£560
310035	RNAscope 2.0 FFPE Reagent Kit – BROWN	Reagent Kits	£1,067	£747
310036	RNAscope 2.0 FFPE Reagent Kit - Red	Reagent Kits (2-plex)	£1,067	£747
320071	RNAscope 2-plex Chromogenic Detection Kit	Reagent Kits (2-plex)	£1,250	£875
320701	RNAscope 2-plex Detection Kit	Reagent Kits (2-plex)	£1,459	£1,021
320700	RNAscope 2-plex FFPE Reagent Kit	Reagent Kits (2-plex)	£1,600	£1,120
300041	RNAscope Blank Probe - C1	Control Probes	£67	£47
310041	RNAscope 1.0 Positive Control Probe _ Hs-UbC	Control Probes	£99	£69
310043	RNAscope Negative Control Probe _ DapB (for both 1.0 and 2.0)	Control Probes	£99	£69
310451	RNAscope 2.0 Positive Control Probe _ Hs-POLAR2A	Control Probes	£99	£69
310771	RNAscope 1.0 Positive Control Probe _ Mm-UbC	Control Probes	£99	£69
312011	RNAscope 1.0 Positive Control Probe _ Rn-UbC	Control Probes	£99	£69
312471	RNAscope 2.0 Positive Control Probe _ Mm-POLAR2A	Control Probes	£99	£69
312481	RNAscope 2.0 Positive Control Probe _ Rn-POLAR2A	Control Probes	£99	£69
313901	RNAscope Positive Control Probe _ Hs-PPIB	Control Probes	£99	£69
313902	RNAscope Positive Control Probe _ Mm-PPIB	Control Probes	£99	£69
313903	RNAscope Positive Control Probe _ Rn-PPIB	Control Probes	£99	£69
320600	RNAscopeVS Chromogenic Reagent Kit - Brown	Control Probes (VS)	£4,267	£2,987
310751	RNAscope 2-plex Negative Control Probe	Control Probes	£199	£139
310045	RNAscope Control Slides	Reagents	£267	£187
320842	RNAscope Pretreatment Kit - Fresh Frozen Tissue	Reagents	£135	£95
310091	RNAscope Wash Buffer	Reagents	£135	£95
310013	HybEZ Hybridization System (220VAC)	Hybridization Products	£3,646	£3,099
310012	HybEZ Humidifying Tray (with lid)	Hybridization Products	£365	£310
310014	HybEZ Slide Rack	Hybridization Products	£365	£310
310015	HybEZ Humidifying Paper (15 pack)	Hybridization Products	£73	£62
310007	EZ-Lock Slide Batch Processing System	Hybridization Products	£391	£274
310019	EZ-Lock Wash Tray	Hybridization Products	£113	£79
310017	EZ-Lock Slide Holder	Hybridization Products	£352	£246

** The above table includes only a subsection of RNAscope products. All RNAscope products have been uploaded to our website, www.insightbio.com. Can't find what you're looking for or want to discuss your experiments. Contact our technical team by Email info@insightbio.com or Telephone +44(0)208 385 0303.

Live cell RNA detection:

1. MilliporeSigma/EMD Millipore “SmartFlare” does not work reliably … according to a TexasTech postdoc (Brian McFarlane lab), who spent a lot of time on this (and pivoted to something else). That postdoc is now employed by MilliporeSigma, doing something else.
2. I ‘know people’ who are into “Molecular Beacons” for live cell FISH. Mo’Beacons have a quencher-stem-loop-fluorophore, such that the molecules are dark when free in solution (or cytoplasm), bright when bound to their specific target. These are the same principle as used in PCR, though details in the reagents may differ (and need a good way to get the reagents into cells).

Tyramide signal amplification (TSA)

1. Increase immunofluorescence brightness by ~100x.
    a. A key part of using HRP/TSA is that the use of multiple, sequential, modest size, molecules, is preferable to one giant molecule with an equivalent number of fluorophores. This is in part because it is not practical to get such large molecules to diffuse into the middle of your specimen.
2. Enable use of lower concentration of primary antibody (i.e. 1:1000 dilution instead of 1:100).
   You will likely have to use a lower concentration of primary antibody, because TSA detects all your antibody on the specimen, both specific and non-specific. Decreasing concentration will likely decrease non-specific event more.

PeroxAbolish (BioCare) to kill HRP between rounds

Sequential TSA is possible by “killing” the HRP between antibody cycles. I especially like “PeroxAbolish” http://biocare.net/product/peroxabolish/ which I learned about from former colleagues, Takahashi et al 2012 Cell Transplant
https://www.ncbi.nlm.nih.gov/pubmed/21929847 (PubMed)
http://www.ingentaconnect.com/content/cog/ct/2012/00000021/00000001/art00010 (full text)
https://www.ncbi.nlm.nih.gov/pmc/articles/PMC3777543/figure/F2 (key figure).

Takahashi … Ichii 2012 dual Tyramide with PeroxAbolish to kill HRP

Cell Transplant. 2012;21(1):113-25. doi: 10.3727/096368911X586747. Epub 2011 Sep 16.
Quantitative in situ analysis of FoxP3+ T regulatory cells on transplant tissue using laser scanning cytometry.
Takahashi H[1], Ruiz P, Ricordi C, Delacruz V, Miki A, Mita A, Misawa R, Barker S, Burke GW, Tzakis AG, Ichii H.

Abstract
There is abundant evidence that immune cells infiltrating into a transplanted organ play a critical role for destructive inflammatory or regulatory immune reactions. Quantitative in situ analysis (i.e., in tissue sections) of immune cells remains challenging due to a lack of objective methodology. Laser scanning cytometry (LSC) is an imaging-based methodology that performs quantitative measurements on fluorescently and/ or chromatically stained tissue or cellular specimens at a single-cell level. In this study, we have developed a novel objective method for analysis of immune cells, including Foxp3(+) T regulatory cells (Tregs), on formalin-fixed /paraffin-embedded (FFPE) transplant biopsy sections using iCys® Research Imaging Cytometer. The development of multiple immunofluorescent staining was established using FFPE human tonsil sample. The CD4/CD8 ratio and the population of Tregs among CD4(+) cells were analyzed using iCys and compared with the results from conventional flow cytometry analysis (FCM). Our multiple immunofluorescent staining techniques allow obtaining clear staining on FFPE sections. The CD4/CD8 ratio analyzed by iCys was concordant with those obtained by FCM. This method was also applicable for liver, small intestine, kidney, pancreas, and heart transplant biopsy sections and provide an objective quantification of Tregs within the grafts.
PMID: 21929847 PMCID: PMC3777543 DOI: 10.3727/096368911X586747

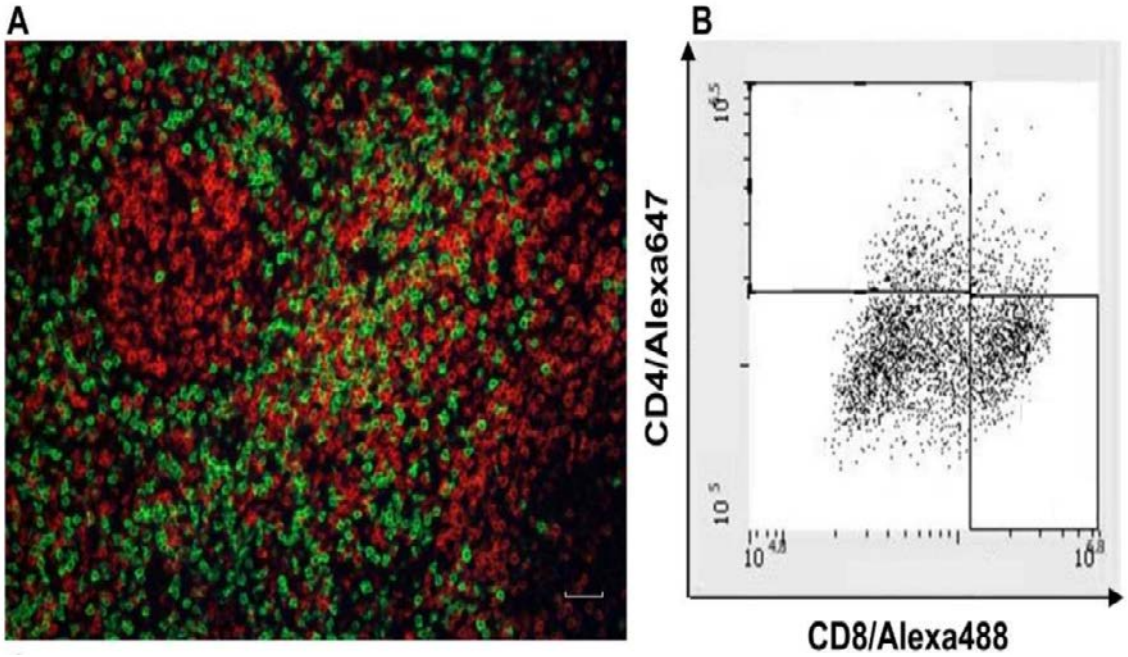

(partial Figure 1) Multiple immunofluorescent staining on FFPE human tonsil section …
(A) FFPE human tonsil section stained for CD4 (Alexa647, red) and CD8 (Alexa488, green) (×200). Nuclear staining by PI was blanked. Scale in figure indicates 50 μ m.
(B) Distribution of signal integral of Alexa488 (CD8) and Alexa647 (CD4) obtained with LSC/iCys. The CD4/CD8 ratio on this sample was revealed 0.38.

3. TSA reagents available from both ThermoFisher, PerkinElmer (Opal) [URLs below], and in principle, could make your own (George can find reference).

Poly-HRP (Fitzgerald Industries)

4. Can be combined with "poly-HRP" (polymer of horseradish peroxidase), and other tech, such as "SuperBoost" https://www.thermofisher.com/us/en/home/life-science/cell-analysis/cellular-imaging/immunofluorescence/tyramide-signal-amplification-tsa.html (though might be more expensive than proportional gains in brightness and/or convenience).
   SuperBoost has the advantage of just having four fluorophore choices, all compatible with the LSM510 (also with widefield fluorescence microscopes):

ThermoFisher / Molecular Probes Tyramide SuperBoost Kits (AF488,555,594,647) and standard TSA Kits

Labeled tyramide (Ex/Em)	Tyramide SuperBoost Kits*		
	Anti–mouse IgG (host: goat)	Anti–rabbit IgG (host: goat)	Streptavidin
Alexa Fluor 488 (495/519 nm)	B40912 B40941 (50 coverslips)	B40922 B40943 (50 coverslips)	B40932
Alexa Fluor 555 (555/565 nm)	B40913	B40923	B40933
Alexa Fluor 594 (591/617 nm)	B40915 B40942 (50 coverslips)	B40925 B40944 (50 coverslips)	B40935
Alexa Fluor 647 (650/668 nm)	B40916	B40926	B40936
Biotin-XX	B40911	B40921	B40931

* Unless otherwise stated, sufficient material is provided for up to 150 18 mm x 18 mm coverslips (if using 150 µL in most critical incubation steps). Volumes can be adjusted for samples of different sizes.

”Standard” ThermoFisher TSA kits have more fluorescent dye choices (all *except* AF350, ok for LSM):
https://tools.thermofisher.com/content/sfs/manuals/mp20911.pdf

Table 2 TSA™ detection kits.

Labeled tyramide	Ex/Em*	Stand-alone†	Horseradish peroxidase conjugate		
			Anti–mouse IgG (host = goat)	Anti–rabbit IgG (host = goat)	Streptavidin
Alexa Fluor® 350	347/442		T20917	T20927	T20937
Alexa Fluor® 488	495/519	T20948	T20912	T20922	T20932
Oregon Green® 488	496/524				T20939
Alexa Fluor® 546	556/573		T20913	T20923	T20933
Alexa Fluor® 555	555/565		T30953	T30954	T30955
Alexa Fluor® 568	579/604	T20949	T20914	T20924	T20934
Alexa Fluor® 594	591/617	T20950	T20915	T20925	T20935
Alexa Fluor® 647	650/668	T20951	T20916	T20926	T20936
Biotin-XX	NA	T20947	T20911	T20921	T20931

* Ex/Em = Fluorescence excitation/emission maxima, in nm. NA = not applicable.

† Tyramide stand-alone reagents kits only provide labeled tyramide (Component A) and amplification buffer (Component E). Other reagents will have to be provided and their concentration optimized by the user. Anhydrous DMSO for dissolving the stand-alone tyramides can be purchased separately from Life Technologies (Cat. no. D12345). We strongly recommend the first time user to purchase and use the whole kit rather than the stand-alone reagent kits.

PerkinElmer “Opal” (two 7plex URL’s shown below, they have other kits, with a screenshot of Opal naming … I note PerkinElmer recommends “microwave treatment” (MWT), aka microwave antigen retrieval … I suggest instead to use Biocare’s PeroxAbolish – see Takahashi 2012 above).
http://www.perkinelmer.com/product/opal-7-immunology-discovery-kit-op7ds1001kt

http://www.perkinelmer.com/lab-solutions/resources/docs/DTS_Opal-7-Discovery_OP7DS1001KT.pdf

Description	Format*	Catalog #	Kit Components
Opal™ 7 Immunology Discovery Kit	50 slides	OP7DS1001KT	• 1X Plus Amplification Diluent (1 X 50mL) • Opal 520 Fluorophore • Opal 540 Fluorophore • Opal 570 Fluorophore • Opal 620 Fluorophore • Opal 650 Fluorophore • Opal 690 Fluorophore • Spectral DAPI solution (1 X 1.5mL) • DMSO (2 X 500 µL) • 10X AR6 buffer (1 X 250ml) • 10X AR9 buffer (1 X 250ml) • Antibody Diluent (1 X 50ml) • Anti-CD4, anti-CD8, anti-CD68 antibodies (human reactivity) • Opal Polymer HRP Ms + Rb (50 mL)

*The format of the kit is based on ~150 µL per slide of Opal Working Solution (see page 4).

Another source of poly-HRP is "Fitzgerald", whose "HRP80" has ~400 HRP enzyme molecules per polymer:
https://www.fitzgerald-fii.com/biological-reagents/poly-hrp-products.html?tag=231
https://www.fitzgerald-fii.com/streptavidin-poly-**hrp20**-conjugate-65r-s107.html
https://www.fitzgerald-fii.com/streptavidin-poly-**hrp40**-conjugate-65r-s104phrp.html
https://www.fitzgerald-fii.com/streptavidin-**poly-hrp80**-conjugate-65r-s105phrp.html
" Streptavidin Poly-HRP Conjugate is streptavidin biotin-binding protein that is conjugated with polymers of horseradish peroxidase, enabling signal amplification and detection of biotinylated antibodies for IHC and other methods. This poly-HRP conjugate is designed to deliver the highest sensitivity and low background in immunoassays where sample volume is limited or when the target molecule is present at low levels. The estimated average number of HRP monomer molecules in SA-PolyHRP20 conjugate is 100 (20 X 5), in SA-PolyHRP40 - 200 (40 X 5) and in **SA-PolyHRP80 - 400 (80 X 5).** Thus, PolyHRP brings in reaction with substrate development system much larger number of enzyme label molecules (per one bound analyte molecule) than conventional conjugates do.

I note that if you are using SA-PolyHRP20 (~100 HRP), SA-PolyHRP40 (~200 HRP) or SA-PolyHRP80 (~400 HRP), you may be able to effectively tune the brightness for each target by some or all combination of:

- Which polymer (HRP20, HRP40, HRP80), for fewer → larger number of surface exposed tyrosines that 'activated' fluorophore-tyramide radical can react with.
- Concentration of fluorophore-tyramide and/or H2O2.
- Incubation time (and temperature) of reaction (I suggest allowing each round to "reach completion", and saturate all local tyrosines and/or kill off the HRP molecules by 'self immolation').
- The PolyHRP you introduce in each round *might provide the major binding site(s) for each round!!! That is: bigger is likely brighter for the simple reason of "size matters". This would have the added value of avoiding mis-interpretation depending on whether some antigen is present in a 'tyrosine desert' vs 'tyrosine rich' target area* … Disclosure: GM when at UMiami filed invention disclosure report related to this … was never filed as a patent application … I refer to my specific concept as "ELImol" for single molecule ELISA [like] assay, could be classic ELISA like assay or microscopy or flow cytometry or other … may be useful to revisit this concept here at JHU.
- Brightness is also dependent on:
    - Intrinsic brightness of dye (Extinction coefficient, quantum yield of fluorescence, quantum yield of "going triplet", quantum yield of non-radiative events [heat transfer to local environment], quantum yield into triplet state(s) … several of these parameters depend on O2 vs deoxy media, viscosity of media, pH, solvent).
    - "Self quenching" of high concentration of dye (and/or potential FRET if more than one dye in vicinity).

- Extrinsic brightness (O2, deoxy, pH, viscosity, solvent, etc), some under your control.
- Refractive index matching, or not: this is under your control (completely if fixed, partially if live). Better match enables brighter imaging at depth (Staudt … Hell 2007, https://www.ncbi.nlm.nih.gov/pubmed/17131355 "TDE" mounting media paper; see also Lam … Bolte 2017 Methods, https://www.ncbi.nlm.nih.gov/pubmed/27826080 though I disagree with some of their recommendations, such as longer confocal dwell time).

Future idea – "Rainbow single molecule immunofluorescence" with sequential TSA:

- "single molecule counting ALL molecules" by many colors: Sequential TSA (see PeroxAbolish above) with cycles of:
  - very dilute primary antibody, such that only 1/10th of the target antigen are bound in any cycle (and zero background).
  - HRP reagent (ex. Fitzgerald PolyHRP80, to bring in new binding site for each molecule.
  - Fluorescent Tyramide

  With each cycle using a different color, such as AF350, AF488, AF546, AF555. AF568, AF594, AF647, would be 7 colors, if AF350 can be excited, and if AF547555/568 can be spectrally resolved (I am hoping Luke Lavis, HHMI Janelia Research Campus will develop 10 LSM510 friendly colors).

Zeiss LSM510 confocal:

- Argon ion laser … operate at 6.1 A (Amp), under Lasers (drop down section).
  The 6.1 A setting will prolong the laser life compared to "max power" (6.5 and above), and improve stability compared to default (5.0 A).
  Only exception is for researchers doing FRAP with an Argion ion laser line (though you will probably not see a big improvement at 6.5, 7.0, or 7.5 A).
- PMT "digital gain" … 1.0 is the best setting. This is a multiplier of the 'raw' intensity value. You could do the same thing in MetaMorph, Fiji ImageJ or Excel.
- PMT offset … I recommend 0.1 (all the way to the right).
- PMT gain … I suggest starting at 700, and changing in steps of 100 (ex. 600 if bright, 800 if dim). You can "fine tune' by going with steps of 50 (ex. 650). There is no real benefit to weird values like 737. Round numbers are easier to remember and keep you from looking like a weirdo when writing up how you worked.

The LSM510 is "showing its age". It is not the most sensitive confocal microscope at JHU, and it occasionally "flakes out" and requires a "power off, wait, turn on, hold "RTC Reset button", wait 30 seconds, start ZEN.

➔ RTC Reset button … be sure to have George show you where it is and that you will occasionally get to use it (with ZEN not running).

20170706H: PerkinElmer Tyramide Signal Amplification (TSA) Opal 6plex excitation and emission maxima

Part Number	Wave Length	Type	List Price (purchase price may be less, ignoring shipping $).
FP1487001KT	494/525 nm	Opal 520	118.00 USD
FP1494001KT	523/536 nm	Opal 540	118.00 USD
FP1488001KT	550/570 nm	Opal 570	118.00 USD
FP1495001KT	588/616 nm	Opal 620	118.00 USD
FP1496001KT	627/650 nm	Opal 650	134.00 USD
FP1497001KT	676/694 nm	Opal 690	134.00 USD

http://www.perkinelmer.com/product/opal-540-reagent-pack-fp1494001kt
http://www.perkinelmer.com/lab-solutions/resources/docs/BRO_Phenoptics-Workflow_012380A_04.pdf

//

Note: PerkinElmer likes to use “microwave Ab strip” (see figure below) between rounds (they may have a patent on it, and/or recommend it to avoid infringement of other’s patents, such as GE Healthcare’s chemical methods to destroy Cy3 and Cy5).
To me, “strip” is stupid: many of the tyramides reacted with the tyrosines on the antibody (Ab) or HRP (HRP-polymer may have hundreds of HRP molecules), so going to all the money, time and effort to get tyramides attached to the Ab and HRP, and then strip the Ab and HRP off (before imaging!!!) is stupid. I recommend Biocare’s PeroxAbolish reagent (see above).

http://www.perkinelmer.com/lab-solutions/resources/docs/APP_MultiplexBiomarkerImaging-CancerImmunology-CapturingImmuneStatusinFFPESections.pdf

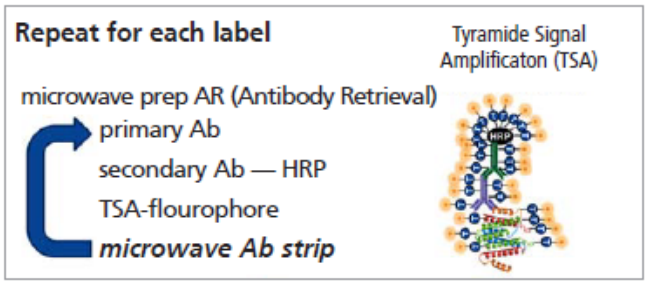

Figure 1. Same-species serial TSA immunofluorescence labeling

Table 1. Label-fluorophore conjugation

Marker	Cell Type	Fluorophore
CD4	Helper T cell	Fluorescein
CD8	Killer T cell	Cyanine 3
CD20	B cell	Cyanine 5
Cytokeratin	Epithelial cell	Coumarin
Counterstain	Nuclei	DAPI

20170730: Click Tyrosine with fluorophore-methyl-luminol may be much more efficient than tyramide!!!

This is a very cool paper (if reproducible) because:
methyl-luminol is apparently much more efficient a substrate for labeling target molecules on (protein surface exposed tyrosines) than classic tyramide.
H2O2 or NADH each work as co-substrate for HRP.
My expectation (ok, hope) methyl-luminol will also be a great substrate for Alice ting’s APEX2 “proximity ligation” assay (see below for references and addgene plasmids).

Sato et al 2017 Chembiochem 18: 475-478. doi: 10.1002/cbic.201600649.
Horseradish-Peroxidase-Catalyzed Tyrosine Click Reaction.
Sato S[1], Nakamura K[1], Nakamura H[1].
Abstract
The efficiency of protein chemical modification on **tyrosine** residues with N-methylluminol derivatives was drastically improved by using horseradish peroxidase (HRP). In the previous method, based on the use of hemin and H_2O_2, oxidative side reactions such as cysteine oxidation were problematic for functionalization of proteins selectively on **tyrosine** residues. Oxidative activation of N-methylluminol derivatives with a minimum amount of H_2O_2 prevented the occurrence of oxidative side reactions under HRP-catalyzed conditions. As probes for HRP-catalyzed protein modification, N-methylluminol derivatives showed much higher efficiency than tyramide without inducing oligomerization of probe molecules. **Tyrosine** modification also proceeded in the presence of β-nicotinamide adenine dinucleotide (NADH, H_2O_2-free conditions).
KEYWORDS: heme proteins; horseradish peroxidase; protein labeling; protein modifications; **tyrosine** modification
PMID: 28009088 DOI: 10.1002/cbic.201600649

20170730: Proximity Ligation with “ProteinX”-APEX2 fusion and Biotin-tyramide for proteomic mass spectrometry … also EMARS

Note: biotin-tyramide and "biotin-phenol" are the same thing.
Label on or in live cells, then follow by mass spectrometry to identify ALL the proteins within ~20 nm of ProteinX fused to APEX2.
Modest expression level.

➔GM thinking: can use fluorophore-tyramide, or fluorophore-methyl-luminol (Sato 2017, above, may work a lot better), as the "handle" instead of (or in addition to) biotin. For example: biotin-linker-fluorophore-linker-tyramide [or methyl-luminol]. Then each fluorophore, ex. fluorescein, Cy3, Cy5, or their Alexa Fluor equivalents (or Luke Lavis's Janelia Fluor's), could provide the "mass tags" instead of standard light and heavy N and C atomsisobaric mass tags.

APEX2 = engineered ascorbate peroxidase. Available in addgene.org.

https://www.addgene.org/Alice_Ting

Note – these are back to back papers:
An Approach to Spatiotemporally Resolve Protein Interaction Networks in Living Cells.
Lobingier BT, Hüttenhain R, Eichel K, Miller KB, Ting AY, von Zastrow M, Krogan NJ.
Cell. 2017 Apr 6;169(2):350-360.e12. doi: 10.1016/j.cell.2017.03.022.
PMID: 28388416
Multidimensional Tracking of GPCR Signaling via Peroxidase-Catalyzed Proximity Labeling.
Paek J, Kalocsay M, Staus DP, Wingler L, Pascolutti R, Paulo JA, Gygi SP, Kruse AC.
Cell. 2017 Apr 6;169(2):338-349.e11. doi: 10.1016/j.cell.2017.03.028.
PMID: 28388415

Lobingier … Ting graphical abstract:

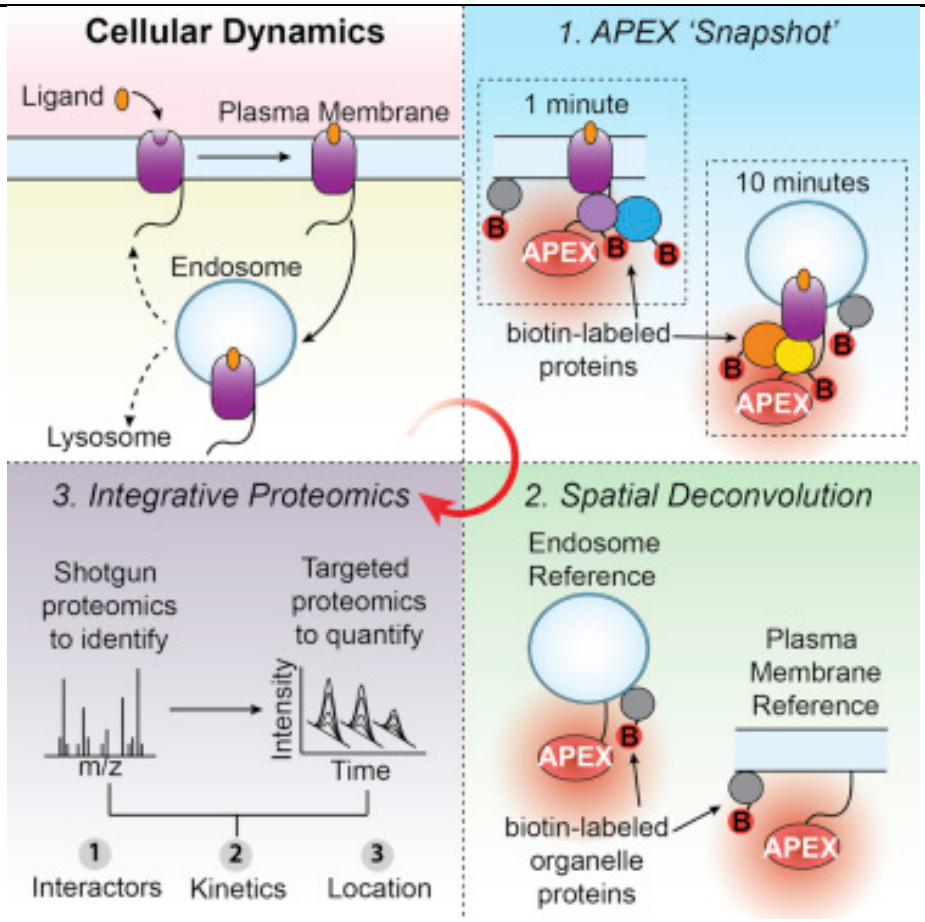

Additional information on APEX2:

Proteomic mapping of cytosol-facing outer mitochondrial and ER membranes in living human cells by proximity biotinylation.
Hung V, Lam SS, Udeshi ND, Svinkina T, Guzman G, Mootha VK, Carr SA, Ting AY.
Elife. 2017 Apr 25;6. pii: e24463. doi: 10.7554/eLife.24463.
PMID: 28441135

Proximity Biotinylation as a Method for Mapping Proteins Associated with mtDNA in Living Cells.
Han S, Udeshi ND, Deerinck TJ, Svinkina T, Ellisman MH, Carr SA, Ting AY.
Cell Chem Biol. 2017 Mar 16;24(3):404-414. doi: 10.1016/j.chembiol.2017.02.002. Epub 2017 Feb 23.
PMID: 28238724

Spatially resolved proteomic mapping in living cells with the engineered peroxidase **APEX2**.
Hung V, Udeshi ND, Lam SS, Loh KH, Cox KJ, Pedram K, Carr SA, Ting AY.
Nat Protoc. 2016 Mar;11(3):456-75. doi: 10.1038/nprot.2016.018. Epub 2016 Feb 11.
PMID: 26866790

Directed evolution of **APEX2** for electron microscopy and proximity labeling.
Lam SS, Martell JD, Kamer KJ, Deerinck TJ, Ellisman MH, Mootha VK, Ting AY.
Nat Methods. 2015 Jan;12(1):51-4. doi: 10.1038/nmeth.3179. Epub 2014 Nov 24.
PMID: 25419960

APEX is an engineered peroxidase that functions as an electron microscopy tag and a promiscuous labeling enzyme for live-cell proteomics. Because limited sensitivity precludes applications requiring low APEX expression, we used yeast-display evolution to improve its catalytic efficiency. **APEX2** is far more active in cells, enabling the use of electron microscopy to resolve the submitochondrial localization of calcium uptake regulatory protein

MICU1. **APEX2** also permits superior enrichment of endogenous mitochondrial and endoplasmic reticulum membrane proteins.

➔ For GFP (EGFP, EYFP and closely related Aequorea FPs), an APEX2-nanobody is available in addgene:

https://www.addgene.org/67651

Modular Detection of GFP-Labeled Proteins for Rapid Screening by Electron Microscopy in Cells and Organisms. Ariotti N, Hall TE, Rae J, Ferguson C, McMahon KA, Martel N, Webb RE, Webb RI, Teasdale RD, Parton RG. *Dev Cell. 2015 Nov 23;35(4):513-25. doi: 10.1016/j.devcel.2015.10.016. Epub 2015 Nov 12.* 10.1016/j.devcel.2015.10.016 PubMed 26585296

EMARS (Enzyme mediated activation of radical sources) and BioID (Biotin Identification)

A few references shown below.

Miyagawa-Yamaguchi A, Kotani N, Honke K. Each GPI-anchored protein species forms a specific lipid raft depending on its GPI attachment signal. Glycoconj J. 2015 Oct;32(7):531-40. doi: 10.1007/s10719-015-9595-5. PMID: 25948169

Li P, Li J, Wang L, Di LJ. Proximity labeling of interacting proteins: Application of BioID as a discovery tool. Proteomics. 2017 Mar 8. doi: 10.1002/pmic.201700002. Review. PMID: 28271636

Ramberger E, Dittmar G. Tissue Specific Labeling in Proteomics. Proteomes. 2017 Jul 18;5(3). pii: E17. doi: 10.3390/proteomes5030017. Review. PMID: 28718811

Roux KJ, Kim DI, Burke B. **BioID**: a screen for protein-protein interactions. Curr Protoc Protein Sci. 2013 Nov 5;74:Unit 19.23.. doi: 10.1002/0471140864.ps1923s74. PMID: 24510646

Roux KJ. Marked by association: techniques for proximity-dependent labeling of proteins in eukaryotic cells. Cell Mol Life Sci. 2013 Oct;70(19):3657-64. doi: 10.1007/s00018-013-1287-3. Review. PMID: 23420482

I have a new Current Protocols unit, Light Microscopy and Image Analysis (page proofs 5/2017)
update from:
Microscopy and image analysis.
McNamara G, Difilippantonio MJ, Ried T.
Curr Protoc Hum Genet. 2005 Aug; Chapter 4:Unit 4.4. doi: 10.1002/0471142905.hg0404s46.
PMID: 18428379

http://onlinelibrary.wiley.com/doi/10.1002/cphg.42/abstract
This unit provides an overview of light microscopy, including objectives, light sources, filters, film, and color photography for fluorescence microscopy and fluorescence in situ hybridization (FISH). We believe there are excellent opportunities for cytogeneticists, pathologists, and other biomedical readers, to take advantage of specimen optical clearing techniques and expansion microscopy—we briefly point to these new opportunities. © 2017 by John Wiley & Sons, Inc.
Keywords: light microscopy; digital imaging; fluorescence in situ hybridization; functional genomics

The new version of the Unit has lots of web links to vendors, specific product, and research labs.

http://onlinelibrary.wiley.com/doi/10.1002/cphg.42/tables

View table Table 4.4.1. Fluorescent Proteins Photophysics Data[a]
View table Table 4.4.2. Fluorophores Photophysics Data[a]

View table Table 4.4.3. Fluorescent Protein Biosensors (FPB)[a]
View table Table 4.4.4. Useful Light Microscopy Web Sites

View table Table 4.4.5. Light Sheet Manufacturers[a]
View table Table 4.4.6. Radiation Wavelength Ranges[a]

Temporal Area Maps for quantifying cell motility
https://vimeo.com/175151196
https://works.bepress.com/gmcnamara/73 (use a web browser other than Google Chrome).
➔ poster on wall near Olga's lab.

Command in MetaMorph is: Process menu → Stack Arithmetic → Sum.

Maximum Intensity Projections are also done using Process → Stack Arithmetic → Sum.